TECHNISCHE UNIVERSITÄT MÜNCHEN

Department Chemie

Lehrstuhl Biotechnologie

Functional analysis of the co-chaperones Aha1 and Cns1 from *S. cerevisiae*

Lars Mitschke

Vollständiger Abdruck der von der Fakultät der Chemie der Technischen Universität München zur Erlangung des akademischen Grades eines Doktors der Naturwissenschaften genehmigten Dissertation.

Vorsitzender: Univ.-Prof. Dr. A. Itzen

Prüfer der Dissertation:

1. Univ.-Prof. Dr. J. Buchner
2. Univ.-Prof. Dr. Th. Hugel

Die Dissertation wurde am 26.06.2012 bei der Technischen Universität München eingereicht und durch die Fakultät für Chemie am 27.08.2012 angenommen.

1. Introduction

1.1. Molecular Chaperones

Proteins are essential components of the cell. They are synthesized at the ribosome and afterward they must adopt a defined three-dimensional structure. Protein folding is the process which leads to the native state of proteins. Entropic and enthalpic forces are involved in the process of protein folding (GO et al., 1978; KORTEMME et al., 1998; KLOSS et al., 2008). The three dimensional structure of proteins is determined by their amino acid sequence (ANFINSEN et al., 1961). However, prediction of the structure of the native state based the amino acid composition it is still challenging (FERSHT AND DAGGETT; 2002; CHEN et al., 2008; ZHANG; 2009). Misfolding or aggregation of proteins results from particular exposure of hydrophobic surfaces during the folding process (JAENICKE AND RUDOLPH, 1986; DOBSON, 2004).

Cells have evolved several mechanism and machineries in order to minimize aggregation or misfolding of proteins. These are the molecular chaperones, which display highly-conserved protein machineries (ELLIS AND VAN DER VIES, 1991; HARTL AND HAYER-HARTL, 2002 and 2009; RICHTER et al., 2010). Molecular chaperones are able to bind specifically to newly synthesized or aggregation-prone proteins. This leads to prevention of protein aggregation (BUCHNER, 1996; WALTER AND BUCHNER, 2002). First hints for the chaperone-assisted protein folding came from the Hsp60 dependence resulted of an imported mitochondrial protein (CHENG et al., 1989; OSTERMANN et al., 1989; HORWICH et al., 1990). Cellular stress such as unphysiological high temperatures leads to the upregulation of most of the chaperones, therefore termed heat shock proteins (GEORGOPOULOS AND WELCH, 1993). Upregulation of chaperones can also result from other cellular stresses (GETHING AND SAMBROOK, 1992; RUDDOCK AND KLAPPA, 1999; AKERFELT et al., 2007). Additionally, it was shown that thermotolarance is associated with expression of molecular chaperones (LINDQUIST AND CRAIG, 1988).

Molecular chaperones are classified according sequence homologies and their molecular weight. Heat shock proteins are separated into different families. Hsp60, Hsp70, Hsp90, Hsp90, Hsp100 and the small heat shock proteins are the main chaperone families. All

chaperones except the small heat shock proteins assist protein folding combined with hydrolysis of ATP, which classified them as foldases.

The Hsp60 family includes bacterial GroEL and the mitochondrial Tric/CCT from eukaryotes (CHENG et al., 1989; OSTERMANN et al.1989, GOLOUBINOFF et al., 1989, HORWICH et al., 1990; LORIMER, 1996; BEISSINGER et al., 1999; WALTER AND BUCHNER, 2002). Hsp60 family members assemble into oligomeric complexes resulting in a barrel-like structure. Hsp10/GroES forms the cap of the barrel structure of Hsp60. Assembly of the chaperone leads to formation of a cavity which is able to bind non-native proteins. Protein folding of the substrate proteins is supported by hydrolysis of ATP. The affinity for the substrate proteins is changing in the different nucleotide-bound states of the chaperone (FENTON AND HORWICH, 2003). A strong binding of substrate proteins is observable in the nucleotide-free state of the chaperone. The ATP-bound state and capping of the chaperone lead to changes in the surface for substrate binding (XU et al., 1997). The non-native protein is trapped inside the chaperone. After formation of its native conformation, the substrate protein is released which is triggered by hydrolysis of ATP (RYE et al., 1997; CHAKRABORTY et al., 2010). Additionally, structural information of the chaperone leads to a more detailed view of protein folding assisted by these large molecular chaperones (BRAIG et al., 1994; XU et al., 1997; BUKAU AND HORWICH, 1998; CHEN et al., 1999; HOFMANN et al., 2010; CLARE et al., 2012).

The Hsp70 family is the class of chaperones with the largest number of family members and Hsp70s are found in every organism. In *S. cerevisiae*, fourteen genes encoding Hsp70 proteins were found (WERNER-WASHBURNE AND CRAIG, 1989). Hsp70 proteins show a two domain architecture with a N-terminal ATPase domain and a C-terminal substrate binding domain (BUKAU AND HORWICH, 1998). Additionally, binding of nucleotides results in allosteric conformational changes in both domains of Hsp70 regulating the ATP hydrolysis and the substrate release (SCHWEIZER et al., 2011; SCHLECHT et al., 2011; MARCINOWSKI et al., 2011). The crystal structure of the substrate binding domain of bacterial DnaK gave insights into the substrate discrimination of Hs70. It is proposed that Hsp70 prefer binding of linear, hydrophobic peptides (ZHU et al., 1996). The Hsp70 chaperone machinery is associated with a vast set of cellular processes like nascent polypeptide binding at the ribosome, membrane-crossing protein translocation cytoskeleton reorganization and protein refolding (NELSON et al., 1992; UNGERMANN et al., 1994; LIANG AND MACRAE, 1997; GOLOUBINOFF et al., 1999). Binding of co-chaperones to Hsp70 regulate substrate binding and hydrolysis of ATP (SCHRODER et al., 1993; HARRISON, 2003; CRAIG et al., 2006; KAMPINGA AND GRAIG; 2010).

Members of the Hsp90 family are able to bind and stabilize non-native proteins. Hsp90 proteins are responsible for stabilization, regulation and activation of specific Hsp90 substrate proteins (MILLSON et al., 2005; ZHAO et al., 2005; MCCLELLAN et al., 2007). The interactome of yeast Hsp90, displaying putative substrate proteins and co-chaperones, revealed that Hsp90 is interacting with around 10% of the yeast proteome (ZHAO et al., 2005). However, a conserved structural motif among the substrates which mediate binding to Hsp90 was never found. This may result from the fact that the substrates of Hsp90 show dramatic differences in sequence and structure. So, substrate discrimination has to be rather flexible and possible mediated by co-chaperone recruitment. Hsp90 forms dimers and for maturation of the substrate proteins of Hsp90 the ATPase activity is essential (OBERMANN et al., 1998; PANARETOU et al., 1998). Three conserved domains are found in the Hsp90 structure: the N-terminal ATPase domain, a middle domain and a C-terminal dimerization domain (PRODROMOU et al., 1997; RICHTER AND BUCHNER, 2001). The middle domain is involved in co-chaperone binding and in discrimination of Hsp90 substrate proteins (YAMADA et al., 2003; LOTZ et al., 2003; HAWLE et al., 2006; HAGN et al., 2011).

The Hsp100 family members act together with Hsp70 and its co-chaperone Hsp40 to gain a protein remodeling activity of aggregated proteins (GLOVER et al., 1998; GOLOUBINOFF et al., 1999; ZOLKIEWSKI et al., 2012). Family members of this class of chaperones assemble into complexes consisting of two hexameric ring structures containing two sites for ATP binding per subunit (WENDLER AND SAIBIL, 2010). Additionally, for Hsp104 from *S. cerevisiae* it was shown that it is involved in the development and inheritance of the prion phenotype (CHERNOFF et al., 1995; EAGLESTONE et al., 2000; HELSEN et al., 2012; HALFMANN et al., 2012).

The small heat shock proteins display another family of molecular chaperones. Their main function is prevention or control of protein aggregation (HORWITZ, 1992; JAKOB AND BUCHNER, 1994). Binding of unfolded proteins by the small heat shock proteins leads to soluble oligomeric complexes (EHRNSPERGER et al., 1997; KIM et al., 1998; HASLBECK; 1999). The class of the small heat shock proteins is classified as holdases as they are not containing an ATPase activity. Refolding of the substrate proteins is performed in cooperation with the Hsp70 or the Hsp100 chaperone machinery (EHRNSBERGER et al., 1997; HASLBECK et al., 2005; CASHIKAR et al., 2005).

1.2. The molecular chaperone Hsp70

Hsp70 is one of the key components of the chaperone system. Proteins from the Hsp70 family are found in all organisms.

DnaK, Hsc66 and Hsc62 represent three members of the Hsp70 family, which are found in *E. coli* (ITOH et al., 1999). In eukaryotic cells, Hsp70 proteins are present in the cytosol, in chloroplasts, in mitochondria and in the endoplasmatic reticulum. In mammals, two cytoplasmic isoforms of Hsp70 are present, where Hsc70 is constitutivly expressed and expression of Hsp70 is stress-induced. These molecular chaperones are important for different functions and thereby function under different conditions. Up to 20% of the newly synthesized proteins use the Hsp70 chaperone machinery during their biogenesis (THULASIRAMAN et al., 1999). Binding of substrate proteins to Hsp70 is mainly maintained by hydrophobic sequences (BECKMANN et al., 1990; HENDRICK AND HARTL, 1993; FRYDMAN et al., 1994; MOGK et al., 1999; RÜDIGER et al., 2000; HARTL AND HAYER-HARTL, 2009). Hsp70 is also able to bind directly to nascent polypeptides which are associated with the ribosome (NELSON et al., 1993; HANSEN et al., 1994; KIM et al., 1998; HARTL AND HAYER-HARTL, 2009). In this process, Hsp70 binds to hydrophobic parts of polypeptides and correct folding of the substrate proteins is facilitated. Additionally, Hsp70 is also involved in several cellular processes like protein transport across membranes, regulation of the heat-shock response and disassembly of clathrin-coated vesicles (DESHAIES et al., 1988; SCHATZ et al., 1996; HERRMANN AND NEUPERT, 2000; MAYER AND BUKAU, 2005; BUKAU et al., 2006; ROTHNIE et al., 2011; BÖCKING et al., 2011).

In *S. cerevisiae*, fourteen members of the Hsp90 family are found (WERNER-WASHBOURNE AND CRAIG, 1989). Nine Hsp70 proteins located in the cytosol are classified as Ssa, Ssb, Sse and Ssz subfamilies. Proteins from the Ssa subfamily (Ssa1-Ssa4) are involved in protein translocation and regulation of the heat-shock response (DESHIAES et al., 1988). Additionally, among the Hsp70 proteins from *S. cerevisiae* the Ssa subfamily show the strongest homology to Hsp70 from higher eukaryotes. The Ssb subfamily (Ssb1, Ssb2) gained a more specialized function as members were found in complexes with ribosomes and nascent polypeptide chains (NELSON et al., 1992; PFUND et al., 1998). This indicates direct involvement in protein translation and protein folding at the ribosome. Regulation of the Hsp70 activity by cochaperones leads to further differentiation of the Hsp70 proteins. Proteins from the Hsp40 family are responsible for fine-tuning of the Hsp70 activity (DIAMANT AND GOLOUBINOFF; 1998; CRAIG et al, 2006; KEMPINGA AND CRAIG; 2010). The Hsp40 cochaperones Ydj1 and Sis1 regulate the turnover of the proteins from the Ssa subfamily.

However, the Ssz protein is able to form complexes with the Hsp40 cochaperone Zuo1 (CYR et al., 1992; LU et al., 1998; GAUTSCHI et al., 2001; HUNDLEY et al., 2002). The protein Ssz is involved in recruitment of Ssbs and the Hsp40 Zuo1 to form a ribosomal associated folding complex (KRAMER et al., 2009). Proteins from the Sse subfamily contain a low intrinsical ATPase activity and are therefore not directly involved in protein folding, but seem to be holdases (SHANER et al., 2004; SHANER AND MORANO, 2007; GOECKELER et al., 2008). These proteins belong to the Hsp110 subfamily, which are able to bind to Hsp70 proteins in an ATP dependent manner as nucleotide exchange factors (SHANER et al., 2005; DRAGOVIC et al., 2006; SHANER et al., 2006; ANDREASSON et al., 2008; POLIER et al., 2010). In addition, they were also involved in the Hsp90 chaperone machinery (LIU et al., 1999; MANDAL et al., 2010).

1.2.1. Structure of Hsp70

In general, Hsp70 contain a N-terminal ATPase domain and a C-terminal substrate-binding domain (FLAHERTY et al., 1990; ZHU et al., 1996). The N-terminal domain which contains the ATPase function is highly conserved. Additionally, few Hsp70s contain a C-terminal EEVD motif which is responsible for binding to several co-chaperones. The solution structure of DnaK complexed with ADP and substrate was solved by NMR (BERTELSEN et al., 2009).

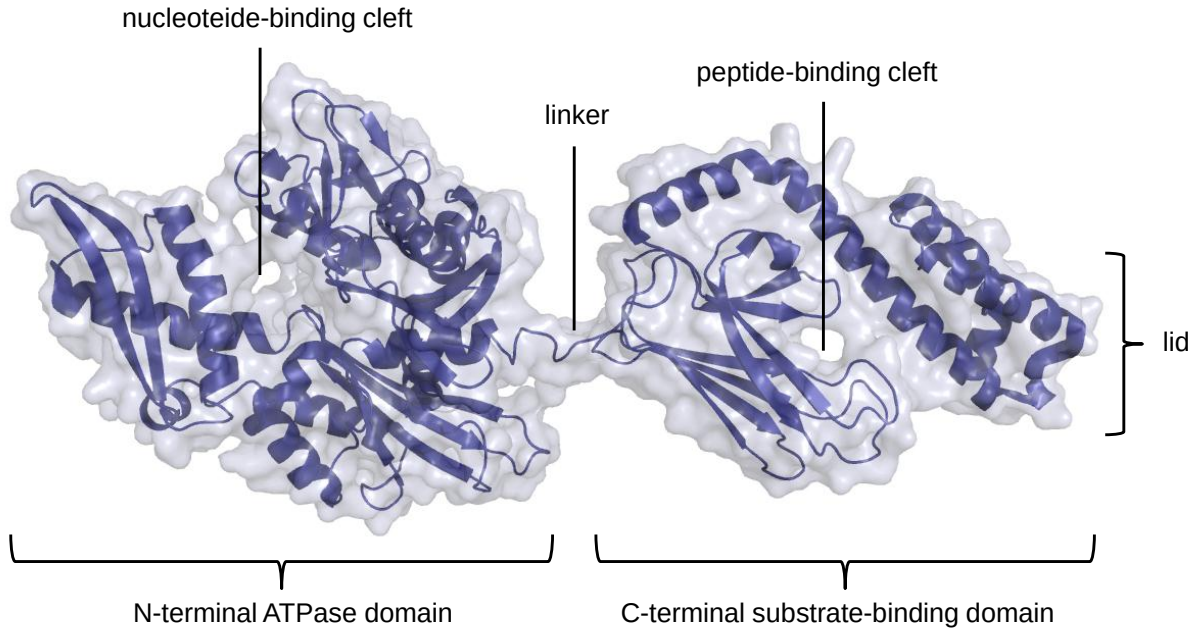

Figure 1-1: Solution structure of DnaK.
Structure of DnaK solved by NMR (pdb-code: 2KHO) with ADP bound to the nucleotide binding domain (BERTELSEN et al., 2009). The N-terminal domain contains the ATPase whereas the C-terminal domain is responsible for substrate binding. Interdomain communication is mediated by the flexible linker.

As shown above, the N-terminal ATPase domain and the C-terminal substrate-binding domain are connected by a short, flexible linker which is involved in allosteric coupling of the two domains (KUMAR et al., 2010). In the ATP-bound state both domains dock. In addition, the lid is also displaced by ATP binding resulting in a better access and egress of the client protein (VOGEL et al., 2006; SWAIN et al., 2007; SCHLECHT et al., 2011; MARCINOWSKI et al., 2011). The C-terminal domain is responsible for client protein binding. A common binding motif among substrate proteins for Hsp70 was not found, as they represent different folding confomers. This includes unfolded polypeptides which emerge at ribosomes or translocation pores and native proteins such as kinases, transcription factors, clathrin and proteins involved in DNA replication (WICKNER et al., 1991; PRATT et al., 1992; HUPP et al., 1992; GAMER et al., 1992; SONG et al., 2001; HUNDLEY et al., 2002; GAUTSCHI et al., 2002; MAYER AND BUKAU, 2005; BUKAU et al., 2006; ROTHNIE et al., 2011; BÖCKING et al., 2011). In contrast to this wide spectrum of substrates, the Hsp70 homologues Hsc66 from *E. coli* and Ssq1 from yeast were found to interact with iron-sulfur-cluster containing substrate proteins (HOFF et al., 2000; LUTZ et al., 2001; VOISINE et al., 2001). So, the substrate proteins of Hsp70 differ in structure and sequence which indicates a degenerated binding motif. According to structural features of Hsp70, substrate proteins were bound in an elongated form. Further analysis with peptide libraries revealed that binding of Hsp70 to hydrophobic

peptides is favored (FLYNN et al., 1991; BLOND-ELGUINDI et al., 1993; RÜDIGER et al., 1997; KNARR et al., 1999). The binding motif of peptides which are able to bind to DnaK is described by a hydrophobic core and flanking charged residues. The binding affinities of the peptides to DnaK range from 5 nM to 5 µM (RÜDIGER et al., 1997). The segments which mediate binding to Hsp70 were found inside hydrophobic cores of folded proteins or at domain interfaces, whereas native proteins bind via exposed loop structures at their surface (GREENE et al., 1995). Conformation of the C-terminal substrate binding domain and conformational flexibility of the lid influence the binding to substrate proteins (VOGEL et al., 2006; SCHLECHT et al., 2011; MARCINOWSKI et al., 2011). The solution structure of DnaK revealed different conformational states which are mediated by binding to nucleotides or substrates (BERTELSEN et al., 2009).

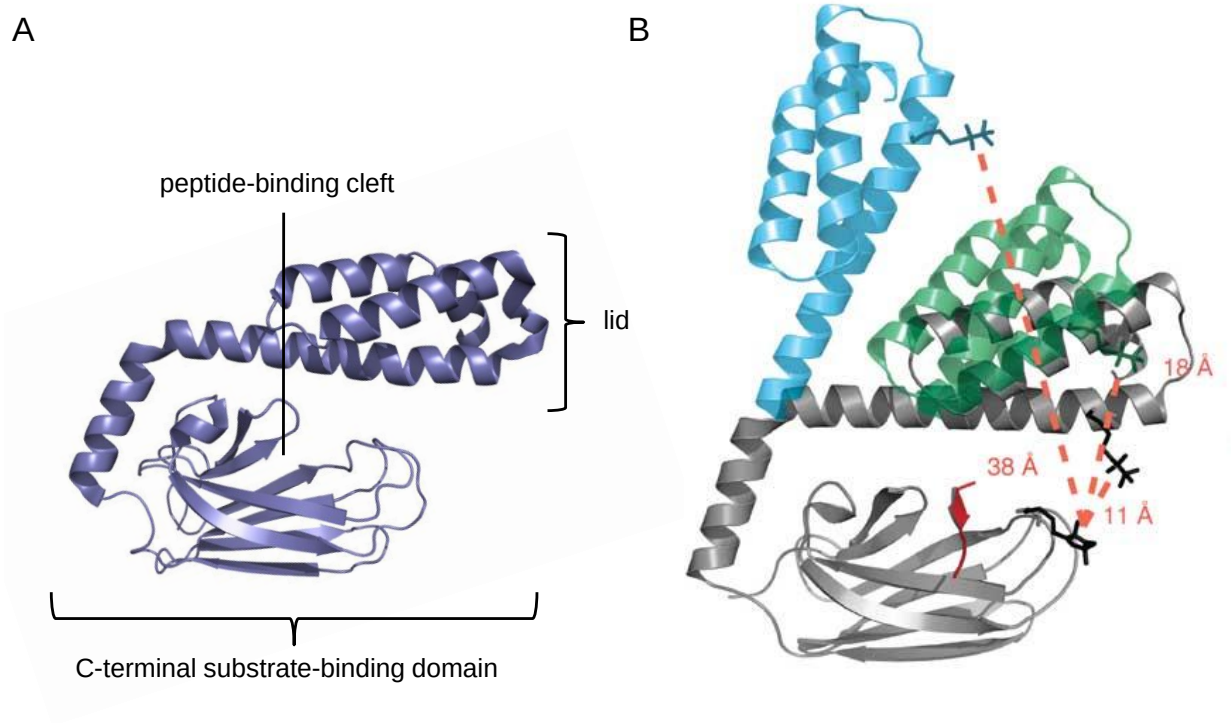

Figure 1-2: C-terminal substrate binding domain of DnaK.
(A) Solution structure of the C-terminal domain of DnaK.
(B) Conformational changes of the lid of DnaK induced by substrate binding. Figure adapted by permission from Macmillan Publishers Ltd (SCHLECHT et al., 2011,).

Different conformations of the lid were observed in the solution structure of DnaK by addition of nucleotides and substrates (BERTELSEN et al., 2009). The helix of the lid stabilizes the complex with substrates and controls their binding and release from Hsp70. For the lid-forming helix of DnaK, at least three conformational states were found. A conformation where the helix is closed over bound peptides was not found, implicating that DnaK can also

bind to substrate proteins with substantial tertiary structure (MAYER et al., 2000; SCHLECHT et al., 2011). Additionally, the lid-forming helix is connected to the substrate-binding pocket by the peptide backbone and various salt bridges. Substrate binding of Hsp70 is destabilized by disruption of the salt bridges (HA et al., 1997).

1.2.2. ATP binding and hydrolysis of Hsp70

The conserved N-terminal ATPase domain of Hsp70 consists of two subdomains and is separated by the nucleotide binding pocket (FLAHERTY et al., 1990; HA et al., 1995; BERTELSEN et al., 2009). Binding of nucleotides to Hsp70 is mediated by Mg^{2+} and K^{+} ions. Additionally, the nucleotide binding pocket is solvent inaccessible. The structure of the N-terminal ATPase domain of Hsp70 shows homology to the structure of actin (KABSCH et al., 1990, FLAHERTY et al., 1991).

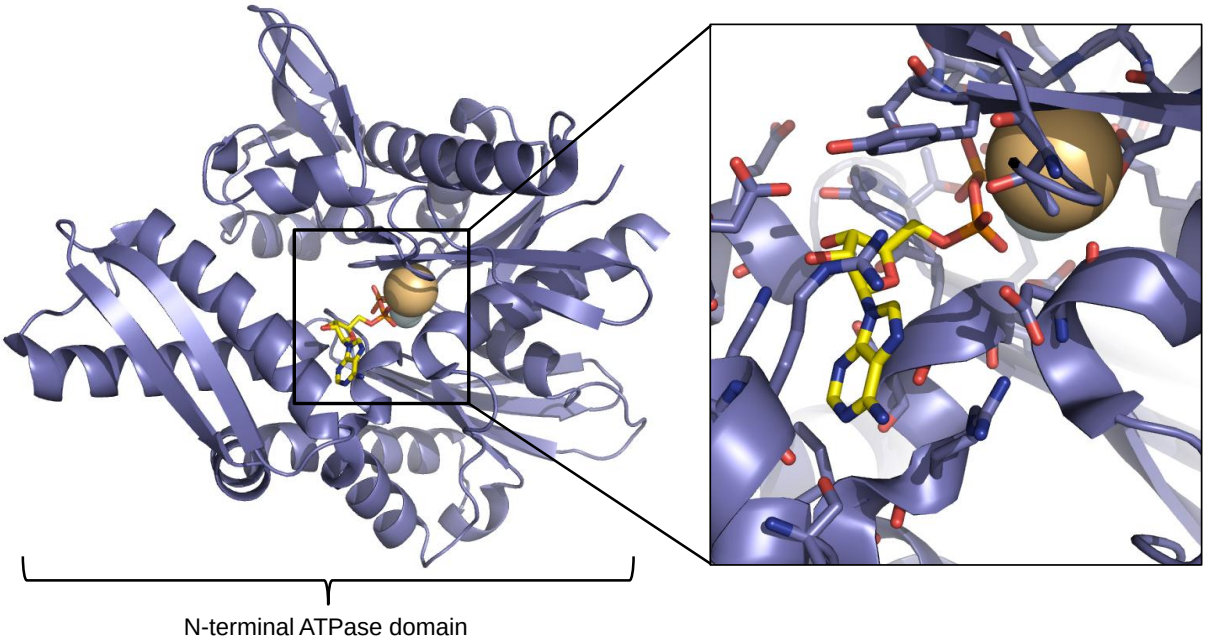

Figure 1-3: N-terminal ATPase domain of Hsp70.
N-terminal ATPase domain of the human Hsp70 (pdb-code: 3AY9). ADP is bound in the nucleotide binding pocket and is complexed with Mg^{2+} (cyan sphere) and K^{+} ions (orange sphere).

Protein folding by Hsp70 is facilitated in cooperation with ATP binding, hydrolysis and nucleotide exchange (PALLEROS et al., 1993; MCCARTY et al., 1995; BANECKI et al., 1996, MAYER AND BUKAU, 2005). Interaction of Hsp70 with substrates is influenced by binding to

nucleotides. The ATP-bound state Hsp70 shows a weak affinity to substrates whereas binding of ADP results in a high affinity state of Hsp70 for substrates (PALLEROS et al., 1993; SCHMID et al., 1994). Hsp70 show an intrinsically low hydrolysis rate for ATP (0.02 – 1 min^{-1}). Mg-ATP is bound to Hsp70 with affinities of 0.1 - 1 µM (GAO et al., 1994; HA et al., 1994; THEYSSEN et al., 1996; KLOSTERMEIER et al., 1998). So, the rate limiting step for the enzymatic cycle of Hsp70 is the hydrolysis of ATP (GAO et al., 1993; MCCARTY et al., 1995; THEYSSEN et al., 1996). In addition, acceleration of ATP hydrolysis and nucleotide exchange are important for the function of Hsp70 in the context of the catalytic cycle (SHANER et al., 2008; POLIER et al., 2008; SCHUERMANN et al., 2008; KABANI, 2009). The ATPase activity is also regulated by the interdomain communication of Hsp70 (LOPEZ-BUESA et al., 1998; VOGEL et al., 2006; SWAIN et al., 2007). The activity for ATP hydrolysis is dependent on Mg^{2+} and K^{+}. Other monovalent ions influence the affinity for ATP binding and the hydrolysis rate of ATP (O´BRIAN et al., 1995). Whereas Mg^{2+} is responsible for complex formation of the phosphate groups of ATP, monovalent ions are needed for orientation and electrostatic interactions of the nucleotide in the binding pocket of Hsp70 (WILBANKS et al., 1995).

1.2.3. Co-chaperones of Hsp70

Hsp70 is regulated by interaction with several co-chaperones which influence different steps in the catalytic cycle (BUKAU et al., 1998; LU et al., 1998; TZANKOV et al., 2008). Nucleotide binding leads to different affinities of Hsp70 for substrate binding. In the ATP-bound state of Hsp70, the on and off rates for substrate binding are rapid, whereas the the rates for the ADP-bound state are slow. The ATPase activity of Hsp70 is intrinsically low and nucleotides binds generally stable, resulting in extremely low transitions between both states. So the Hsp70 machinery requires co-chaperones. The Hsp70 co-chaperones are able to accelerate the intrinsically low ATPase activity of Hsp70 or influence the nucleotide exchange (SONDERMANN et al., 2001; DRAGOVIC et al., 2006; QIU et al., 2006; RAVIOL et al., 2006; POLIER et al., 2008; KAMPINGA AND CRAIG, 2010).

Proteins from the Hsp40 family are responsible for stimulation of the ATPase activity of Hsp70 and for facilitating substrate capture. These proteins are referred as J-proteins, according to their conserved binding motif. Binding to Hsp70 is mediated by the J-domain, which displays a conserved signature region of around 70 amino acids. Exposed residues of the J-domain are responsible for interaction with Hsp70 (GREENE et al., 1998; JIANG et al., 2007). J-proteins bind to the ATPase domain and the adjacent flexible region of Hsp70. The crucial conformational changes which are necessary for closing of the peptide-binding pocket

are mediated by the J-protein interaction (SUH et al., 1998; GASSLER et al., 1998; VOGEL et al., 2006; HUANG et al., 2005; SWAIN et al., 2007; JIANG et al., 2007). Various J-proteins exist, which often outnumber Hsp70s and nucleotide exchange factors in a defined cellular compartment (CRAIG et al., 2006; HAGEMAN AND KAMPINGA; 2009). The structures of the J-proteins Ydj1 and Sis1 from *S. cerevisiae* were solved (SHA et al., 2000; LI et al., 2003; WU et al., 2005). The J-proteins Ydj1 and Sis1 from *S. cerevisiae* are able to stimulate the ATPase activity of Hsp70 (CYR et al., 1992 and 1994; LU et al., 1998).

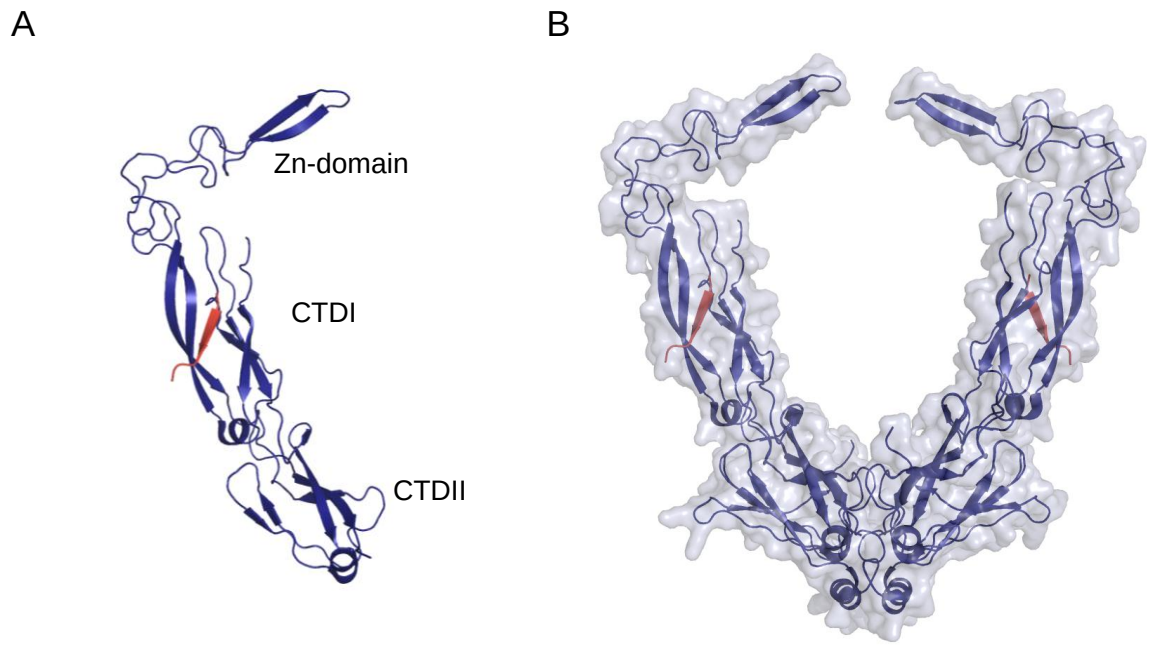

Figure 1-4: Structure of Ydj1 from *S. cerevisiea*
(A) Monomer structure of yeast Ydj1 and domain architecture is shown (red: cocrystallized peptide; pdb-code: 1NLT). Ydj1 has two adjacent domains which are composed of ß-sheets, termed CTDI and CTDII. Additionally, Ydj1 has two zinc fingers in the Zn-domain. A CAAX motif for farnesylation of Ydj1 was also found. This is important for membrane association and client binding (CAPLAN et al., 1992; FLOM et al., 2008).
(B) Dimeric structure of Ydj1 (pdb-code: 1NLT and 1XAO).

Nucleotide exchange factors are able to enhance the exchange of ADP for ATP (PIERPAOLI et al., 1997 and 1998; PACKSCHIES et al., 1997). Binding of NEFs to the nucleotide-binding domain of Hsp70 showed an opened nucleotide binding pocket. So, access and egress of nucleotides is enhanced. An induced-fit mechanism for active opening of the nucleotide-binding pocket by the NEFs was proposed (HARRISON et al., 1997; SONDERMANN et al., 2001). However, it is more reasonable that NEFs bind to the nucleotide-binding domain of Hsp70 and capture transient opening states (BHATTACHARYA et al., 2009). Several structures

of NEFs bound to the nucleotide-binding domain of Hsp70 are available (HARRISON et al., 1997; SONDERMANN et al., 2001; LIU et al., 2007; SCHUERMANN et al., 2008; XU et al., 2008).

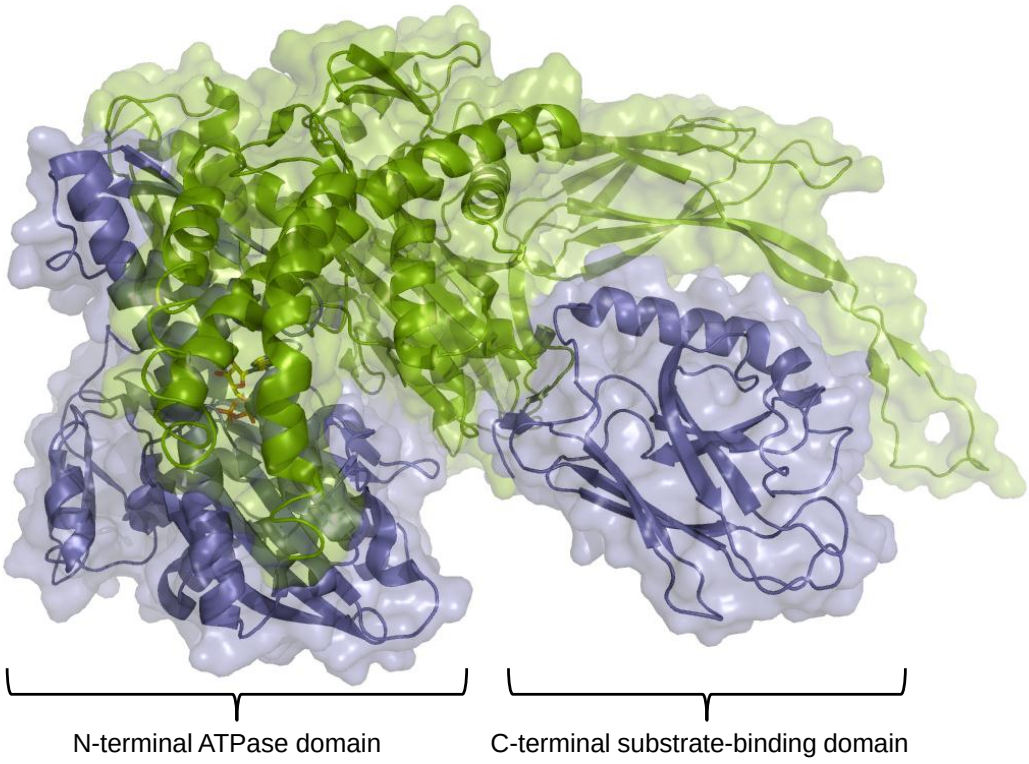

Figure 1-5: Hsp70 in association with nucleotide exchange factor.
Co-crystal structure of Hsp70 bound to the NEF Sse1 (SCHUERMANN, et al., 2008; pdb-code: 3C7N). Hsp70 is colored in blue, Sse1 in green.

1.2.4. Chaperone cycle of Hsp70

Regulation of the Hsp70 cycle leads to a canonical model for the Hsp70 machinery´s mode of action. In this model J-proteins recognize and bind to the substrate and transfer them to Hsp70 protein. After formation of the J-protein-Hsp70-substrate complex, the substrate is transferred to the peptide-binding pocket of Hsp70. ATP binding leads to an open conformation and the peptide-binding pocket is accessible for the substrate. Hydrolysis of ATP leads to conformational changes within Hsp70 resulting in an increased affinity for the substrate. A nucleotide exchange factor is than able to bind to the ADP-bound Hsp70-substrate complex, releases ADP and ATP is bound. The substrate is released as the affinity

to Hsp70 is decreased upon nucleotide exchange (KAMPINGA AND CRAIG, 2010; ZUIDERWEG et al., 2012).

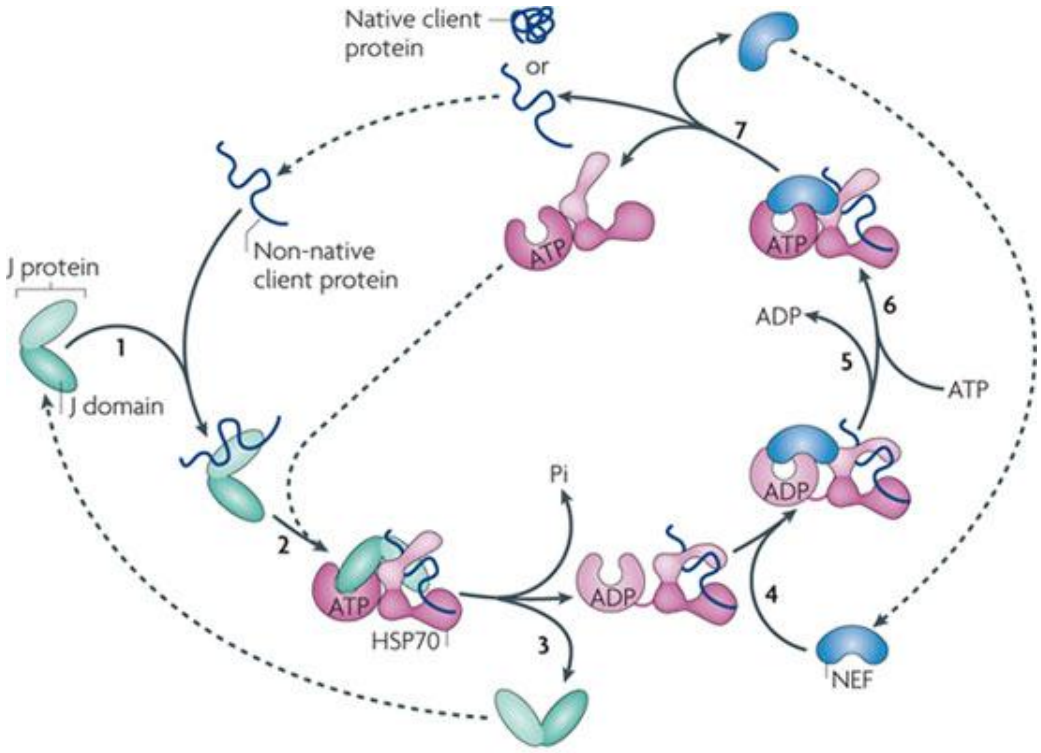

Figure 1-6: Canonical model of the Hsp70 chaperone machinery.
Based on in vitro refolding studies of denatured proteins a model of the core Hsp70 machinery´s mode of action is proposed. Figure is adapted by permission from Macmillan Publishers Ltd (KAMPINGA AND CRAIG, 2010).

In addition, Hsp70 is involved in folding processes of proteins. The Hsp70 machinery is able to refold heat-denatured luciferase, polymerase, and can resolubilize protein aggregates. However, refolding of proteins seems to include an unfolding process of the substrate (SFATOS et al., 1996; DE LOS RIOS et al., 2006; SHARMA et al., 2010). Different mechanisms of the unfolding process are postulated (DIAMANT et al., 2000; GOLOUBINOFF et al., 2007; MORENO-DEL ALAMO et al., 2010).

1.3. The molecular chaperone Hsp90

Hsp90 is a highly conserved molecular chaperone and a global regulator for the folding and regulation of several cellular proteins. Formation of the correct conformation and activation of more than 200 proteins, termed clients, is mediated by Hsp90 (PRATT AND TOFT, 1997; PICARD; 2002; ZHAO et al., 2005; MCCLELLAN et al., 2007). Hsp90 is highly abundant compromising up to 1-2% of the whole soluble cellular proteins (JAKOB et al., 1996).

Hsp90 exist in eubacteria and eukaryotes. Archea generally lack genes encoding for Hsp90 proteins (LARGE et al., 2009). Hsp90 is essential for viability of eukaryotic cells, whereas in bacteria Hsp90 is only required under stress conditions (BARDWELL et al., 1988; BORKOVICH et al., 1989; SPENCE et al., 1989 and 1990; PEARL AND PRODROMOU, 2000; PRATT AND TOFT, 2003). In higher eukaryotes, different homologs of Hsp90 were found. Two genes encoding for cytosolic Hsp90, Hsp90α and Hsp90β, were identified in mammals. Both proteins show a 85% sequence homology and are highly homologue to Hsp90 from lower eukaryotes and prokaryotes (HICKEY et al., 1989).

Furthermore, Hsp90 is also found in mitochondria and in the endoplasmic reticulum. Trap1 (tumor necrosis factor receptor-associated protein 1) is the mitochondrial Hsp90 (SONG et al., 1995; CHEN et al., 1996; FELTS et al., 2000). A function assigned to Trap1 is protection against mitochondrial apoptosis (MASUDA et al., 2004; LU et al., 2006; HUA et al., 2007). Additionally, multi-drug resistance of human colorectal cancer cells was associated with upregulation of Trap1 (COSTANTINO et al., 2009). The Hsp90 family member in the endoplasmic reticulum is termed Grp94 (Glucose-regulated protein 94). Maturation of several proteins like MHC class II proteins, nascent immunoglobulin chains, integrins, Toll-like receptors, thyroglobulin and collagen in the ER is mediated by Grp94 (SCHAIFF et al., 1992; MELNICK et al., 1992; FERREIRA et al., 1994; MURESAN et al., 1997; YANG et al., 2007; LIU et al., 2008; WU et al., 2012). In *A. thaliana* seven Hsp90 family members were found. Four are located in the cytosol and three in plastides (KRISHNA AND GLOOR, 2001). In lower eukaryotes, such as *S. cerevisiae*, Hsp90 is only found in the cytosol, where it is essential for viability (BORKOVICH et al., 1989).

1.3.1. Structure of Hsp90

Hsp90 is a homodimer consisting of three conserved domains. The highly conserved N-terminal domain contains the ATP binding site (PRODROMOU et al., 1997). The individual N-terminal domain itself shows no significant activity for hydrolysis of ATP (OBERMANN et al., 1998; WEGELE et al., 2003). In order to achieve a hydrolysis competent state of Hsp90, a catalytic loop of the middle domain and transient N-terminal dimerization is required (MCLAUGHLIN et al., 2002; ALI et al., 2006; RICHTER et al., 2006). Binding of co-chaperones, like Sba1, Cdc37, Aha1 and Sgt1, is also maintained by the N-terminal domain of Hsp90 (PEARL, 2005; ALI et al., 2006; PEARL AND PRODROMOU, 2006; ZHANG et al., 2008; RETZLAFF et al., 2010). The middle domain of Hsp90 is implicated in client protein binding (MEYER et al., 2003; VAUGHAN et al., 2006; PARK et al., 2011; STREET et al., 2011; HAGN et al., 2011). Additionally, the middle domain of Hsp90 is also involved in binding of co-chaperones (MEYER et al., 2004; ALI et al., 2006; RETZLAFF et al., 2010). Dimerization of Hsp90 is mediated by the C-terminal domain. Additionally, dynamics of the C-terminal dimerization is also possible in the presence of transient N-terminal dimerization of Hsp90 (RATZKE et al., 2010). Eukaryotic cytosolic Hsp90 family members contain the MEEVD motif at the very C-terminus. This motif is recognized by TPR-containing co-chaperones (CHEN et al., 1998; PRODROMOU et al., 1999; CARRELLO et al., 1999; RAMSEY et al., 2000; SCHEUFLER et al., 2000; RICHTER et al., 2003; SCHMID et al., 2012). The three domains are conserved in Hsp90 homologues. However, the C- and N-terminal extensions and linkers connecting the domains of Hsp90 differ between Hsp90 homologues. The N- and C-terminal domain of Hsp90 is connected by a charged and flexible linker, which affects Hsp90 function, co-chaperone interaction and conformation. Length and amino acid composition of this linker differ between Hsp90 homologues. In bacterial and mitochondrial Hsp90, the linker is considerably shortened (HAINZL et al., 2009; TSUTSUMI et al., 2012).

The binding constant of dimerization of Hsp90 is in the nM range, so Hsp90 is almost exclusively dimeric in vivo (MARUYA et al., 1999; HARRIS et al., 2001; RICHTER et al., 2001). Additionally, in higher eukaryotes also heterodimers (α-β) were found besides the homodimers (α-α; β-β) (PERDEW et al., 1993; NEMOTO et al., 1996).

The Hsp90 dimer is highly flexible and adopts different states during the chaperone cycle. Conformational changes of Hsp90 are triggered by nucleotides (HESSLING et al., 2009).

The crystal structure of the nucleotide-bound, closed state of Hsp90 in complex with Sba1 was solved. In order to obtain crystal formation the charged linker of Hsp90 was shortened

and replaced (ALI et al., 2006). Structures of the nucleotide-free, open state and the ADP-bound state of Hsp90 were solved for the bacterial Hsp90 (SHIAU et al., 2006).

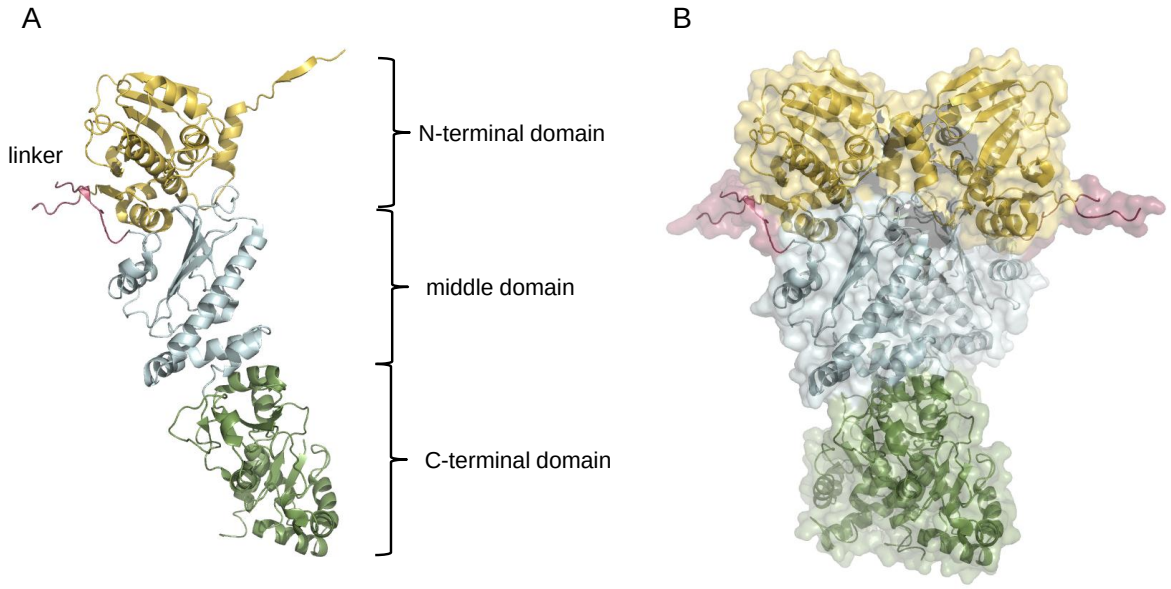

Figure 1-7: Crystal structure of Hsp90.
Crystal structure of yeast Hsp90 bound to AMP-PNP was solved (ALI et al., 2006; pdb-code: 1CG9).
(A) Monomer of Hsp90 and domain architecture of Hsp90 is shown.
(B) Hsp90 form homodimers. In the presence of AMP-PNP, Hsp90 is in the closed conformation.

The structure of the N-terminal domain of Hsp90 was solved previously (PRODROMOU et al., 1999). This domain is responsible for binding of nucleotides as well as for several Hsp90 inhibitors (STEBBINS et al., 1997; PRODROMOU et al., 1999; ROE et al., 1999). It showed a β-sheet and an alpha helical structure. Similarities to this structure are found in type II and type IV DNA topoisomerase, the MutL family of DNA repair proteins and the bacterial DNA gyrase B protein (BERGERAT et al., 1997).

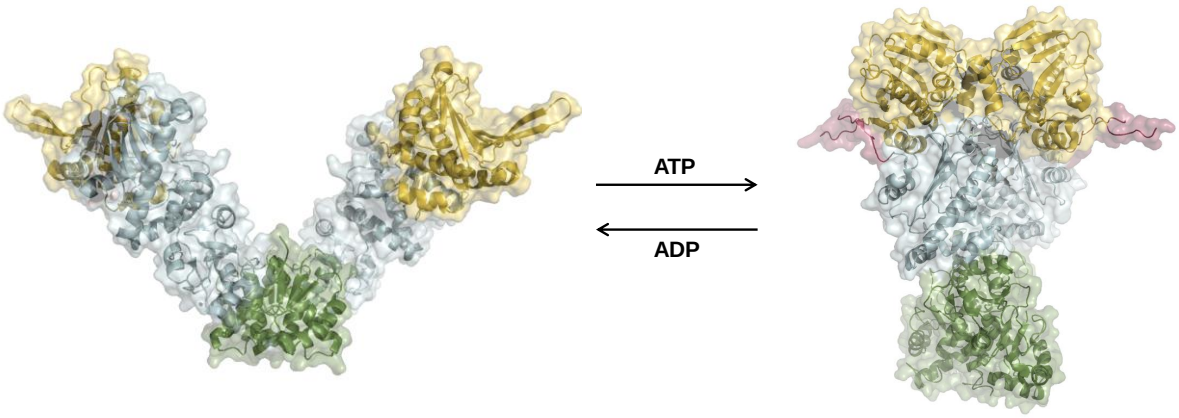

Figure 1-8: Different conformations of Hsp90.
Crystal structures of HtpG in the open (pdb-code: 2IOQ) and yeast Hsp90 in the closed conformation (pdb-code: 2CG9) are shown. Upon nucleotide binding different conformational changes of Hsp90 are induced. Binding of ATP induce the closed conformation, whereas binding to ADP adopt the open conformation.

1.3.2. ATP binding and hydrolysis by Hsp90

The ATPase activity is essential for the function of Hsp90 as ATPase-inactive mutants result in lethality of yeast cells (OBERMANN et al., 1998; PANARETOU et al., 1998). Substrates are able to bind to Hsp90 independent of the nucleotide-bound state of Hsp90. However, maturation of substrates is performed together with the Hsp70 machinery in an ATP-dependent manner (FREEMAN et al., 1996; SCHUMACHER et al., 1996; MINAMI et al., 2001). The N-terminal domain of Hsp90 is responsible for nucleotide binding. However, Hsp90 shows quite low affinity to ATP (K_D ~ 400 µM) (PRODROMOU et al., 1997; SCHEIBEL et al., 1997; WEIKL et al., 2000). As shown by the crystal structure, ATP is bound in a kinked conformation which results in higher affinity to ADP (PRODROMOU et al., 1997).

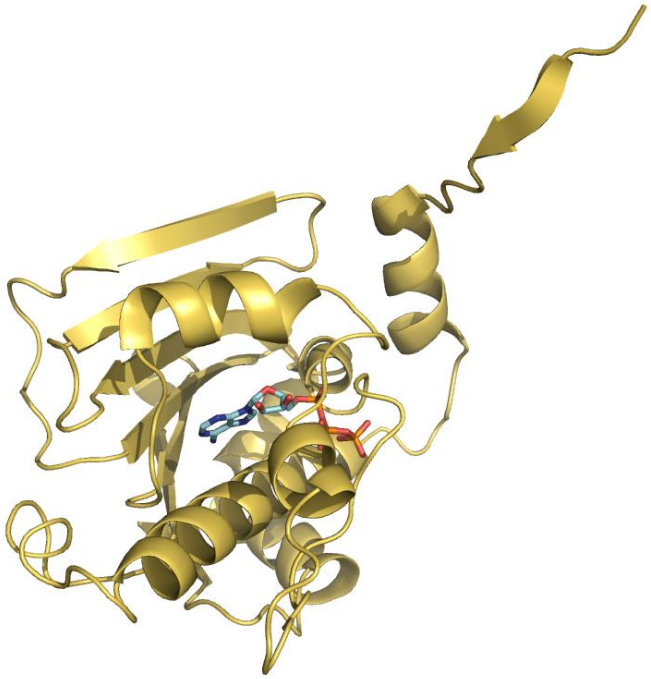

Figure 1-8: N-terminal domain of Hsp90.
The N-terminal domain of Hsp90 (pdb-code: 2CG9) is responsible for binding and hydrolysis of ATP. ATP was fitted in the structure and is shown in stick representation.

Hsp90 contains an intrinsically low ATPase activity (PANARETOU et al., 1998; SCHEIBEL et al., 1998; WEIKL et al.; 2000; YOUNG et al., 2000; MCLAUGHLIN et al., 2002). Analysis of the reaction kinetics revealed that other regions within Hsp90 are also involved in the hydrolysis reaction (WEIKL et al., 2000). ATP hydrolysis is also coupled to N-terminal dimerization mainly mediated by the first 24 residues of Hsp90 (PRODROMOU et al., 2000; RICHTER et al., 2002; HESSLING et al., 2009).

In order to achieve the catalytically active state of Hsp90, structural rearrangements of its ATP lid occur. This includes closing of the ATP lid over the bound nucleotide. Additionally, this closing reaction results in involvement of the catalytic loop of the middle domain (PRODROMOU, 2012). ATP turnover is kinetically limited by structural rearrangements proceeding hydrolysis (WEIKL et al., 2000; GRAF et al., 2009; HESSLING et al., 2009). Thereby, Hsp90 is not only switching between two conformational states. The catalytic cycle of Hsp90 includes different conformational states of Hsp90 (HESSLING et al., 2009).

1.3.3. Co-chaperones of Hsp90

Various co-chaperones interact with Hsp90 within the chaperone cycle. They were found as regulators of the ATPase activity of Hsp90 and are recruited according to specific clients of Hsp90 (CHEN et al., 1998; PRODROMOU et al., 1999; PANARETOU et al., 2002; RICHTER et al., 2004; ROE et al., 2004).

Sti1/Hop

The protein Sti1/Hop acts as adaptor protein in order to connect the Hsp70 and the Hsp90 cycle. For client delivery such as steroid hormone receptors both chaperone cycles are involved and Sti1 mediates the substrate transfer to the Hsp90 system. Sti1 was shown as a potent inhibitor of the Hsp90 ATPase. Binding of Sti1 to Hsp90 leads to stabilization of the open conformation which results in inhibition of the ATPase activity of Hsp90 (Figure 1-10, a) (JOHNSON et al., 1998, PRODROMOU et al., 1999, RICHTER et al., 2003). The protein is composed of multiple TPR-domains. So, Sti1 is able to bind simultaneously to Hsp90 and Hsp70. So, Sti1 serves as adaptor protein for the substrate transfer to the Hsp90 system (CHEN, 1998; WEGELE et al., 2003 and 2006, SCHMID et al., 2012). Sti1 is a monomeric protein and one Sti1 molecule is sufficient to inhibit the ATPase activity of Hsp90 (YI et al., 2010; LI et al., 2011). Sti1 is not essential in yeast. However, lethality of yeast cells is inducible in combination with deletion of either Sba1 or Ydj1 (FANG et al., 1998; FLOM et al., 2005).

Large prolylisomerases

In *S. cerevisiae*, Cpr6 and Cpr7 represent the PPIase co-chaperones of Hsp90. Peptidyl-prolyl-isomerases catalyze the interconversion of cis-trans isomerization of peptide bonds prior to proline residues (DUINA et al., 1996; FANGHANEL et al., 2004). They were found to be involved in Hsp90-assisted maturation of steroide hormone receptors (JOHNSON et al., 1994; RATAJCZAK et al., 2009). They contain a TPR-domain which mediates binding to Hsp90 (Figure 1-10, e). Additionally, independent chaperone activity of the PPIases was also shown (BOSE et al., 1996; FREEMAN et al., 1996; MAYR et al., 2000; PIRKL AND BUCHNER; 2001). For the progression of the chaperone cycle, the recruitment of different co-chaperones is necessary. For Cpr6 it was shown that it forms mixed complexes with Sti1 and Hsp90 (LI et al., 2011). The specific role of the PPIases in client maturation is not understood. However,

they are thought to act after loading of the steroid hormone receptors on Hsp90 (SMITH et al., 1995; SMITH AND TOFT, 2008).

Ppt1

Ppt1 is a protein phosphatase and binds to Hsp90 via its N-terminal TPR-domain (Figure 1-10, f). The function of the phosphatase domain is intrinsically inhibited. After binding of Ppt1 to Hsp90, the phosphatase function is active (KANG et al., 2001). Dephosphorylation of Hsp90 and Cdc37 is specifically catalyzed by Ppt1 (WANDINGER et al., 2006; VAUGHAN et al., 2008). Regulation of Hsp90 phosphorylation is important for maturation of the clients as deletion of Ppt1 reduced Hsp90 client activity (WANDINGER et al., 2006).

Cdc37

Another inhibitor of the Hsp90 ATPase activity is Cdc37 (SILIGARDI et al., 2002; GAISER et al., 2010). Cdc37 was found as an essential component for progression of the cell cycle and in Hsp90-client-complexes (REED et al., 1980; FERGUSON et al., 1986 BRUGGE et al., 1986; DEY et al., 1996). Furthermore, Cdc37 is specific for binding and chaperoning kinases (MACLEAN AND PICARD, 2003). In *S. cerevisiae*, deletion of Cdc37 results in lethality implicating essential functions (BRETER et al., 1983; MANDAL et al., 2007).

Cns1

Cns1 was found as a multicopy suppressor of a slow-growth phenotype in yeast cells resulting from deletion of Cpr7. Overexpression of other Hsp90 interacting proteins were not able to rescue this phenotype (DOLINSKI et al., 1998). Additionally, overexpression of Cpr7 leads to viability of yeast cells when Cns1 function is impaired. However, Cpr6 showed no effect (TESIC et al., 2003). For rescue of the viability of yeast cells, the PPIase domain of Cpr7 is essential. However, the specific function of this domain can be inhibited. A chimera of the TPR-domain of Cpr7 and the PPIase domain of Cpr6 was not able to restore viability (TESIC et al., 2003). Thus, Cpr7 and Cns1 share an essential function in yeast. For Cns1 it was shown, that for the viability of yeast cells only the TPR-domain is essential (TESIC et al., 2003, HAINZL et al., 2004).

Cns1 consists of a N-terminal TPR-domain and C-terminal domain with unknown function. Interaction with Hsp90 and Hsp70 is mediated by the TPR-domain of Cns1 (Figure 1-10, g) and was shown previously (HAINZL et al., 2004). In contrast to other co-chaperones of Hsp90, Cns1 is not upregulated upon heat shock (GASCH et al., 2000). However, function of Cns1 remained still unclear.

In higher eukaryotes, homologues of Cns1 were found (CREVEL et al., 2001 and 2008). TTC4 is a putative co-chaperone of Hsp90 and Hsp70 and showed sequence similarities to Cns1 (CREVEL et al., 2008). Additionally, in the gene encoding for TTC4 several mutations were detected in various cancer cells (POETSCH et al., 2000; SU et al., 2000). However, structural informations of TTC4 are not available.

Sba1

Sba1 is known to stabilize the closed conformation of Hsp90 (Figure 1-10, b) (SULLIVAN et al., 2002; RICHTER et al., 2004; MCLAUGHLIN et al., 2006, ALI et al., 2006). This protein is able to partially inhibit the ATPase activity of Hsp90 (RICHTER et al., 2004; MCLAUGHLIN et al., 2006). It was also found in steroide hormone receptor complexes with Hsp90 (JOHNSON et al., 1994). For Sba1, it was also shown that it serves as component of the Hsp70/Hsp90 chaperone system and stabilizes the client protein (MORISHIMA et al., 2003). Additionally, Sba1 is maybe directly involved in client binding as it also show chaperone activity (BOSE et al., 1996; FREEMAN et al., 1996, WEAVER et al., 2000). However, the functional interactome of Sba1 revealed also functionality independently of Hsp90 (ECHTENKAMP et al., 2011).

The activator of the Hsp90 ATPase, Aha1

Aha1 is the most potent co-chaperone which is able to accelerate the ATP turnover of Hsp90 (PANARETOU et al., 2002; MEYER et al., 2004). Aha1 prefers binding to specific nucleotide-bound states of Hsp90 which lead to changes in the equilibrium of the conformational states of Hsp90 (HESSLING et al., 2009). Aha1 and its homologue Hch1 are not essential in yeast. However, specific Hsp90 clients are affected upon deletion of Aha1 and Hch1 (LOTZ et al., 2003). Additionally, Aha1 display a critical role in the misfolding disease cystic fibrosis (WANG et al., 2008). The cystic fibrosis transmembrane regulator (CFTR) is a multi-membrane spanning protein critical for regulation the balance of chloride ions in secretory organs (RIORDAN 2005 and 2008). Loss of function of the CFTR is responsible for cystic fibrosis. The most common disease-associated allele of CFTR is

deletion of Phe 508. Stability and export of both wild-type and the ΔF508 CFTR are sensitive to expression levels of Aha1 (WANG et al., 2006).

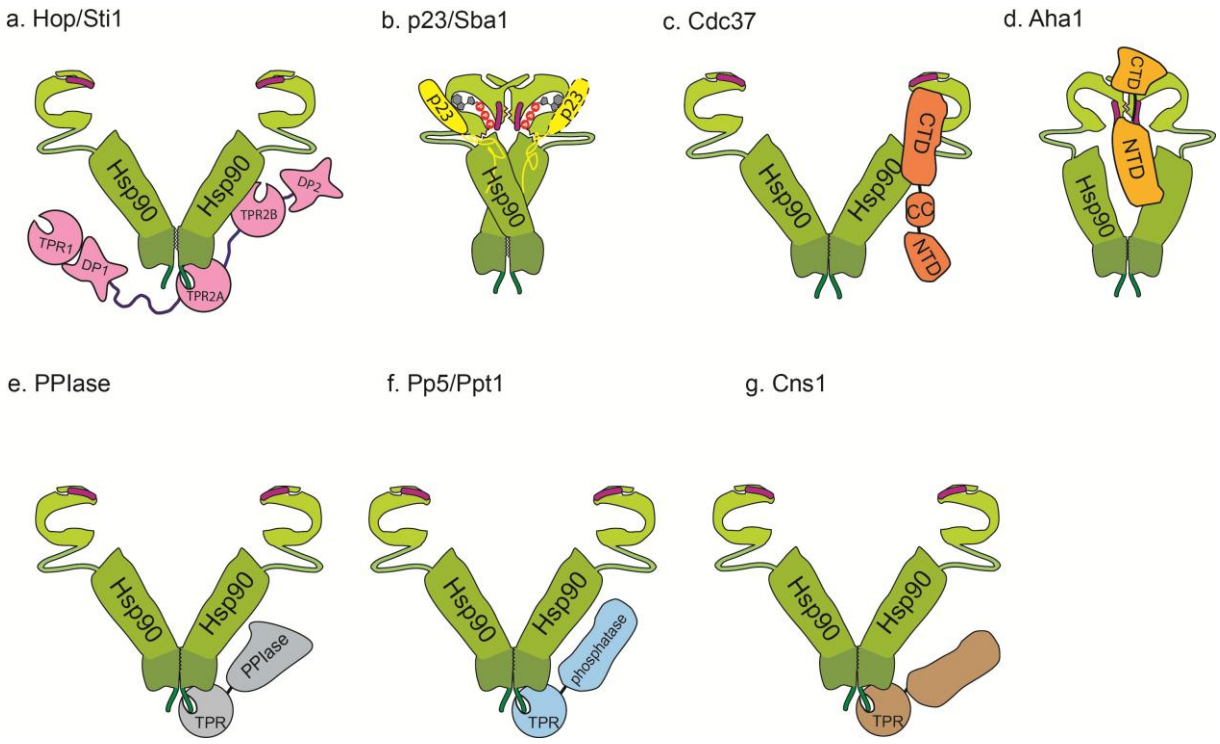

Figure 1-10: Interaction of Hsp90 with co-chaperones.
Various co-chaperones are able to bind to Hsp90. The different binding mechanisms of the co-chaperones are represented as cartoons.

1.3.4. Chaperone cycle of Hsp90

During the Hsp90 chaperone cycle different conformational states are present (HESSLING et al., 2009). Maturation of several clients of Hsp90 is performed in cooperation with the Hsp70 chaperone cycle. Sti1 serves as adaptor protein which connects both chaperone cycles (JOHNSON et al., 1998; WEGELE et al., 2006; SCHMID et al., 2012). The minimal system for reconstitution of complexes of Hsp90 and steroid hormone receptor consists of Hsp90, Hsp70, Hsp40 and Sba1/p23 (DITTMAR et al., 1998, KOSANO et al., 1998, CINTRON et al., 2008). Various co-chaperones are able to bind to Hsp90. However, they act at different stages in the Hsp90 cycle. Based on maturation of steroid hormone receptors several Hsp90-co-chaperone complexes were identified (SMITH et al., 1992; SMITH, 1993, JOHNSON et al., 1994, PRATT AND TOFT, 1997). The intermediate complex involves Sti1 (SMITH, 1993).

Sti1 is able to bind simultaneously Hsp70 and Hsp90, connecting the both chaperone cycles (JOHNSON et al., 1998; WEGELE et al., 2006; SCHMID et al., 2012). It was shown that co-chaperones can bind simultaneously to Hsp90 which is important for progression of the chaperone cycle (LI et al., 2011). Sba1 and the PPIases are also involved in the Hsp90 chaperone cycle but act at later stages (JOHNSON et al., 1995; FREEMAN et al., 2000; MCLAUGHLIN et al., 2006; LI et al., 2011). Analysis of competitive and simultaneous binding of co-chaperones leads to a model of the Hsp90 chaperone cycle (Figure 1-11) (LI et al., 2012).

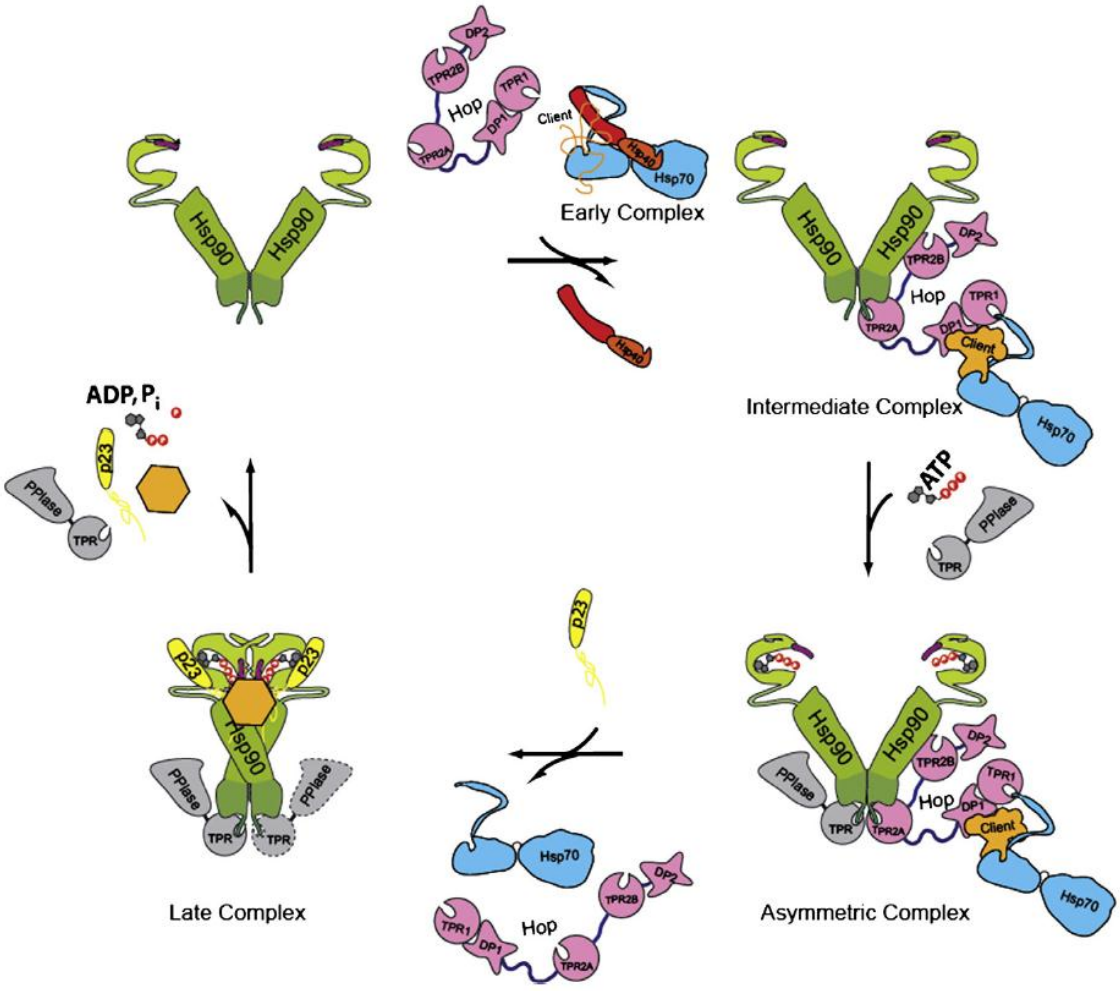

Figure 1-11: Chaperone cycle of Hsp90.
Proposed model of the chaperone cycle of Hsp90 is shown (Figure adopted from LI et al., 2012). Sti1 serves as adaptor protein and is responsible for the substrate transfer to the Hsp90 system. As Sti1 stabilize the open conformation of Hsp90. However, the other binding site for TPR-containing chaperones is free for interaction with other co-chaperones. That leads to formation of asymmetric Hsp90 complexes. Sba1 stabilize the closed state of Hsp90 and the late complex is formed. After ATP hydrolysis, co-chaperones and the potential client is released.

2. Objective

During this work, on two projects dealing with the regulation of the Hsp90/Hsp70 chaperone cycle were focused.

First, regulation of the ATPase activity of Hsp90 by its co-chaperone Aha1 was analyzed to get a more detailed view of the stimulatory effect on the Hsp90 ATPase activity. This project was initialized by Marco Retzlaff, who was responsible for first insights in the recognition of both domains of Aha1 within the Hsp90 dimer and NMR analysis. This work includes besides cloning and purification, mainly kinetic analysis and biophysical methods for protein-protein associations. Different Hsp90 mutants were cloned and purified in order to get a more detailed view on the specific regulation of the ATP turnover within the Hsp90 dimer. During this heterodimers should be investigated in order to determine the mechanism of the stimulation of Hsp90 ATPase activity by Aha1. Additionally, this includes discrimination between specific activation mechanisms. With methods for identification of protein-protein associations, the specific binding mechanism of Aha1 to the Hsp90 dimer should be developed.

The second main project includes co-chaperone interactions within the Hsp70 and Hsp90 chaperone cycle. Cns1 is a co-chaperone which is able to bind to either Hsp70 or Hsp90. The aim of the work was to get more detailed view of Cns1 function within the Hsp90 and the Hsp70 chaperone cycle. As structural data from the C-terminal domain are available, different constructs were used for crystallization of the TPR-domain. Additionally, the function of Cns1 in context of the Hsp90 and Hs70 cycle should be analyzed. With methods for identification of protein-protein associations, specific co-chaperone organization and recruitment of Hsp90 and Hsp70 should be developed. Here, either competitive or simultaneous binding to Hsp90 and Hsp70 should give more information about the mechanism of co-chaperone organization. This work includes mainly protein purification and biochemical methods to confirm specific binding to Hsp90 or Hs70. Besides the *in vitro* analysis, different methods were used to get more details of the *in vivo* function of Cns1 in yeast *S. cerevisiae*. This mainly includes the generation of a yeast strain where genomically encoded Cns1 is deleted. By use of this strain and the plasmid shuffling method, various fragments of Cns1 should be analyzed for functionality.

3. Material and Methods

3.1. Materials

3.1.1. Chemicals

β-Mercaptoethanol	Sigma, St. Louis, USA
Acrylamid/Bis solution 38:2 (40% w:v)	Serva, Heidelberg, Germany
Adenosin-5'-diphosphate (ADP) disodium salt	Roche, Mannheim, Germany
Adenosin-5'-triphosphate (ATP) disodium salt	Roche, Mannheim, Germany
Adenylyl Imidodiphosphat (AMP-PNP)	Roche, Mannheim, Germany
Agar Agar	Serva, Heidelberg, Germany
Agarose	Serva, Heidelberg, Germany
Ammonium persulfate (APS)	Roth, Karlsruhe, Germany
Ampicilin sodium salt	Roth, Karlsruhe, Germany
Bacto-pepton	BD Biosciences, Franklin Lakes, USA
Bacto-trypton	BD Biosciences, Franklin Lakes, USA
Coomassie Brilliant Blue R-250	Serva, Heidelberg, Germany
Desoxynucleotide triphosphates (dNTPs)	Roche, Mannheim, Germany
Dimethyl sulfoxide (DMSO)	Sigma, St. Louis, USA
Dithiothreitol (DTT)	Roth, Karlsruhe, Germany
Ethidium bromide	Sigma, St. Louis, USA
Ethylenediaminetetraactetic acid (EDTA)	Merck, Darmstadt, Germany
Galactose	Merck, Darmstadt, Germany

Glucose	Merck, Darmstadt, Germany
Glycerol	Roth, Karlsruhe, Germany
Imidazole	Sigma, St. Louis, USA
Isopropyl β-D-1-thiogalaktopyranoside (IPTG)	Serva, Heidelberg, Germany
Kanamycin sulfate	Roth, Karlsruhe, Germany
LB medium	Serva, Heidelberg, Germany
Milk powder	Roth, Karlsruhe, Germany
N-(2-Hydroxyethyl)-piperazine-N´-2-ethanesulfonic acid (HEPES)	Roth, Karlsruhe, Germany
Nicotine amide dinucleotide (NADH)	Roche, Mannheim, Germany
Phosphoenolpyruvate (PEP)	Sigma, St. Louis, USA
Protease inhibitor Mix FY, G, HP, M	Serva, Heidelberg, Germany
Sodium dodecylsulfate (SDS)	Serva, Heidelberg, Germany
Stain G	Sigma, St. Louis, USA
Tris-(hydroxymethyl)-aminomethane (TRIS)	Roth, Karlsruhe, Germany
Tween-20	Merck, Darmstadt, Germany
Yeast Nitrogen Base	Serva, Heidelberg, Germany

3.1.1. Enzymes, standards and kits

1 kb DNA ladder	Peqlab, Erlangen, Germany
Wizard Miniprep kit	Promega, Madison, USA
Wizard PCR product purification and gel extraction kit	Promega, Madison, USA
T4 ligase	Promega, Madison, USA
Pfu DNA polymerase	Promega, Madison, USA
High Fidelity DNA polymerase	Promega, Madison, USA

GoTaq DNA polymerase	Promega, Madison, USA
Restriction enzymes	NEB, Ipswich, USA
Low-Range-molecular weight marker (LMW for SDS-PAGE)	BioRAd, München, Germany
Roti-Mark Prestained	Roth, Karsruhe, Germany
Alkaline phosphatase	Roche, Mannheim, Germany

3.1.2. Proteins and antibodies

Polyclonal serum against Cns1 (rabbit)	Dr. J. Pineda Antikörper Service, Berlin, Germany
Monoclonal IgG-Peroxidase conjugate against rabbit IgG (sheep)	Peqlab, Madison, USA
Monoclonal IgG-Peroxidase conjugate against mouse IgG (sheep)	Promega, Madison, USA
Monoclonal IgG-Peroxidase conjugate against His-tag (mouse)	Promega, Madison, USA
Pyruvate kinase (PK)	Promega, Madison, USA
Lactate dehydrogenase (LDH)	Promega, Madison, USA
Thrombin	Roche, Mannheim, Germany
Immobilized thrombin	Sigma, St. Louis, USA

3.1.3. Chromatography materials and columns

Resource-Q; Source 15 (6 mL)	GE Healthcare, Freiburg, Germany
Superdex 200 Prep Grade	GE Healthcare, Freiburg, Germany

Superdex 75 Prep Grade	GE Healthcare, Freiburg, Germany
HiPrep 26/10 Desalting column	GE Healthcare, Freiburg, Germany
HisTrap FF	GE Healthcare, Freiburg, Germany
Q Sepharose Fast Flow	GE Healthcare, Freiburg, Germany
SP Sepharose Fast Flow	GE Healthcare, Freiburg, Germany
Hydroxy apatite column	Biorad, München, Germany

3.1.4. Consumables

Amicon Ultra-15 Centrifugal Filter Units	Millipore, Bedford, USA
Amicon Ultra-4 Centrifugal Filter Units	Millipore, Bedford, USA
Blotting paper	Whatman, Maidstone, USA
Cuvettes, plastic, half-micro	Zefa, München, Germany
Dialysis membranes Spectra/Por 6000–8000 Da (various MWCOs)	Spectrum Laboratories, Houston, USA
Immobilon-P membrane (PVDF)	Roth, Karlsruhe, Germany
PE tubes (50/15 ml)	Greiner & Söhne, Nürtingen, Germany
Immobilion-P (PVDF) membrane	Millipore, Bedford, USA
Petri dishes, PS, 94 mm	Greiner & Söhne, Nürtingen, Germany
pH-indicator strips	Merck, Darmstadt, Germany
Reaction tubes, various volumes	Sarstedt, Nümbrecht, Germany
Silica glass Suprasil cuvettes	Hellma, Jena, Germany
X-ray film X-OMAT AR	Kodak, Rochester, USA

3.1.5. Equipement

Centrifuges:

Avanti J 25 with JA-10 and JA-25.50 rotors	Beckmann, Wien, Austria
Beckmann XL-I analytical ultracentrifugation	Beckmann, Wien, Austria
Eppendorf table-top centrifuge 5415 C	Eppendorf, Hamburg, Germany
Rotina 46 R coolable centrifuge	Hettich, Tuttlingen, Germany
Chromatographic machines:	
FPLC machine	Amersham, Uppsala, Sweeden
Äkta-system	Amersham, Uppsala, Sweeden
Super loop, 150 ml	Amersham, Uppsala, Sweden
Gelelectrophoresis and blotting:	
Fast Blot B44 apparatus	Biometra, Göttingen, Germany
Hoefer Mighty Small II gelelectrophoresis unit	Amersham, Uppsala, Sweden
RHU10X	Roth, Karlsruhe, Germany
Calorimeter:	
VP-ITC MicroCalorimeter	MicroCal Inc., Northampton, USA
VP-ITC200 MicroCalorimter	MicroCal Inc., Northampton, USA
Spectrophotometer:	
Biotech Ultrospec 3000	Amersham, Uppsala, Sweden
UV-VIS-spectrophotometer	
Cary 50 UV-VIS-spectrophotometer	Varian, Palo Alto, USA
Cary 100 UV-VIS-spectrophotometer	Varian, Palo Alto, USA
FluoroMax-3 with thermostable cuvette holder	Spex, Edison, USA
J-715 spectropolarimeter with PTC 343	Jasco, Groß-Umstadt, Germany
peltier tempering unit	

Further equipment:

Air circulation incubator	New Brunswick Scientific, Nürtlingen, Germany
Cell disruption machine Basic Z	Constant Systems, Warwick, England
Culture shaker Certomat S	Braun Biotech, Melsungen, Germany
Eppendorf Thermomixer	Eppendorf, Hamburg, Germany
Magnetic stirrer Heidolph MR 2000	Heidolph, Kelheim, Germany
Metal Thermo Block TB 1	Biometra, Göttingen, Germany
pH-meter	WTW, Weilheim, Germany
Thermocycler Primus	MWG, Ebersberg, Germany
Test tube roller	Heidolph, Kelheim, Germany
Varioklav steam	H+P, Oberschleißheim, Germany

3.1.6. Computer software

Adobe Photoshop CS 2	Adobe Inc., San Jose, USA
Adobe Reader	Adobe Inc., San Jose, USA
Multialin	http://multalin.toulouse.inra.fr/multalin/
Espript	http://espript.ibcp.fr/ESPript/ESPript/
Microsoft Office 2007	Microsoft, Unterschleißheim, Germany
Origin 8.0	OriginLab Corp., Northampton, USA
ProtParamTool	ExPasy (www.expasy.ch)
Endnote	Endnote X5
PyMOL	PyMOL 1.5 (www.pymol.org)
DCDT+	J. S. PHILO; Anal Biochem (2011)

3.2. Organisms and cultivation

3.2.1. Strains

Following bacterial strains were used in this work.

Strain	Genotype	Origin/Company
E. coli DH10B	F$^-$araD 139Δ(*ara leu*) 7697 DlacX74 galU galK mcrA Δ(*mrr hsd*RMS- *mcr*BC) *rps*L *dec*R 380 ΔlacZ ΔM15 *end*A1 *nup*G *rec*A1	Berthesda Research Laboratories, Berhesda, USA
E. coli Mach1	F$^-$ ϕ80(lacZ)ΔM15 Δ*lac*X74 *hsd*R(r_K^- m_K^+) Δ*rec*A1398 *end*A1 *ton*A	Invitrogen, Groningen, Netherlands
E. coli BL21 (DE3) CodonPlus	F$^-$ *omp*T *hsd*S_B (r_B^- m_B^-) gal *end*A argU ileY leuW Cam^R	Stratgene, La Jolla, USA
E. coli BL21 (DE3) Star	F$^-$ *omp*T *hsd*S_B (r_B^- m_B^-) *gal dcm me 131* (DE3)	Invitrogen, Groningen, Netherlands
E. coli HB101 pUBS	supE44, Δ(*mcr*C-*mrr*) *rec*A13, *ara*-14 *pro*A2 *lac*Y1 *gal*K2, *rps*L20 *xyl*-5 *mtl*-1 *leu*B6 *thi*-1; pUBS: Kan^R, lacI^q	Promega, Mannheim, Germany

E. coli DH10B and *E. coli* Mach1 were used for cloning and amplification of plasmids. For gene expression controlled by either the T7 or the T5 promotor, *E. coli* BL21 CodonPlus, *E. coli* BL21 Star and *E. coli* HB101 were used.

Following *S. cerevisiae* and *P. pastoris* strains were used in this work.

Strain	Genotype	Origin/Company
Y00000 (*wild type*)	BY4741; MATa, his∆1; Leu2∆0; met15∆0; ura3∆0	Euroscarf, Frankfurt, Germany
Cns1 (YBR155w), *knockout*, diploid	BY4741; MATa/α, his∆1/ his∆1; leu2∆0/leu2∆0; lys2∆0/LYS2; MET15/met15∆0; ura3∆0/ ura3∆0 YBR155w::kanMX4/ YBR155w	Euroscarf, Frankfurt, Germany
Y06830 (∆*cpr7*)	By4741; Mata, his∆1; Leu2∆0; met15∆0; ura3∆0 YJR032w::kanMX4	Euroscarf, Frankfurt, Germany
MC100-3; His_6-Ssa1	arg4 his4 aox∆1::SARG4 aox∆2::Phis4	A. Schmid

3.2.2. Media

Following Media and antibiotics were used for growth of *E. coli*:

LB_0: 20 g/l LB-powder

(12 g/l Bacto Agar for plates)

Antibiotic concentrations (used for growth of E. coli):

Ampicillin: 100 µg/ml

Kanamycin: 50 µg/ml

For growth of yeast strains the following media were used:

YPD:	Yeast Extract	5 g/l
	BactoPepton	10 g/l
	glucose	20 g/l
	(14 g/l Bacto Agar for plates)	
CSM:	YNB	6.7 g/l
	selective amino acid mix	1 g/l
	glucose	20 g/l
FOA-plates:	YNB	1.7 g/l
	selective amino acid mix	1 g/l
	ammonium sulphate	5 g/l
	glucose	20 g/l
	5´-FOA	1 g/l
	Bacto Agar	12 g/l
Selective amino acid-mix:	composition of amino acids were done as described in “Methods in Yeast Genetics: A Cold Spring Harbor Laboratory Course Manual, 2005 Edition	
Pre-Sporulation solution:	YNB	6.7 g/l
	selective amino acid mix	1 g/l
	glucose	0.25%
	KOAc	2 %
	(12 g/l Bacto agar for plates	
Sporulation Solution:	KOAc	2 %

3.2.3. Growth and storage of *E. coli*

Cultures of *E. coli* on agar plates were incubated for around 16 hours at 37°C. Liquid cultures of *E. coli* in LB-media were grown at 37°C and for selection of the respective plasmid the corresponding antibiotic was added. Growth of *E. coli* was monitored by measuring absorption at a wavelength of 600 nm. An optical density at 600 nm (OD_{600}) of one equates to around 8x108 cells.

For long term storage of *E. coli* strains, glycerol stocks were made. Therefor 1 ml of an exponentially growing culture was mixed with 500 µl of 60% sterile glycerol, shock-frozen in liquid nitrogen and stored at -80°C.

3.2.4. Growth and storage of *S. cerevisiae*

Cultures of *S. cerevisiae* or *P. pastoris* on YPD or CSM plates were incubated for 2-3 days at 30°C. Growth of liquid cultures of in LB-media was also performedat 30°C for 2-3 days. Growth of cells was monitored photometrically at a wavelength of 600 nm. An OD_{600} of one equates to around $2x10^7$ cells.

For short-time storage, yeast cells were kept on plates or in liquid media at 4°C. Glycerol stocks were used for long-term storage. Therefor 1 ml of an exponentially growing culture was mixed with 500 µl of 60% sterile glycerol and stored at -80°C.

3.2.5. Sporulation of *S. cerevisiae*

Sporulation of yeast cells is observable in response to nitrogen starvation and the presence of a poor carbon source. Under these conditions, diploid yeast cells undergo meiosis and pack the produced haploid nuclei into spores.

To obtain sporulation, the diploid yeast strain was plated on Pre-Sporulation plates and incubated for 2 days at 30°C. Afterwards, one colony was transferred to Pre-Sporulation media and further incubated at 30°C for additional 2 days. Then 500 µl of the culture were centrifuged and washed twice with sterile water. After washing steps, the cell pellet was resuspended in 1 ml sporulation media for 2 -3 days. Formation of tetrads was monitored microscopically.

3.3. Methods of molecular biology

3.3.1. Plasmids

Plasmid	Insert/restriction site	Origin
pQE30-Cns1	Cns1; BamHI/SalI	O. Hainzl
pQE30-Cns1-218C	Cns1 (res. 218-385); BamHI/SalI	O. Hainzl
pQE30-Cns1-N204	Cns1 (res. 1-294); BamHI/SalI	O. Hainzl
pQE30-Cns1-TPR	Cns1 (res. 83-189); BamHI/SalI	O. Hainzl
pQE30-Cns1-NΔ60	Cns1 (res. 60-385) + thrombin cleavage site; BamHI/SalI	Created in this work
pET-SUMO-Cns1-TPR$^{70-204}$	Cns1 (res. 70-204); BamHI/XhoI	Created in this work
pET-SUMO-Cns1-TPR$^{60-204}$	Cns1 (res. 60-204); BamHI/XhoI	Created in this work
pET28-TTC4	TTC4, NheI/XhoI	Created in this work
pQE-Cns1-218C_M231C	Cns1 (res. 218-385) M231C; BamHI/SalI	Created in this work
pQE-Cns1-218C_T237C	Cns1 (res. 218-385) T237C; BamHI/SalI	Created in this work
pQE-Cns1-218C_D246C	Cns1 (res. 218-385) D246C; BamHI/SalI	Created in this work
pQE-Cns1-218C_D278C	Cns1 (res. 218-385) D278C; BamHI/SalI	Created in this work
pQE-Cns1-218C_E280C	Cns1 (res. 218-385) E280C; BamHI/SalI	Created in this work
pQE-Cns1-218C_S286C	Cns1 (res. 218-385) S286C; BamHI/SalI	Created in this work

pQE-Cns1-218C_S367C	Cns1 (res. 218-385) S367C; BamHI/SalI	Created in this work
pQE-Cns1-218C_S372C	Cns1 (res. 218-385) S372C; BamHI/SalI	Created in this work
pET-SUMO-Sti1	Sti1, BamHI/XhoI	A. Schmid
pET-SUMO-Ydj1	Ydj1; BamHI/XhoI	GeneArt, Regensburg, Germany
pET28-Aha1	Aha1; NdeI/BamHI	K. Richter
pET28-Aha1-N	Aha1 (res. 1-156); NdeI/BamHI	M. Retzlaff
pET28-Aha1-C	Aha1 (res. 157-356); NdeI/BamHI	M. Retzlaff
pET28-yHsp90	Yeast Hsp90; NdeI/XhoI	K. Richter
pET28-yHsp90_D79N	Yeast Hsp90 D79N; NdeI/XhoI	M. Retzlaff
pET28-yHsp90_V391E	Yeast Hsp90 V391E; NdeI/XhoI	M. Retzlaff
pET28-yHsp90_V209A	Yeast Hsp90 V209; NdeI/XhoI	Created in this work
pET28-yHsp90_D79N/V391E	Yeast Hsp90 D79N/V391E; NdeI/XhoI	Created in this work
pET28-yHsp90_V209A/V391E	Yeast Hsp90 V209A/V391E; NdeI/XhoI	Created in this work
p426-GPD-Cns1	Cns1; BamHI/XhoI	O. Hainzl
p425-GPD-Cns1	Cns1; BamHI/XhoI	O. Hainzl
p425-GPD-Cns1-218C	Cns1 (res. 218-385); BamHI/XhoI	O. Hainzl
p425-GPD-Cns1-N204	Cns1 (res. 1-204); BamHI/XhoI	O. Hainzl
p425-GPD-Cns1-TPR	Cns1 (res. 60-204); BamHI/XhoI	O. Hainzl

p425-GPD-Cns1-TPR$^{80-204}$	Cns1 (res. 80-204); BamHI/XhoI	Created in this work
p425-GPD-Cns1-TPR$^{70-204}$	Cns1 (res. 70-204); BamHI/XhoI	Created in this work
p425-GPD-Cns1-TPR$^{70-196}$	Cns1 (res. 70-196); BamHI/XhoI	Created in this work
p425-GPD-Cns1-NΔ60	Cns1 (res. 60-204); BamHI/XhoI	Created in this work

3.3.2. Oligonucleotides

Following primers were used for amplification. Primers for Quick change mutagenesis were designed according to the standard protocol.

Primer	Sequence 5´-3´
Cns1-BamH1-Fwd	GATCGGATCCATGAGCTCCGTTAACGCAAATGGA
Cns1N60-BamHI-Fwd	GATCGGATCC GGTGGTGAAAACGTGGAGTTAGAAGCTTT
Cns1N70-BamHI-Fwd	GATCGGATCCAAGGCATTAGCTTATGAAGGCGAACCACACG
Cns1C204-XhoI-Bwd	GATCCTCGAGTTATTGTTCTTTTCTATCAATCACTGATAACATATTC
Cns1C196-XhoI-Bwd	GATCCTCGAGTTACATATTCAAAATTGATTTGTTCTCTGGGTC
Cns1N60-p425-Fwd	GATCGGATCCATGGGTGGTGAAAACGTGGAGTT
Cns1N70-p425-Fwd	GATCGGATCCATGAAGGCATTAGCTTATGAAGGCG
Cns1N80-p425-Fwd	GATCGGATCCATGGAAATCGCTGAAAATTTCAAG
Cns1-XhoI-Bwd	GATCCTCGAGTCACACAGATCTTCTTTCTAAGGC
Cns1-SalI-Bwd	GATC GTCGAC TCACACAGATCTTCTTTCTAAGGCTTTTTGC
TPR-TEV-BamH1-Fwd	GATC GGATCC GAAAACCTCTACTTCCAAGGTGGTGGTGAAAACGTGGAGTT
TPR-THR-BamH1-Fwd	GATCGGATCCCTGGTGCCGCGCGGCTCGGGTGGTGAAAACG
Cns1-UPstream45	CTAGCAAGTAAAAGAAAAGAATAAATTGGTTTTGCATCTAGAATG

Cns1-DNstream45	TATCTACAACTTTGCGTTACATATTTTTAACTATTTGACACTTCA
CNS1-UPTAG	GGTTTTGCATCTAGAATGGATGTCCACGAGGTCTCTAATGGCGTCGCACGTCCTATCGTACGCTGCAGGTCGAC
Cns1-DNTAG	TAACTATTTGACACTTCACGGTGTCGGTCTCGTAGAATCGCGTGGCAGCCTTTCTATCGATGAATTCGAGCTCG
Cns1-Confirm A	GTTTAGGCACCTTGTACAGTTTCAC
Cns1-Confirm B	GTCATTGCGCTCTCTAACATAATTT
TTC4-NheI-Fwd	GATCCATATGGAACAACCTGGGCAGGATC
TTC4-XhoI-Bwd	GATCCTCGAGTCATCGTATCTGGTACACCT

3.3.3. Molecularbiological solutions

TEA(50x): 2 M Tris/Acetate, pH 8.0

50 mM EDTA

Gel Loading buffer (10x): 50 % (v/v) glycerin

10 mM EDTA (pH 8.0)

0.2 % (w/v) Bromphenole Blue

Agarose solution: 1% Agarose in TEA(1x)

Stain G

dNTP-Mix: 10 mMdATP

10 mMdGTP

10 mMdCTP

10 mMdTTP

ColonyPCR-Mix (20 µl): 4 µl 5xGoTaq-buffer

0.5 µl dNTP-Mix

0.2 µl each Primer

0.1 µl GoTaq-Polymerase

Solution A:	1.3 % (v/v) 3M NaAc, pH 5.5
	10 % (v/v) 1 M CaCl2
	2.5 % (v/v) 2.8% MnCl2
Solution A-Glycerin:	17.25 % (v/v) Glyzerin (97%) in Solution A
PLATE-Solution:	40% PEG
	10 mM TRIS (pH 7.5)
	1 mM EDTA
	0.1 M LiAc

3.3.4. Isolation of *E.coli* plasmid DNA

Plasmid DNA from *E.coli* was isolated from 4 ml overnight cultures. The preparation was done with the WIZARD Plus SV mini-Prep kit according to the standard protocol (PROMEGA, USA).

3.3.5. Agarose gel electrophoresis

Separation of DNA was performed in 1 % (w/V) agarose gels containing 0.0 µg/ml Stain G. Electrophoresis was carried out in 1x TAE buffer with a constant voltage of 120 V. Afterwards, UV irradiation was used to detect the separated DNA.

3.3.6. Isolation of DNA from agarose gels

DNA isolation was performed with the PCR product purification kit. Therefore the separated DNA was excised from the agarose gels and purified according standard protocol. DNA was stored at –20°C.

3.3.7. Transformation of *E. coli*

For transformation of *E. coli*, the respective strain were made chemically competent. Therefore 2 ml of sterile $MgCl_2$ was added to 100 ml of exponentially growing culture of *E. coli* (OD_{600} = 0.6 – 0.8) for 10 min at 37°C. Afterwards the culture was cooled on ice for one hour and centrifuged with 4500 g at 4°C for 5 minutes. Sedimented cells were resuspended in 20 ml Solution A and incubated for one hour on ice. Then the cells were pelleted by centrifugation at 4°C for 5 minutes and resuspended in 2 ml of Solution A-Glycerol. 100 µl aliquots were either directly transformed with plasmid DNA or frozen in liquid nitrogen and stored at -80°C.

For transformation 100 µl competent cells were mixed with 50-200 ngplasmid DNA and incubated on ice for 15-30 minutes. The cells were heat-shocked at 42°C for 1 minute and then cooled on ice for 5 minutes. After addition of 1 ml LB0-Media cells were incubated at 37°C for 1 hour. Then the cells were plated on the respective selection plates.

3.3.8. Transformation of *S. cerevisiae*

For transformation of *S. cerevisiae* yeast cells, 200 µl of an overnight culture were centrifuged and the supernatant was discarded. After addition of 100-200 ng plasmid DNA and 1 µl of single stranded carrier DNA (salmon testis single-stranded DNA) cells were resuspended in 150 µl PLATE-Solution. The cells were then incubated at room temperature for 24 hours. The mixture was heat-shocked at 42°C for 1 hour and afterwards plated on the respective selection plates.

3.3.9. PCR Amplification

PCR was used to amplify fragments from coding regions of plasmids or genomic DNA. All PCR reactions were performed with either the High Fidelity Polymerase or the *Pfu*-Polymerase. Primers were designed to have a melting temperature of around 60°C. Following mixture were used to perform the PCR reaction:

template DNA:	50-100 ng
Primer (100 pmol/µl):	1 µl each
10x reaction buffer:	10 µl
dNTPs:	2 µl
HiFi-Polymerase:	1 µl
H_2O:	ad 100 µl

According to the length of the amplified PCR product temperature and synthesis time were adjusted. For desired PCR products over 3 kb synthesis the temperature was set to 68°C otherwise synthesis temperature was 72°C. The following settings for DNA amplification were chosen.

Denaturation	95°C for 45 s
Annealing	50-55°C for 45 s
Synthesis	68°C or 72°C for about 1 min per 1 kb of PCR product
Cycles	30

For colony PCR with *E. coli* one colony was resuspended in the GoTaq-Mastermix. PCR Reaction was performed as described above.

For *S. cerevisiae* one colony was resuspended in 9 µl steril water. Then 1 µl Lyticase was added and the mixture was incubated for 20 minutes at 30°C. After Addition of the GoTaq-Mastermix PCR reaction was started with the set up described above.

PCR was also used for Quick-Change Mutagenesis. Primers were designed as described by manufacturer´s protocol. PCR reactions were performed with the Pfu-polymerase. Following mixture were used to perform the PCR reaction:

template DNA:	50-100 ng
Primer (100 pmol/µl):	1 µl each
10x reaction buffer:	2 µl
dNTP-mix:	2 µl
Pfu-Polymerase:	1 µl
H_2O:	ad 20 µl

3.3.10. DNA digestion

For analytical and preparative purposes, digestion of DNA with restriction enzymes was performed. Analytical DNA digestion was done in 10 µl sample volume. Therefore 5 µl plasmid DNA, 1 µl restriction buffer, 1 µl each restriction enzyme and water were mixed resulting in a final reaction volume of 10 µl. The mixture was incubated at 37°C for 30 minutes and analyzed by agarose gel electrophoresis. Preparative DNA digestion was performed in 100 µl reaction volume. Therefore 3-5 µg of plasmid DNA were incubated with 10 µl of 10x reaction buffer and 1 µl of each restriction enzyme at 37°C for 3-4 hours. DNA restriction was analyzed by agarose gel electrophoresis and, if needed for further cloning, DNA fragments were excised from the gel and purified with the WIZARD PCR Purification Kit.

3.3.11. Dephosphorylation of DNA ends

To prevent relegation, vectors were treated with rapid alkaline phosphatase after digestion with the restriction enzymes. For dephosphorylation of the DNA ends, 2 µl of rapid alkaline phosphatise (0.5 U/µl), 10 µl 10x reaction buffer and 88 µl cut vector were mixed and incubated at 37°C for 2 hours. Afterwards DNA was purified with the WIZARD PCR Purification Kit.

3.3.12. Ligation of DNA

For ligation of DNA, 100 ng of cut vector were mixed with 3-fold molar excess of the insert. The respective volumina of vector-insert were mixed and sterile water was added to a final volume of 9 µl. Afterwards, 10 µl 2x Quick Ligation buffer and 1 µl of T4 DNA Ligase was added. The mixture was incubated for 30-40 minutes at room temperature. The mixture was then used for transformation in competent *E. coli* cells.

3.4. Preparative methods

3.4.1. Gene expression in *E. coli*

Large scale productions of proteins were done in 3x 2 l LB_0 media with the respective antibiotic. Different expression strains were used depending on the respective type of promoter. Gene expression under the control of the T7 promotor was performed in *E. coli* BL21CodonPlus. The *E. coli* strain HB101 (pUBS) was used for gene expression under control of the T5 promotor. Basically 2 liter of LB_0 media were inoculated with 50 ml of an overnight culture. The flasks were shaked at 37°C until an OD_{600} of 0.6 - 0.8 was reached. Afterwards cells were cooled on ice for 10 minutes and gene expression was induced by addition of 1 mM IPTG. Cells were incubated under shaking at 25°C over night. Cells were harvested by centrifugation with 6500 g for 15 minutes.

3.4.2. Gene expression in *Pichia pastoris*

For large scale production of Ssa1 gene expression in *Pichia pastoris* was used. Three 100 ml flasks were inoculated with *P. pastoris* strain containing His-tagged Ssa1. After stationary phase was reached, 2 liter of YNB/Sorbitol-media was inoculated and incubated for 24 hours at 30°C. Gene expression was then induced by addition of Methanol (0.5% v/v). For better aeration cover of the flasks were removed. After incubation for 24 hours at 30°C Methanol was added again and additionaly incubated for 24 hours. Additional induction is necessary because on one hand Methanol is used by *P. pastoris* as carbon source, on the

other hand methanol evaporates in course of time. After two times of induction cells were harvested by centrifugation (4500 g, 4°C, 15 min)

3.4.3. Cell disruption

For lysis of the harvested cells (*E. coli or P. pastoris*) a cell disrupter was used. The pelleted cells were resuspended in lysis buffer (5 ml/g of cells), wich was usually Buffer A of the first chromatography step. DNAse I and protease inhibitor mix HP (Serva) was added before lysis of the cells. Lysis of the cells was performed in a Basic Z model cell disruption system at a pressure of 1.8 kbar (*E. coli*) or 2.4 kbar (*P. pastoris*). The lysate was cleared from remaining cells and cell debris by centrifugation at 4°C and 40000 g for 30 min.

3.4.4. Tetrad dissection

In order to dissect the tetrads the remaining ascus was digested by treatment with Lyticase. Therefore 500 µl of the sporulated culture were centrifuged and washed twice with sterile water to get rid of the sporulation media. Than 10 µl of sterile Lyticase were added and incubated at 30°C for 30 min. After that digestion step the cells were plated on thin URA^--plates. With the micromanipulator the tetrads were dissected and the single spores were spotted on the plate. After colonies were grown on URA^-plates, spores were respotted on G418-plates. In order to check the mating type and the respective ORF, colony PCRs were performed.

3.5. Methods for protein purification

Following chromatographic methods were used for protein purification in this work. Success of purification was determined by SDS-PAGE.

3.5.1. Immobilzed Metal Ion Affinity Chromtography

This method is based on specific and reversible interaction of a molecule to a matrix-bound partner. In the affinity chromatography used in this work, Ni-ions are complexed to immobilized nitrile triacetic acid anchor (NTA). The matrix comlexed Ni-ions interact with the His_6-tag fused to the protein with high specificity and selectivity. The elution of the bound protein is either achieved by displacement with a competitive binding partner or by pH induced conformational changes. Increasing the concentration of imidazole in the running buffer leads to competitive displacement of the His6-tagged proteins from the matrix. For affinity chromatography HisTrap FF column was used.

3.5.2. Ion Exchange Chromatography

The principle of the ion exchange chromatography is the competitive interaction of charged ions. A particle competes with ions for binding to the charged surface of the matrix. Proteins have either a positive or negative charge depending on their amino acid sequence. The overall charge of proteins is determined by its specific isoelectric point (pI) and depends on the pH of the running buffer. Based on this characteristic, binding of a charged protein to a surface is enabled. The protein is displaced and eluted from the matrix by gradually increasing the salt concentration of the running buffer.

Purification of proteins with either cation or anion exchange was performed with the Resource S/Q columns (GE Healthcare, Freiburg, Germany).

3.5.3. Size Exclusion Chromatography

Gel filtration chromatography was used to separate proteins based on their specific hydrodynamic radius. The matrix of the columns is composed of a porous carrier matrix of defined pore size. To prevent unspecific interactions of proteins with the matrix running buffer with high ionic strength were used. Superdex75 Prep Grade or Superdex200 Prep Grade were used depending on the required range of separation.

3.5.4. Concentration of proteins

For concentration of protein solutions two methods were applied. Protein solutions with volumes up to 50 ml were concentrated using Millipore Ultra-15 concentrators. The principle of this method is to reduce the volume of a protein solution through a membrane of defined pore size (molecular weight cut off) by centrifugation. The proteins are concentrated above the membrane. Depending on the size of the protein 3 kDa, 10 kDa or 30 kDa molecular weight cut-offs were used. For larger volumes Amicon cells were used. With nitrogen gas (3 bar) and gentle stirring the protein solution is pressed through a filter of defined pore size.

3.5.5. Protein dialysis

Dialysis was used to change buffer compositions of the protein solution. In a bag of defined pore size the protein solution was dialyzed in a 100fold larger volume to the sample volume Dialysis was performed at 4°C over night.

3.5.6. Purification of His_6-tagged proteins from *E. coli*

Solutions:

Ni-NTA:	Buffer A:	50 mM K_2HPO_4/KH_2PO_4, pH 8.0
		300 mM KCl
		20 mM imidazole
	Buffer B:	50 mM K_2HPO_4/KH_2PO_4, pH 8.0
		300 mM KCl
		300 mM imidazole
IEC:	Buffer 1:	50 mM K_2HPO_4/KH_2PO_4

		50 mMKCl
	Buffer 2:	50 mM K_2HPO_4/KH_2PO_4
		1 M KCl
SEC:	Buffer.	40 mM HEPES, pH 7.5
		150 mM KCl
		5 mM $MgCl_2$

procedure:

3 x 2 liter of LB_0-Media with the respective antibiotic were inoculated with 50 ml of overnight culture. After incubation at 37°C and OD_{600} of 0.6 - 0.8 was reached cells were cooled on ice for 10 minutes. Afterwards, gene expression was induced by addition of 1 mM IPTG and cells were incubated at 25°C. Cells were harvested by centrifugation and resuspended in Buffer A containing DNAse I and Protease Inhibitor Mix HP (SERVA). After cell disruption and centrifugation, the cleared lysate was loaded on a HisTrap FF column (2.5 ml/min). The column was washed with 20x of the column size with Buffer A. To get rid of further unspecific bound proteins, 20x of the column size were washed with 5% Buffer B. Elution of the protein was performed by step gradient to 60% Buffer B. In case of cleavable His_6-tags, thrombin, TEV-protease or SUMO-protease were added and incubated at 4°C over night. Followed affinity chromatography was used to remove remaining undigested proteins and His-tagged proteases (TEV- and SUMO-protease). The flow through was collected, concentrated and loaded on gel filtration column equilibrated with SEC-running-buffer. Size exclusion chromatography was performed and purity of the protein was checked by SDS-PAGE. Whenever necessary, additional ion exchange chromatography was performed.

3.5.7. Purification of His_6-tagged Ssa1 from *P. pastoris*

As described by A. SCHMID (PhD Thesis, 2009) Ssa1 from *P. pastoris* was purified using following buffers:

NiNTA:	Buffer A:	40 mM HEPES, pH 7.5
		350 mM NaCl
		150 mM KCl
		20 mM $MgCl_2$
		5 % glycerine
		2 mM β-Mercaptoethanol
		1 mM ATP
		10 mM Imidazole
	Buffer B:	40 mM HEPES, pH 7.5
		350 mM NaCl
		150 mM KCl
		20 mM $MgCl_2$
		5 % glycerine
		2 mM β-Mercaptoethanol
		1 mM ATP
		300 mM Imidazole
SEC:	Buffer:	40 mM HEPES, pH 7.5
		150 mM KCl
		5 mM $MgCl_2$

procedure:

The cleared lysate was loaded on a HisTrap FF column (2.5 ml/min) and the column was washed with 20 times the column volume with Buffer A. After additional washing step with 20 times the column volume 7% Buffer B, the protein was eluted by step gradient to 100%

Buffer B. The protein was dialyzed against SEC buffer. Afterwards, size exclusion chromatography was performed. Fractions that contained pure Ssa1 protein were pooled, concentrated and frozen in liquid nitrogen. The protein was stored at -80°C.

3.6. Protein analytic

3.6.1. solutions

running buffer 10x:	0.25 M Tris
	2 M Glycine
	1 % (w/v) SDS
Leammli-buffer 5x:	10 % (w/v) SDS
	50 % (w/v) glycerine
	300 mMTris
	0.05 % (w/v) Bromphenole blue
	5 % (v/v) β-Mercaptoethanol
Transfer buffer:	192 mM glycine
	25 mM Tris
	20 % (v/v) Methanol
	0.3 % (w/v) SDS
PBS (-T):	115 mM NaCl
	4 mM K_2HPO_4
	16 mM NaH_2PO_4
	(0.1 % Tween-20)

Stripping buffer:	2 % SDS
	62.5 mM Tris
	100 mM β-Mercaptoethanol

3.6.2. SDS-polyacrylamide electrophoresis

To analyze protein extracts and cell lysates, discontinuous SDS-Polyacrylamide gelelectrophoresis (SDS-PAGE) was performed. Separation of proteins was done using vertical 7 x 9 x 0.075 cm SDS-PAGE gels at a constant current of 30 mA per gel. The samples were mixed with Laemmli laoding buffer and heated at 95°C for 5 minutes. As molecular weight standards either LMW marker or ROTI-Prestained marker was used.

3.6.3. Coomassie staining of SDS-gels

Visualisation of the proteins after SDS-PAGE was performed using following solutions:

Fairbanks A Solution:	25% (v/v) Isopropanol, 10 % (v/v) acetic acid, 0.05 % Commassie Blue R
Fairbanks D Solution:	10 % (v/v) acetic acid

SDS-polyacrylamide gels were stained with Fairbanks Solution A and destaining was performed with Fairbanks D solution. To reduce incubation times, solutions were heated up. Staining was carried out for 20 minutes, destaining was done for up to 2 hours.

3.6.4. Western Blot

Immunoblotting was performed in a Semi-Dry blotting apparatus (Biometra, Germany). Seperated proteins by SDS-polyacrylamide gels were transferred electrophoretically on a PVDF membrane. In front of the blotting procedure, the methanol-activated PVDF membrane and Whatman 3MM filter papers were incubated in transfer buffer for 20 minutes. The SDS-polyacrylamide-gel was put on the PVDF membrane. Stacks of Whatman 3MM filter

papers were placed below and above these two components. The transfer was performed with constant current of 72 mA for 90 minutes.

After transfer reaction, the PVDF membrane was incubated with blocking solution (5 % milk powder in PBS-buffer pH 8.0) for 30 min in order to block unspecific binding sites. After addition of the diluted primary antibody (in 50 ml PBS (pH 8.0), 2 % milk powder), the membrane was incubated for 1 hour. After three washing steps with PBS-T buffer for 10 min, the secondary antibody (peroxidase coupled antibody) was added and the membrane was incubated for 1 hour. Then, additional three washing steps with PBS-T were performed. Detection of the antibody-enzyme was done by using the ECL detection Kit (Amersham, Uppsala, Sweden). Detection is based on the chemoluminescence reaction of the coupled peroxidase, which catalyzes the oxidation of cyclic Diacylhydrazineluminol in the presence of H_2O_2. This reaction leads to emission of light, which was detected on a X-Omat X-ray film (Kodak, USA) by incubation up to 10 minutes.

3.6.5. Analytical Ultracentrifugation

For detection of protein-protein-interaction analytical ultracentrifugation was used. For protein association studies, the protein with the lower molecular mass was labeled with a fluorescence dye. For that reason, only the protein itself and protein complexes formed with the labeled protein are detected by fluorescence optical system. AlexaFlour488 labeled proteins were incubated with different amounts of potential interaction partner in 300 µl reaction volume and excised in an ultracentrifugation cell using the XL1 rotor. The protein solutions were centrifuged at constant speed of 42000 rpm at 25°C. The Label is excited by a laser beam and the resulting fluorescence is detected. Calculation of the sedimentation velocities was done by using the programs SEDVIEW or DCDT+.

3.6.6. Chemical cross link of proteins

For chemical cross link the hetero-bifunctional, crosslinker 4-N maleimido benzophenone was used. This cross linking agents contains a sulfhydryl specific group and a photoreactive group. 4-N maleimido benzophenone was diluted in DMSO to a final concentration of 50 mM. Proteins were incubated with a 50fold molar excess of the crosslinking agent. Reaction was performed at room temperature for 2 hours. Reaction was quenched by addition of molar

excess of Tris (pH 8.0). Afterwards, proteins were dialyzed against buffer (40 mM Tris, pH 7.8, 100 mM KCl, 1 mM EDTA). Mass analysis was performed to proof coupling of 4-N maleimido benzophenone with the protein. Proteins were then incubated with yeast lysate for 30 min at room temperature. Afterwards, UV irradiation was used for activation of the photoreactive group and to achieve cross linking reaction via the diradical state. Various irradiation times were used. Analysis of cross link reaction was visualized by SDS-PAGE and Western blot.

3.6.7. Crystallisation of proteins

Screening for crystallisation conditions was done in the group of Prof..Dr. Michael Groll. (Chair of Biochemistry, TU München). Proteins (Cns1-TPR, NΔ60-Cns1) were mixed with dissolved peptides (10 mM in 100 mM Tris, pH 8.0) for crystallisation. The molar ratio of the protein-peptide-complex was chosen to 1:1.5. The protein concentrations varied from 10-45 mg/ml.

3.6.8. Labeling of proteins

For analytical ultracentrifugation, proteins were labeled with an Alexa488-fluorescence dye, which react with primary amines. The reaction was performed in 40 mM HEPES, pH 7.5; 20-50 mM KCl. Therefore, the proteins (5-7 mg/ml) were incubated with a 5fold molar excess of the Alexa488-fluorescence dye (10 mM in DMSO) for 2 hours on ice. Then, the reaction was quenched by addition of a molar excess of Tris (1M, pH 8.0). Afterwards, the labeled protein was dialyzed against 40 mM HEPES, 20-50 mM KCl at 8°C for 5-12 h. The resulting labelling efficiency was calculated according to manufacturer´s protocol.

3.7. Spectroscopical and calorimetrical methods

3.7.1. UV/VIS-spectroscopy

Absorbtion of electromagnetic radiation is achieved by transfer of the π-electrons to an excited, high-energy state. For protein analysis, wavelengths between 180 nm and 300 nm are used. Peptide bonds are mainly responsible for the absorption in the region of 180 nm to 240 nm. The aromatic residues trytophane, tyrosine and phenylalanine absorb in the region of 250 nm to 300 nm. Additionally, also disulfide bridges are responsible for absorption within these wavelengths. However, the largest contribution of absorption in this region is delivered by tryptophan and tyrosine. The molar extinction coefficients of the aromatic amino acids and their corresponding wavelength of maximum absorption are shown in the following table:

Amino acid	λ_{MAX} in nm	ε_{MAX} in M^{-1} cm^{-1}
Tryptophane	280	5600
Tyrosone	274	1400
Phenylalanine	257	200
Disulfide bridge	250	300
Peptide bond	190	~ 7000

UV spectroscopy was used to determine protein concentrations. For calculation of molar extinction coefficients of proteins, the program ProtParam was used. Protein concentrations were calculated using Lambert-Beer-equation: $A = \varepsilon * c * d$

In this equation, A represents absorption at 280 nm, ε the molar extinction coefficient, d the thickness of the cuvette and c the concentration in mol/l

3.7.2. CD spectroscopy

Circular Dichroism (CD) refers to absorbtion of left and right circularly-polarized light of optically active molecules. Asymmetric carbon atoms and/or aromatic amino acids are responsible for the optical activity of molecules. Proteins are composed of a large number of

optically active amino acids and additionally form secondary structure. That result in different absorption intensities of left and right circularly polarized light. The quantitive measure for circular dichroism is the ellipticity Θ (in degrees). The molar ellipticity is the correlation of the ellipticity, the molecular weight and the amino acid composition of the protein.

$$\Theta_{MRW} = \frac{\Theta \cdot 100 \cdot M}{c \cdot d \cdot N_{AS}}$$

Θ represent the measured ellipticity in mdeg, M the molecular weight of the protein in kDa, c the protein concentration in mg/ml, d the thickness of the cuvette in cm and N_{AS} the number of amino acid of the protein.

Polypeptide chains display characteristic CD-signals in the far-UV region (170 – 250 nm). Two adjacent minima at 208 and 222 nm are resulted from a-helices. A single minimum at 218 nm is caused by ß-sheets. Thus, the CD spectrum leads information about the secondary structure of proteins. Far-UV spectra were recorded from 190 – 260 nm using 10 accumulations. The protein concentrations ranged from 0.1 – 0.3 mg/ml. Parameter of the measurement were set to: Resolution: 0.1 nm; Scan speed: 20 nm/min; Response: 4.0 s; Band width: 1.0 nm.

3.7.3. Isothermal titration calorimetry (ITC)

Isothermal titration calorimetry is a common method to study protein-protein interactions in solution. Biophysical parameters like the dissociation constant K_D, the binding enthalpy ΔH and the stoichiometry of the binding event are determined by ITC. A potential binding partner in the syringe is titrated to protein in the cell. Resulting heat of binding is directly measured, which is monitored as µcal/s.

ITC was performed with the VP-ITC200 (MicroCal). Proteins were dialyzed against the same buffer (40 mM HEPES (pH 7.5); 20 – 150 mM KCl) in order to avoid heat of neutralization. Depending on the expected KD, protein concentrations of 30 – 50 µM in the cell were used. The concentrations of the titrant were set to 300 – 500 µM. In a typically experiment, ITC was

performed at constant temperature of 20°C. 40 – 45 injections with a duration time of 180 s were performed. Origin 8.0 was used for analysis of the ITC data.

3.8. Activity Assays

3.8.1. ATPase assay with an ATP-regenerating system

The ATP hydrolysis rates were determined by using a regenerative ATPase assay. Product inhibition by accumulation of ADP during the hydrolysis reaction is prevented. This assay uses an enzyme-coupled system that converts the produced ADP in ATP. This reaction is performed by pyruvate kinase (PK) and lactate dehydrogenase (LDH) in presence of posphoenol pyruvat and NADH. Consumption of NADH to NAD^+ can be monitored spectroscopically at a wavelength of 340 nm. Following concentrations were used in this assay:

PK	0.1% (v/v)
LDH	0.4% (v/v)
NADH	0.15 mM NADH
PEP	2 mM

ATPase assays were performed in 40 mM HEPES (pH 7.5), 20-150 mM KCl, 5 mM $MgCl_2$. Basically, 120 µl of the premix were used for every 150 µl assay. ATPases, ATP, co-chaperones and buffer were added in the remaining volume. Assays were performed using a Cary 50 Bio UV/Vis spectrometer at 30°C. For data collection, the average time was set to 0.2 sec and reactions were recorded for about 15-30 min. From the slope of the linear decrease of the progression curves, the hydrolysis rates were calculated.

3.8.2. V-Src activity assay in *S. cerevisiae*

The activity of v-Src in wild type yeast cells was compared to yeast cells overexpressing Cns1 or Cns1 fragments. Yeast wild type strain containing a plasmid for galactose inducible v-Src expression (URA) was transformed with plasmids of Cns1wt or Cns1 fragments (LEU). Colonies were then transferred to URA^-/LEU^--Media containing raffinose as carbon source and incubated at 30°C until stationary phases were reached. A series of 1:10 dilutions were spotted afterwards on URA^-/LEU^- plates containing either glucose or galactose. Typically cell density of a culture in stationary phase contained 1 x 10^8 cells/ml. Plates were incubated at 30°C for 3 days.

4. Results and Discussion

4.1. Regulation of Hsp90 ATPase activity by the Co-chaperone Aha1

Hsp90 is interacting with various co-chaperones to function in the context of a complex ATPase cycle (see introduction). These co-chaperones have different effects on Hsp90. They are able to regulate the ATP turnover, induce structural changes or are involved in substrate activation processes (JOHNSON et al., 1994, 1996; PIRKL AND BUCHNER, 2001, RIGGS et al., 2003; SILIGARDI et al., 2004; FORANOV et al., 2008; HESSLING et al., 2009). The ATPase activity of Hsp90 is inhibited by Sba1, Sti1 and Cdc37 (PRODROMOU et al., 1999; SILIGARDI et al., 2004; RICHTER et al., 2003). Sba1, the yeast homolog of human p23, binds preferentially to the closed, nucleotide-bound state (SULLIVAN et al., 2002; RICHTER et al., 2004; MCLOUGHLIN et al., 2006). Also the crystal structure of the nucleotide-bound, closed state of Hsp90 was solved in the presence of Sba1 (ALI et al., 2006). In contrast, Sti1 prefers binding to the open conformation of Hsp90 (RICHTER et al., 2003; ONUOHA et al. 2008). Binding of Sti1 to multiple sites on Hsp90 leads to prevention of the N-terminal closing reaction which inhibits the ATP hydrolysis in a noncompetitive manner (RICHTER et al., 2003).

Other co-chaperones are able to enhance the Hsp90 ATPase activity as shown for Aha1 and Cpr6 (PANARETOU et al. 2002, MCLAUGHLIN et al., 2006). In *S. cerevisiae*, Aha1 was found as a homologue to Hch1 (NATHAN et al. 1999; PANARETOU et al., 2002). The N-terminal domain (residues 1-153) of Aha1 shares high homology to Hch1 (Figure 4-1). Hch1 was characterized as a multicopy suppressor of Hsp90 temperature-sensitive mutants (NATHAN et al. 1999). Whereas homologues of Aha1 have been identified from yeast to mammals, Hch1 is only encoded in lower eukaryotes (PANARETOU et al. 2002; LOTZ et al. 2003).

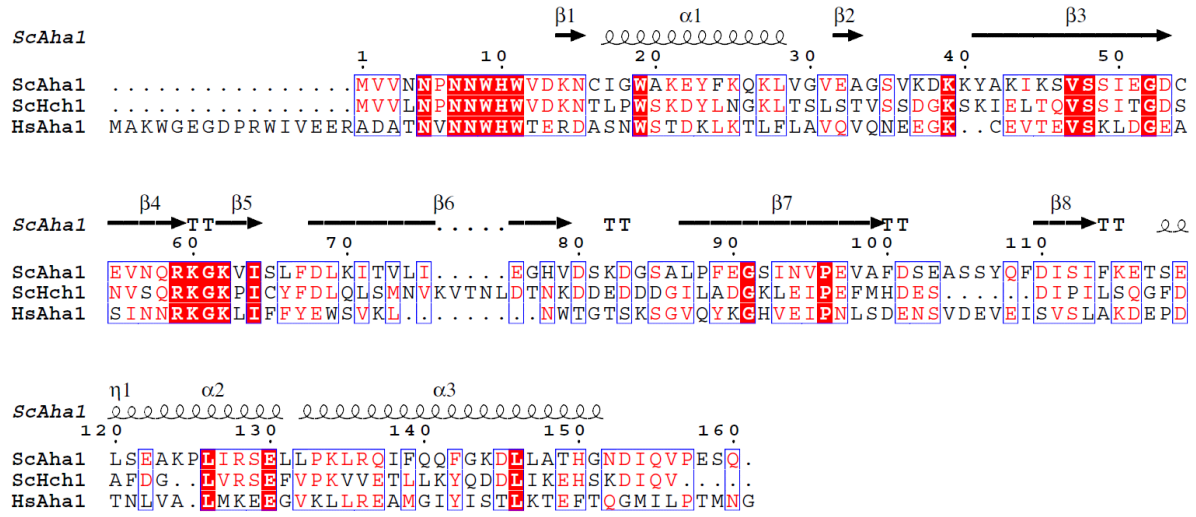

Figure 4-1: Sequence alignment of Hch1 (ScHch1) and the N-terminal domain of yeast (ScAha1) and human Aha1 (HsAha1).
Sequence alignment was performed with yeast Hch1 and the N-terminal domains of Aha1 from yeast and humans using MULTALIN and ESPRIPT. The coordinates of the N-terminal domain of *S. cerevisiae* Aha1 from the crystal structure (pdb-code: 1USV) were used for identification of structural elements.

4.1.1. Structure of Aha1

The structure of Aha1 was solved by co-crystallization with the Hsp90 middle domain (pdb-code: 1USU; MEYER et al., 2004) displaying the core of interaction between Aha1 and Hsp90. The N-terminal domain of Aha1 showed an elongated cylindrical structure consisting of a central four-stranded antiparallel beta-sheet enclosed by two terminal helices (Figure 4-2, A). The structure of the C-terminal domain of human Aha1 was solved by NMR (pdb-code: 1X53). The structure is characterized by a five-stranded antiparallel beta-sheet, an internal and a C-terminal helix (Figure 4-2, B). Whereas the N-terminal domain of Aha1 was known to interact with Hsp90 the function of the C-terminal domain of Aha1 in the regulation of the ATPase activity of Hsp90 remained unclear.

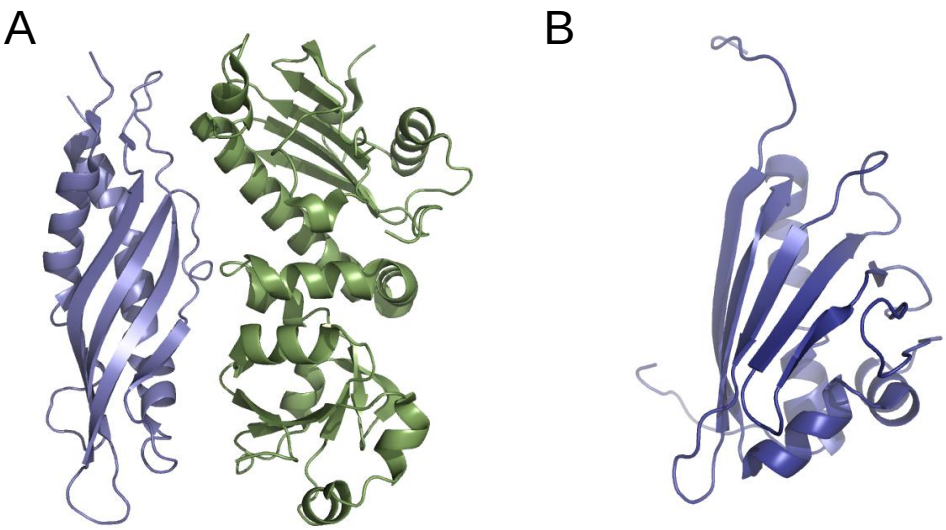

Figure 4-2: Structure of Aha1
(A) Crystal structure of the N-terminal domain of Aha1 bound to the middle domain of Hsp90 (MEYER et al, 2004, pdb-code: 1USV). Aha1-N is colored in blue, middle domain of Hsp90 in green.
(B) Solution structure of the C-terminal domain of human Aha1 (pdb-code: 1X53) solved by NMR.

4.1.2. Influence of Aha1 on Hsp90 ATPase activity

Hsp90, Aha1 and both its N-terminal and C-terminal domain were expressed in *E. coli*. Purification of the His-tagged proteins was performed according to standard protocols (see Material and Methods). As shown by CD spectroscopy and thermal transitions both the N- and C-terminal domains of Aha1 are stable proteins and correctly folded (RETZLAFF et al., 2010).

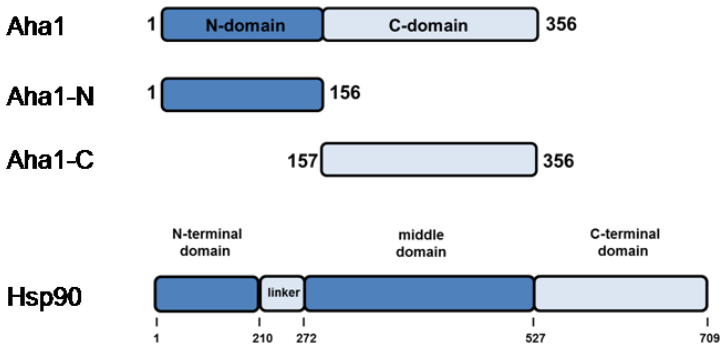

Figure 4-3: Schematic domain architecture of yeast Aha1 and yeast Hsp90.
Aha1 was subdivided into N-terminal domain (Aha1-N) and the C-terminal domain (Aha1-C)

The influence of full length Aha1 and both the N-terminal and the C-terminal domain of Aha1 on the ATPase activity of Hsp90 were measured by an enzyme-coupled ATPase assay.

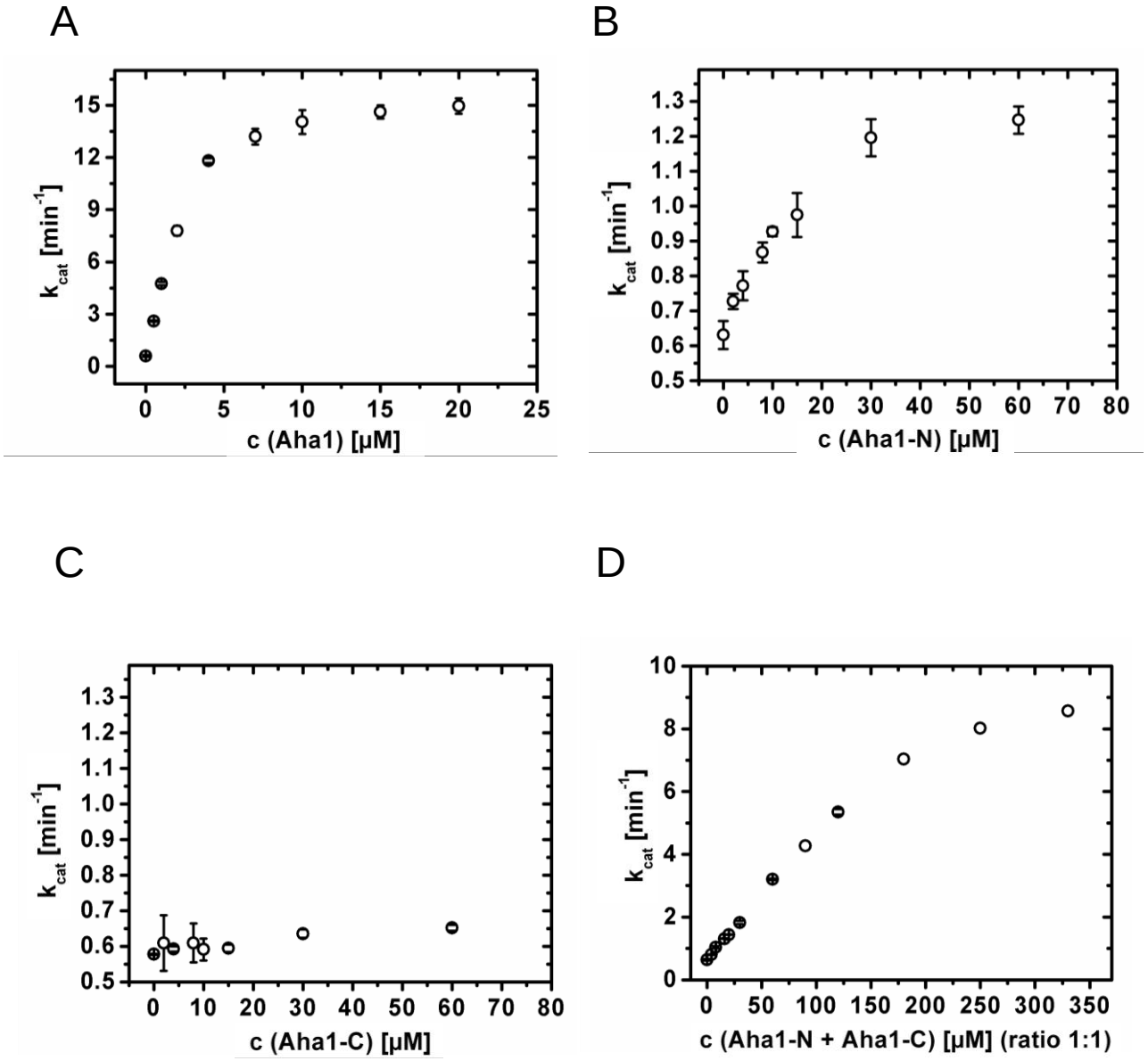

Figure 4-4: ATPase assay to determine the stimulatory effect of Aha1 and Aha1 fragments on the ATPase activity of Hsp90
Effect of full length Aha1 (A) and both the N-terminal domain, Aha1-N, (B) and the C-terminal domain of Aha1, Aha1-C, (C) on Hsp90 ATPase activity. Additionally, effects of both individual domains (molar ratio 1:1) on Hsp90 ATPase were tested (D). Hsp90 was diluted to a final concentration of 1.0 µM. Assays were performed at 30°C in 40 mM HEPES/KOH (pH 7.5), 20 mM KCl, 10 mM $MgCl_2$ and 5 mM ATP. Reactions were corrected for background activity by using 125 µM radicicol.

Aha1 is able to activate the intrinsically low ATPase activity of Hsp90 (k_{cat} ~ 0.8 min^{-1}) by a factor of around 15. The apparent K_M value for this activation is around 3 µM (Figure 4-4, A). Addition of the N-terminal domain of Aha1 to Hsp90 leads also to an activated Hsp90 ATPase activity (Figure 4-4, B). Compared to full-length Aha1, the N-terminal domain of Aha1 is not able to fully activate the ATPase activity of Hsp90. Furthermore, the apparent K_M is increased indicating a lower binding affinity of the N-terminal domain of Aha1 to Hsp90 compared to full length Aha1. The C-terminal domain of Aha1 showed no effect on the ATPase activity of Hsp90 (Figure 4-4, C). These results are in agreement with data published before as binding of Aha1 to Hsp90 is mainly maintained by its N-terminal domain (PANARETOU et al., 2002; MEYER et al., 2004).

However, both individual domains of Aha1 together are able to stimulate the ATP hydrolysis rate of Hsp90 in the range of full length Aha1 (Figure 4-4, D). Hence, the two domains of Aha1 tend to form complexes which have a stronger activation potential then the individual domains alone. Aha1 and both the C- and N-terminal domain are monomeric in solution. By ITC no complex formation of the two domains could be detected (data not shown). This leads to the suggestion that both domains of Aha1 are involved in the activation process of the Hsp90 ATPase activity.

As shown by ATPase assays, both domains of Aha1 are important for the complete activation mechanism of Hsp90 ATPase activity. The activation potential of the two individual domains is strongly depending on the presence of the N-terminal domain of Aha1. These results point towards cooperative binding sites for Aha1 on Hsp90. So, for interaction with Aha1 other domains of Hsp90 besides the middle domain seem to be involved.

4.1.3. Binding site of Aha1 on Hsp90

The complete binding site and the corresponding residues of Aha1 and Hsp90 responsible for interaction were determined by NMR using isotopic labeled proteins (RETZLAFF et al., 2010). NMR spectroscopy and data analysis was done by Marco Retzlaff and Franz Hagn.

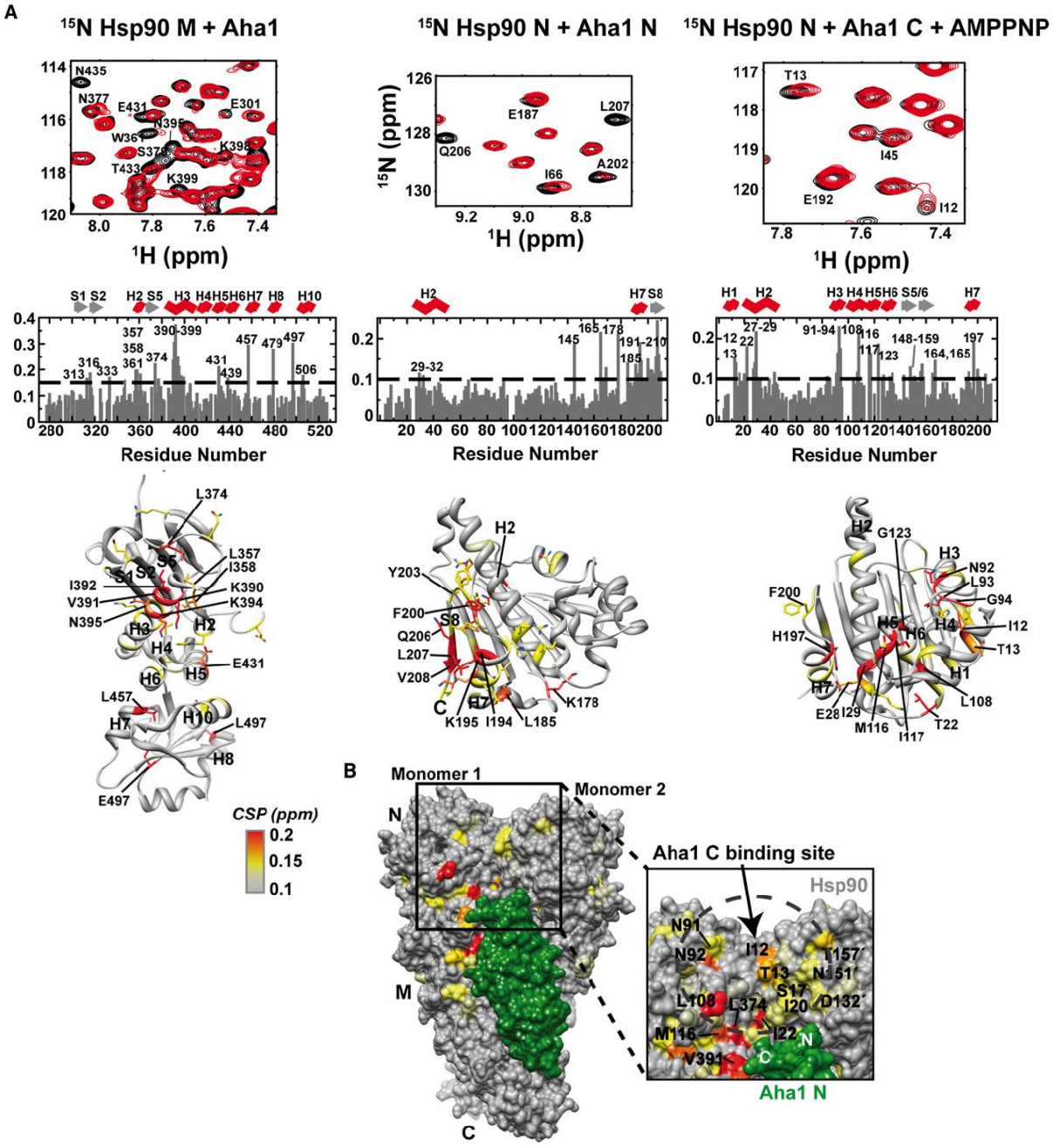

Figure 4-5: Interaction sites between individual domains of Hsp90 and Aha1.
(A) 15N-HSQC spectra of Hsp90 middle domain (left) and Hsp90 N-terminal domain (middle and right) in the presence of the C-terminal domain and N-terminal domain of Aha1 (black, Hsp90 domain alone; red, in presence of Aha1 domains). Aha1-N binds to Hsp90 middle domain (left) and the Hsp90 N-terminal domain (middle). Aha-C is able to interact with the AMP-PNP bound form of the Hsp90 N-terminal domain (right). Chemical shift perturbation (CSP) plots are shown below the 15N-HSQC sections. CSPs were mapped on the structures of the individual domains of Hsp90 (gray, not significant; yellow, significant; red, significant plus one standard error or above).
(B) Chemical shift differences derived from (A) were mapped on the full length structure of the dimeric Hsp90 (pdb-code: 2CG9). Residues from the Hsp90 middle domain involved in binding to Aha1 are in agreement with the structure of the Hsp90 middle domain bound to Aha1-N (pdb-code: 1USU). Therefore, Aha1-N (green) was aligned to the full length structure of Hsp90. Residues from the Hsp90 N-terminal domain which are involved in Aha1 binding are labeled. The surface region where Aha1-C binds is indicated by the arrow. Figure is adopted from RETZLAFF et al. (2010).

For the Hsp90 middle domain the same residues as previously shown in the Aha1-Hsp90 crystal structure (MEYER et al., 2004) were found to be important for interaction. Additional binding sites of the N-terminal domain of Aha1 were determined in the N-terminal domain of Hsp90 (residues 187-210). The C-terminal domain of Aha1 showed no interaction with the N-terminal domain of Hsp90. However, addition of the non-hydrolysable ATP-analog AMP-PNP leads to an interaction of the Hsp90 N-terminal domain with Aha1-C. The nucleotide-induced conformational changes of Hsp90 are responsible for generating the binding site for the C-terminal domain of Aha1.

Using Förster resonance energy transfer (FRET) of labeled Hsp90 dimers (HESSLING et al., 2009), effects of Aha1 on the subunit exchange of the Hsp90 dimer could be determined (RETZLAFF et al., 2010).The apparent half-life of the subunit exchange reaction of Hsp90 was markedly increased by addition of full length Aha1 compared to the reaction in the absence of Aha1. Thus, addition of Aha1 leads to stronger association of the two subunits of Hsp90.The individual domains of Aha1 are not able to stabilize the Hsp90 dimer. The presence of both individual domains of Aha1 in this assay revealed a moderate effect on the Hsp90 subunit exchange reaction (RETZLAFF et al., 2010). Taken together, binding of Aha1 on Hsp90 induces structural changes within the Hsp90 dimer which leads to a stabilization of the ATPase-competent state of Hsp90.

Both domains are involved in binding and stimulation of the ATPase activity of Hsp90. The specific mechanism how Aha1 binds to Hsp90 remained unclear. There are different possibilities how Aha1 could interact with the Hsp90 dimer which leads to an increased ATPase activity. Aha1 could bind to one site of the Hsp90 dimer. The N-terminal domain of Aha1 binds to the middle domain of Hsp90 and the C-terminal domain of Aha1 binds to the N-terminal domain of Hsp90 on the same protomer within the Hsp90 dimer. Binding of Aha1 leads then to a reorientation of the domains and formation of the N-terminal closed conformation of Hsp90. In this case, stimulation of the ATPase activity of Hsp90 by Aha1 can be described by an intermolecular (*cis*) activation process (Figure 4-6).

Another possibility is that Aha1 could bind to both sites of the Hsp90 dimer. Binding of Aha1 across the Hsp90 dimer would also explain the observed effects on the ATPase activity and formation of the compact Hsp90 complex. Here, Aha1 binds via its N-terminal domain to the middle domain of Hsp90 on one subunit and the C-terminal domain of Aha1 binds to the N-terminal domain of Hsp90 on the other subunit. Both subunits of the Hsp90 dimer are involved in binding of Aha1. In this case the mechanism of stimulation of the Hsp90 ATPase activity by Aha1 is intermolecular (*trans*) (Figure 4-6).

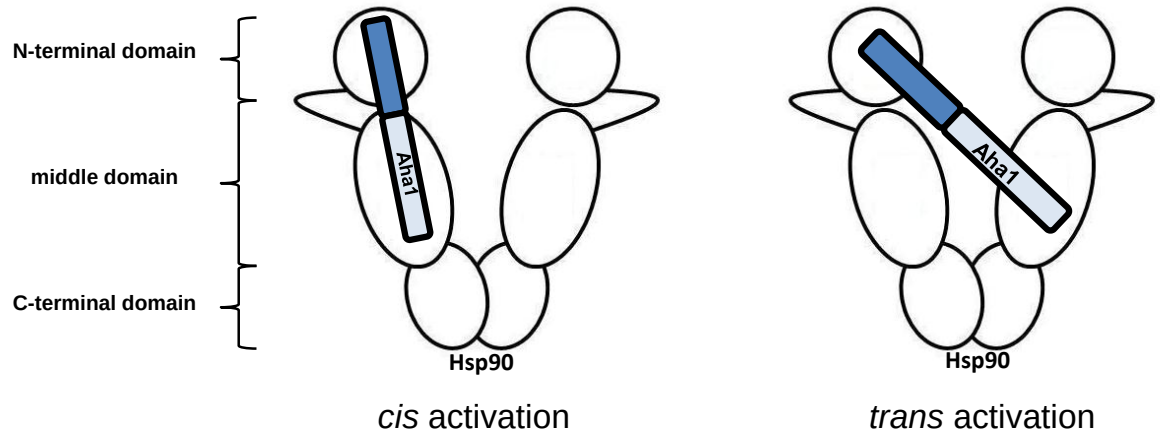

Figure 4-6: Schematic view of Aha1 binding to Hsp90.
The stimulatory effect of Aha1 on the Hsp90 ATPase activity could be achieved by an intramolecular (*cis* activation) or an intermolecular binding mechanism (*trans* activation).

4.1.4. Mechanism of Hsp90 ATPase activation by Aha1

As shown above, different types of activation of the Hsp90 ATPase activity by Aha1 are possible. To address the specific mechanism of activation of the Hsp90 ATPase activity by Aha1, different mutations were introduced in Hsp90. Based on the crystal structure of Aha1 bound to the Hsp90 middle domain (Figure 4-7), the Hsp90 mutant Hsp90V391E was created. The residues Leu 315, Ile 388 and Val 391 of Hsp90 provide the core of the interaction with Aha1. These residues pack against Ile 64, Leu 66 and Phe 100 to form the hydrophobic interface which is supported by polar interactions between Gln 314 from Hsp90 and the main chain of Ile64 and Ser65 of Aha1. An extensive network of hydrogen bonding and ion-pair interactions is formed by exposed lysine residues from Hsp90 with Asp53, Asp68, Glu97, and Asp101 from Aha1 (MEYER et al., 2004).

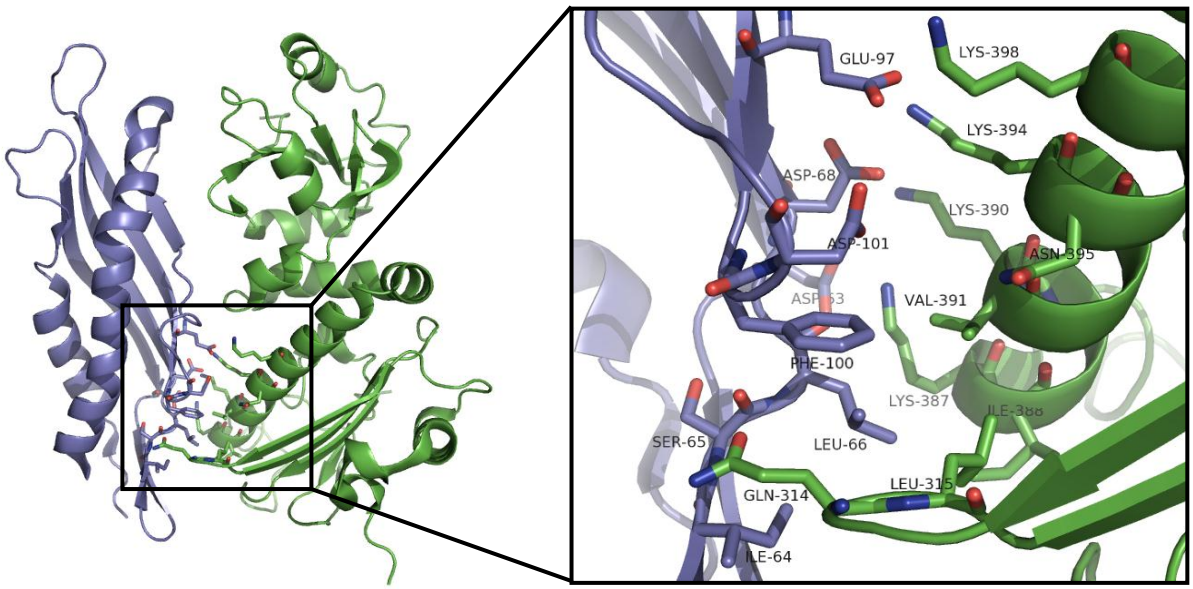

Figure 4-7: Co-crystal structure of the N-terminal domain of Aha1 bound to the Hsp90 middle domain and residues involved in formation of the core of interaction.
Co-crystal structure of N-terminal domain of Aha1 bound Hsp90 middle domain (pdb-code: 1USU). The binding interface of Aha1 and Hsp90 with the residues involved in the formation of the core of interaction is shown in a detailed view on the right.

Based on the interaction sites of Aha1 in the N-terminal domain of Hsp90determined by NMR (Figure 4-5), the Hsp90V209A mutant was generated. The V209 residue of Hsp90is located near the charged linker region and is involved in binding to the C-terminal domain of Aha1.

The ATPase activity of Hsp90V391E and Hsp90V209A were analyzed. Both mutants showed no differences in ATP hydrolysis rate compared to Hsp90wt (data not shown). In order to obtain the stimulatory effect of Aha1 on the ATPase activity of both mutants, ATPase assays in the presence of various amounts of Aha1 were performed.

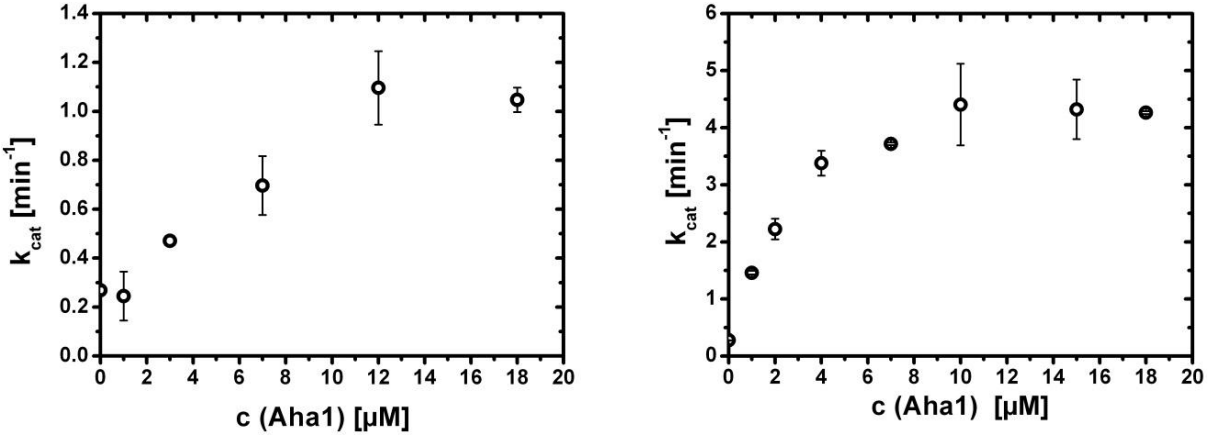

Figure 4-8: Stimulatory effect of Aha1 on ATPase activity of Hsp90V391E and Hsp90V209A. Hsp90V391E or Hsp90V209A was diluted in 40 mM HEPES/KOH (pH 7.5) 20 mM KCl, 5 mM $MgCl_2$, 2 mM PEP, 0.15 mM NADH, 0.1 %PK, and 0.4 % LDH (AH-buffer) to a final concentration of 1.0 µM and was incubated with various amounts of Aha1. Assays were performed at 30°C and were started with addition of ATP to a final concentration of 500 µM.

The stimulatory effect of Aha1 on the ATPase activity of Hsp90V391E is markedly decreased compared to Hsp90wt. Introduction of the polar glutamine into the hydrophobic binding interface of Hsp90 leads to the disruption of Aha1 binding. The apparent K_M is also increased indicating that the binding affinity of this mutant to Aha1 is strongly reduced. This effect was also confirmed by ITC (data not shown) and analytical ultracentrifugation (RETZLAFF et al., 2010) as no binding could be observed between Aha1 and Hsp90V391E under conditions used for detection of binding of Aha1 to Hsp90wt.

The ATPase activity of Hsp90V209A displayed also a lower ability for activation by Aha1. But the activation of the Hsp90 ATPase is only reduced around 2-fold. In this case, Aha1 is still able to bind via its N-terminal domain to the middle domain of Hsp90 which was shown to be the core of interaction. Only the binding affinity of the C-terminal domain of Aha1 to the Hsp90 N-terminal domain is affected which leads to a decreased activation of the Hsp90ATPase activity.

Additionally, for inhibition of the intrinsic activity of Hsp90, the mutant Hsp90D79N was used. This mutant is not able to bind or hydrolyze ATP (PANARETOU et al, 1998; OBERMANN et al., 1998). To disrupt binding to Aha1 in addition to abolishing the ATPase activity, the double mutants Hsp90D79NV391E and Hsp90D79NV209A were created. As expected the

Hsp90D79N and the Hsp90D79NV391E mutant showed no ATPase activity (data not shown).

4.1.5. Activation mechanism in *trans*

In order to dissect specific intra- and intermolecular interactions within the Hsp90 dimer different heterodimers were formed and their specific ATPase activity was measured. The dissociation constant of subunit dimerization of Hsp90 is in the nM range (HARRIS et al, 2001, RICHTER et al., 2001). So, asymmetric dimers harboring different mutations on each monomer can be formed simply by mixing homodimers containing different mutations (RICHTER et al, 2001). Activation of the Hsp90 ATPase activity could be achieved by *cis*- or *trans*-mechanisms. Specific communication between the middle and the N-terminal domain of Hsp90 which are required to facilitate ATP hydrolysis could be detected by heterodimer assays (RICHTER et al., 2001; CUNNINGHAM et al., 2008).

To determine if the stimulating effect of Aha1 is based on intramolecular (*cis*) or intermolecular (trans) activation of the Hsp90 dimer ATPase assays were performed according to heterodimer assays described before (CUNNINGHAM et al., 2008). The analysis of the resulting k_{cat} values of the corresponding molar ratios of Hsp90 would lead to a linear or nonlinear progression which is indicative of a *cis* or *trans*-mechanism (CUNNINGHAM et al., 2008).

First, different heterodimers were used to test activation in *trans*. By using Hsp90 mutants where Aha1 binding is interrupted and the ATPase inactive Hsp90 mutant, the activation mechanism in *cis* is partially inhibited. ATPase assays were performed to test the activation of the ATP turnover of these heterodimers by full length Aha1.

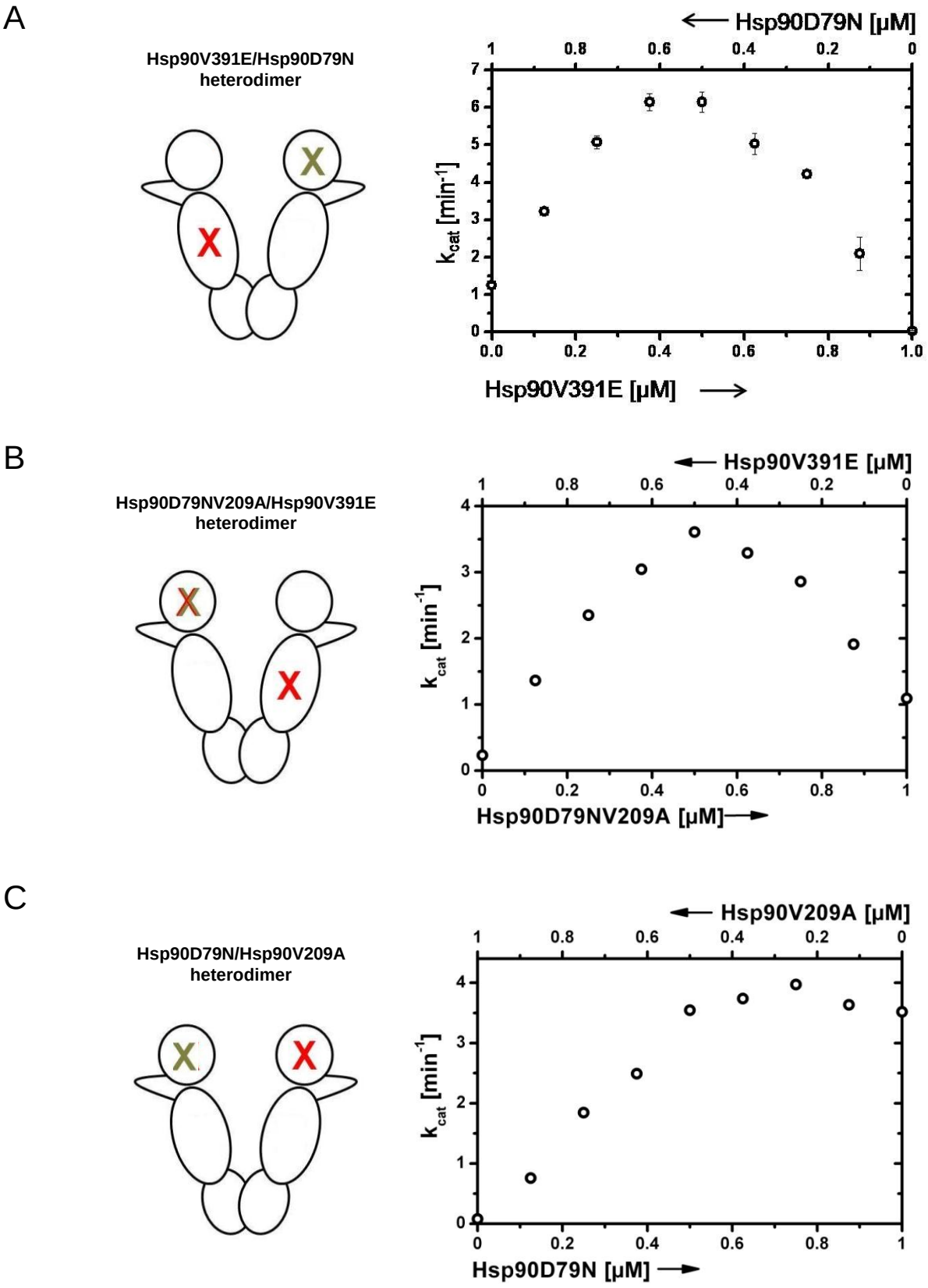

Figure 4-9: Stimulatory effect of Aha1 on ATPase activity of Hsp90 heterodimers.
Hsp90 mutants were mixed in different molar ratios to a final concentration of 1.0 µM. ATPase assays were performed in the presence of saturating amounts of Aha1 (10 µM). Heterodimer formation is visualized by cartoons on the left (red cross, mutations in Aha1 binding; yellow cross, catalytically inactive mutation).

Hsp90D79N and Hsp90V391E were mixed in different ratios with a final concentration of 1 µM. Then, ATPase assays were performed by addition of saturating amounts of Aha1 (10 µM). The Hsp90D79N and Hsp90V391E heterodimers displayed a maximum in Hsp90 ATPase stimulation at equal concentration of both Hsp90 mutants (Figure 4-9, A). Under heterodimer conditions of Hsp90, Aha1 is able to stimulate the ATPase activity. As described by the nonlinear progression of this plot, an activation mechanism in *trans* occurred. A linear progression of the Hsp90 ATPase activity would be expected if stimulation by Aha1 is not mediated by an intermolecular mechanism (Figure 4-9, A). In the *trans* activation mechanism, Aha1 binds to one subunit of Hsp90 and stimulates the ATP turnover in the other subunit. Under these conditions, activation of the ATPase is regulated by only one Aha1 molecule as binding to the other subunit of Hsp90 is interrupted via the V391E mutation. Based on statistical distribution between homo- and heterodimers at equal concentration of each Hsp90 mutant, the amount of heterodimer should be 50%. In this case, it seems that only one Aha1 is able to fully stimulate the Hsp90 dimer.

Heterodimers consisting of Hsp90D79NV209A and Hsp90V391E showed also a *trans* activation mechanism (Figure 4-9, B). Here, additional mutations in the N-terminal domain of Hsp90 were used to further disrupt binding of Aha1. The Hsp90D79N/Hsp90V209A heterodimer is still able to bind Aha1 via the middle domain. In this case only binding of Aha1 to the N-terminal domain is affected. Again, the nonlinear progression supports the *trans* mechanism (Figure 4-9, C).

Further titration experiments with increasing amounts of the ATPase-inactive Hsp90 mutant showed full activation of the ATP turnover compared to Hsp90wt (RETZLAFF et al., 2010). These data conclusively showed that only one Aha1 is sufficient to fully activate the ATPase activity of the Hsp90 dimer.

4.1.6. Activation mechanism in *cis*

Taken together, the determined binding site of Aha1 to Hsp90 in addition to the effects of Aha1 on Hsp90 ATPase activity and the subunit exchange reaction revealed that Aha1 could also bind to only one subunit of the Hsp90 dimer and activate the ATPase activity of the same subunit within the Hsp90 dimer.

In order to check activation in *cis*, heterodimers of the double mutant Hsp90D79NV391E and Hsp90wt were formed. Additionally, heterodimers with Hsp90D79NV209A and Hsp90V209A

were formed and the activation of the ATPase activity by Aha1 was tested. Under heterodimer conditions, Aha1 is able to bind only to one subunit. By using the double mutant Hsp90D79NV391E or Hsp90D79NV209A, the activation mechanism in *trans* is partially inhibited.

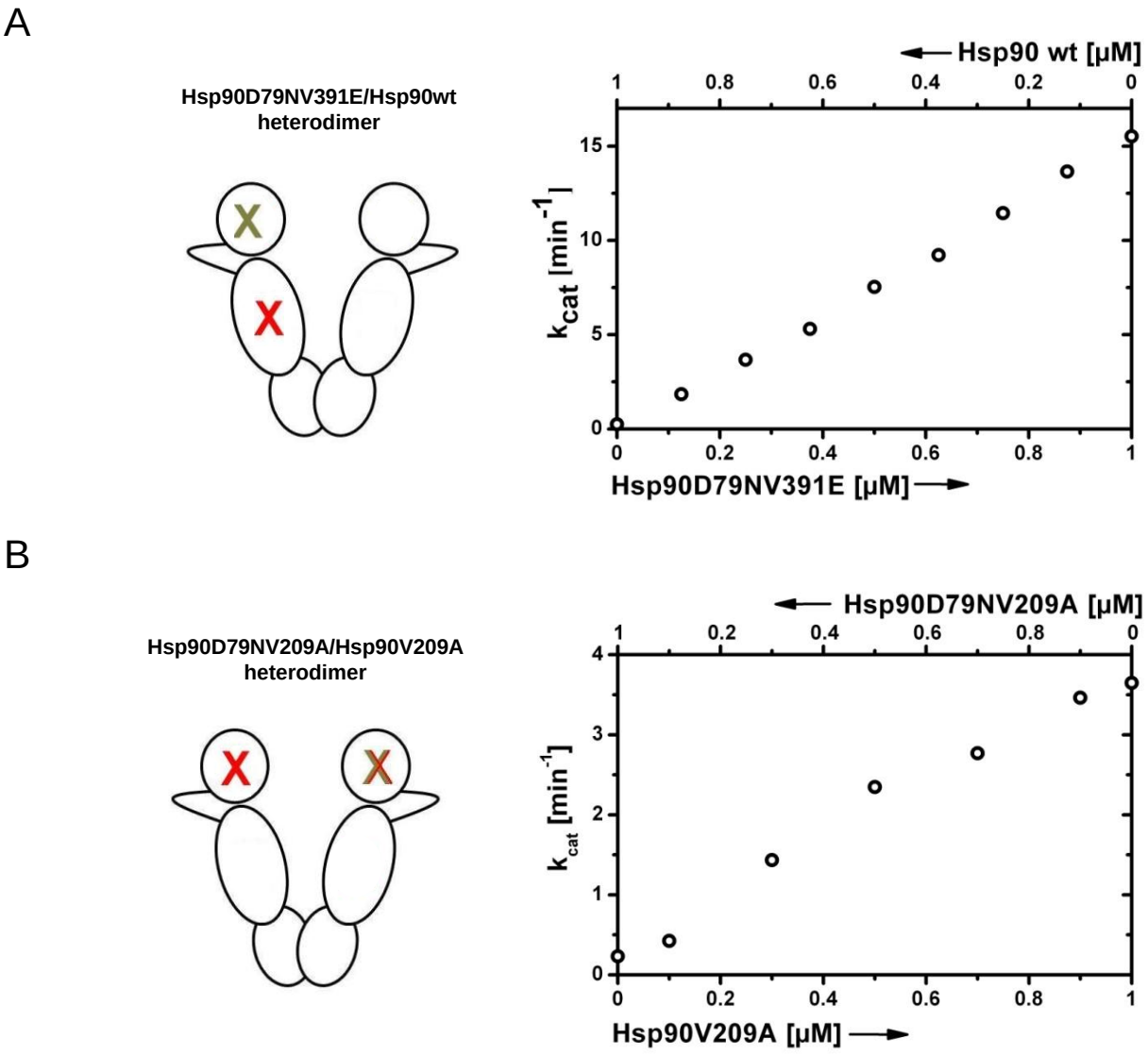

Figure 4-10: Stimulatory effect of Aha1 on ATPase activity of Hsp90 heterodimers.
Hsp90 mutants were mixed in different molar ratios to a final concentration of 1.0 µM. ATPase assays were performed in the presence of saturating amounts of Aha1 (10 µM). Heterodimer formation is visualized by cartoons on the left (red cross, mutations in Aha1 binding; yellow cross, catalytically inactive mutation).

The ATPase activity of heterodimers consisting of Hsp90D79NV391E and Hsp90wt or heterodimers of Hsp90V209A and Hsp90D79NV209A showed a nearly unchanged ability for activation by Aha1. The mechanism in *cis* is described by the linear progression of the plot of the ATPase activity and the corresponding molar ratios of the Hsp90 variants.

Further analysis of heterodimers between Hsp90wt and the C-terminal domain of Hsp90 revealed that *cis* activation in the Hsp90 dimer by Aha1 requires two full-length subunits of Hsp90 (data not shown). However, one of the protomer can be catalytically inactive (RETZLAFF et al., 2010).

4.1.7. Aha1 binding to Hsp90 and Hsp90 heterodimer

Isothermal titration calorimetry (ITC) was performed to confirm the binding of Aha1 and Hsp90. Aha1 was titrated against Hsp90wt and the ATPase-inactive mutant Hsp90D79N.

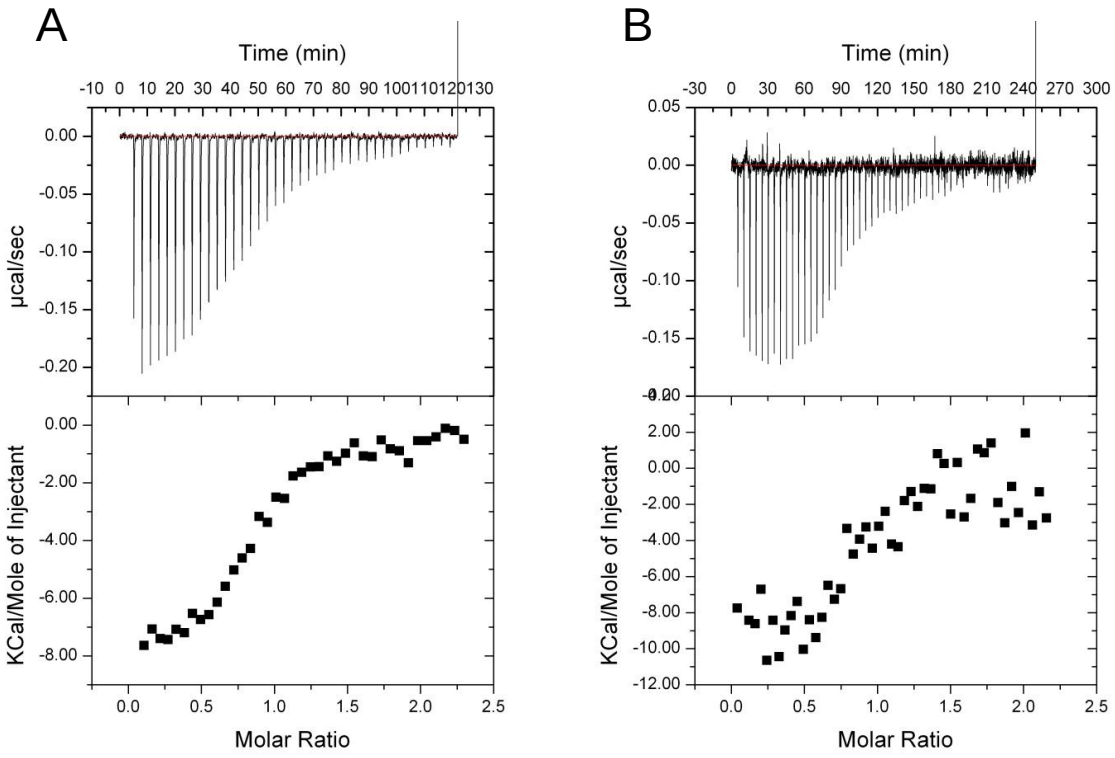

Figure 4-11: Raw ITC data of the titration of Aha1 to Hsp90wt or Hsp90D79N.
Binding of Aha1 to Hsp90wt (A) or Hsp90D79N (B). ITC was performed in 40 mM HEPES/KOH (pH 7.5), 20 mM KCl at 30°C. Calculation of the stoichiometry is based on the concentration of Hsp90 monomers.

These data showed that Aha1 binds to Hsp90wt and the catalytically inactive mutant Hsp90D79N with a stoichiometry of 1:1 and nearly the same binding affinities. This implies that two Aha1 molecules are able to bind to one Hsp90 dimer. These data are in agreement with former analysis (MEYER et al., 2004).

In order to proof that only one Aha1 binds to the heterodimer, Hsp90D79N/Hsp90V391E was used. Heterodimers were generated by a ~5-fold excess of Hsp90V391E which is not able to bind Aha1.

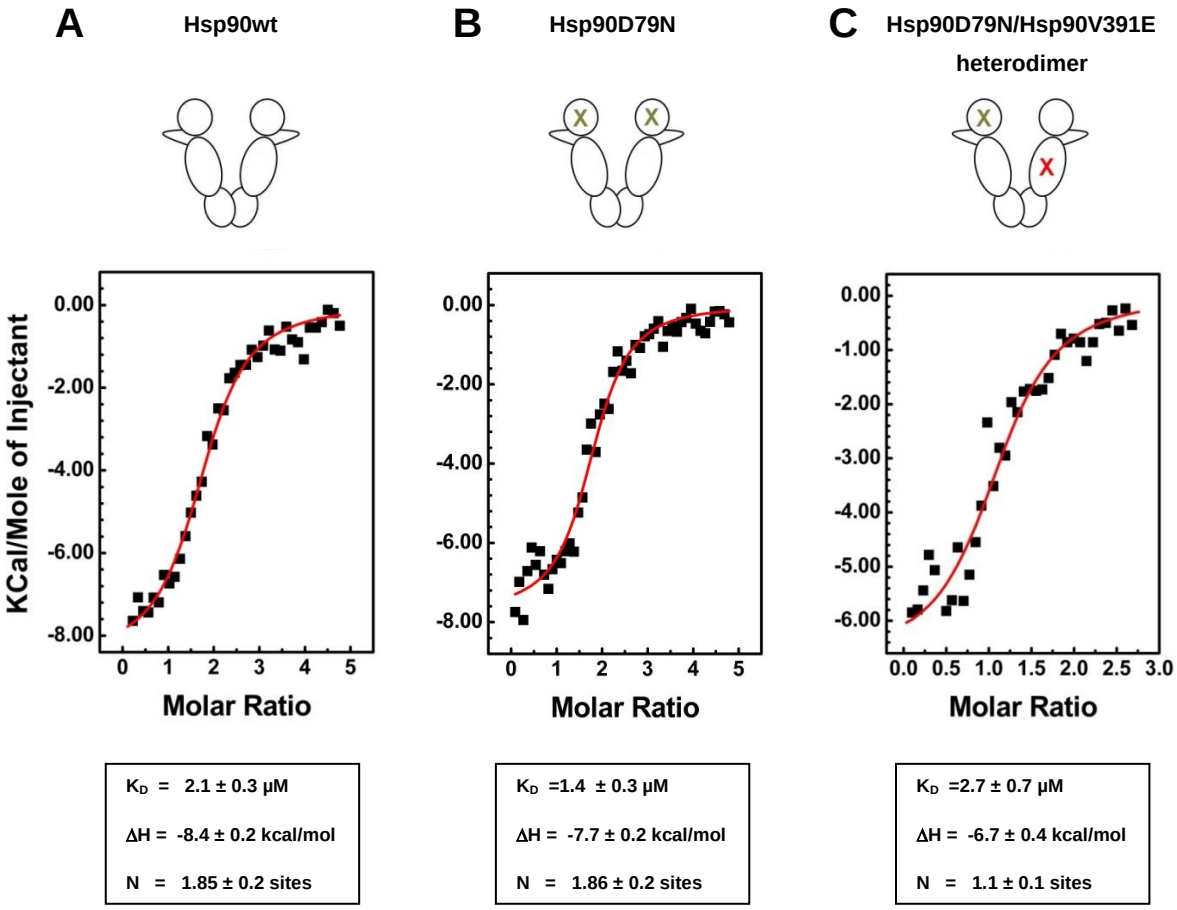

Figure 4-12: Comparison of binding of Aha1 to different Hsp90 variants by ITC.
Binding of Aha1 to Hsp90wt (A), Hsp90D79N (B) and the heterodimer consisting of Hsp90D79N and Hsp90V391E (C) (Figures of the binding curves derived from ITC are adopted from RETZLAFF et al, (2010)). Hsp90 is visualized by cartoons above the corresponding titration curve. Titration curves were recorded and the peak integrals were fit in order to obtain binding affinities and stoichiometries. Calculated parameters are displayed below, where K_D represent the dissociation constant, ΔH the binding enthalpy and N the number of molecules bound per Hsp90 dimer.

The ITC data clearly revealed that Aha1 binding to the Hsp90 heterodimer is interrupted compared to Hsp90wt. In contrast to Hsp90wt and Hsp90D79N where two molecules Aha1 are able to bind to the Hsp90 dimer with nearly the same affinities, the heterodimer displayed an equimolar stoichiometry. The binding affinity to the heterodimer is also only slightly decreased. These data demonstrated in addition to the ATPase assays that one Aha1 is sufficient to fully activate the Hsp90 dimer.

4.1.8. Model of the activation mechanism of Aha1

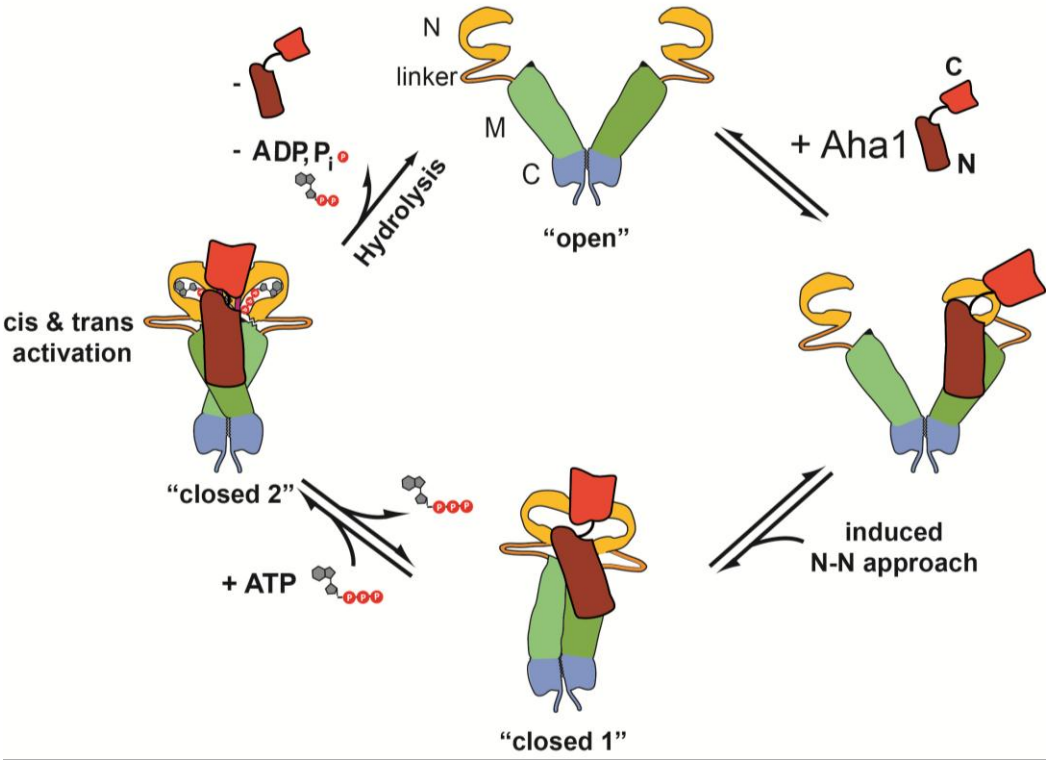

Figure 4-13: Schematic model of the activation model of Aha1
Specific interaction of Aha1 with Hsp90, followed by stimulation of the ATPase activity of Hsp90, includes *cis* and *trans* activation mechanisms. Figure is adopted from RETZLAFF et al. (2010).

In this model Aha1 binds to the open conformation of Hsp90 (termed "open") in an asymmetric manner as only one Aha1 molecule is involved in binding to the Hsp90 dimer. The N-terminal domain of Aha1 is the primary binding domain which leads to complex formation with Hsp90 and positioning of the C-terminal domain of Aha1. Binding of Aha1 induces conformational changes within the Hsp90 as the N-terminal domains come in closer

contact (termed “closed 1”). Binding of ATP induces a second closed state of Hsp90 (termed “closed 2”). Formation of the second closed state leads to a higher affinity and an additional binding site for Aha1. The C-terminal domain of Aha1 is now able to bind to both N-terminal domains of Hsp90. In this case only one Aha1 molecule binds to the Hsp90 dimer and that is sufficient to fully activate the Hsp90 ATPase activity with an activation mechanism in *cis* and *trans*. Additionally, binding of only one Aha1 maintains a free binding site for potential Hsp90 clients. Hsp90 returns to the open state after ATP hydrolysis and release of ADP.

4.1.9. Discussion

Analysis of Aha1 in the context of its regulation of the Hsp90 ATPase activity revealed a novel mechanism of interaction with Hsp90. During this work it could be shown that acceleration of the ATP turnover is mediated by binding of Aha1 to the middle and the N-terminal domain of the Hsp90 dimer. Additionally, for interaction of Aha1, a specific conformation of Hsp90 during the catalytic cycle is favored. The individual N-terminal domain of Aha1 showed activation of the Hsp90 ATPase activity (PANARETOU et al., 2002). To achieve full activation of Hsp90 both domains of Aha1 must act in a cooperative manner. The analysis of binding sites of Aha1 on Hsp90 revealed that binding of Aha1 involves regions in the N-terminal domains of Hsp90 in addition to the previously shown interaction to the middle domain of Hsp90 (MEYER et al., 2004). Binding of the C-terminal domain of Aha1 to the N-terminal domain of Hsp90 is only observable in the presence of nucleotides.

A model for the interaction cycle of Aha1 and Hsp90 was proposed (Figure 4-13), in which the N-terminal domain of Aha1 binds to the middle domain of Hsp90. It traps a N-terminal dimerized state of Hsp90 by binding both N-terminal domains. That leads to a localization of the C-terminal domain of Aha1 close to the N-terminal domains of the Hsp90 dimer. This binding event could lead to more rapid conformational changes to the dimerized, closed state of the Hsp90. Structural rearrangements to the closed state of Hsp90 are the kinetically limiting steps during the chaperone cycle (HESSLING et al., 2009). It seems that binding of Aha1 leads to a mechanical coupling of the middle and N-terminal domains of Hsp90. As consequence of binding of Aha1 and the induced conformational changes, the ATPase activity of Hsp90 is accelerated. The FRET experiments support this model of interaction as Aha1 stabilizes Hsp90 by bridging the Hsp90 dimer.

The heterodimer experiments performed with different Hsp90 mutants revealed that only one Aha1 is sufficient to fully stimulate the ATPase activity of Hsp90. Additionally, binding of

Aha1 to the Hsp90 heterodimer was proven by ITC (Figure 4-12). This asymmetric binding of Aha1 to Hsp90 is also in agreement with the expression levels of these proteins. In the cytosol of *S. cerevisae*, Hsp90 is expressed in more than 30-fold excess compared to Aha1 (GHAEMMAGHAMI et al., 2003). So, the complex of one Aha1 molecule bound to the Hsp90 dimer may represent the physiologically relevant species.

As already shown, co-chaperones are able to bind simultaneously to Hsp90 which is important for the progression of the chaperone cycle and client chaperoning (RICHTER et al., 2004, CHADLI et al., 2008; RETZLAFF et al., 2010; LI et al, 2011). With binding of Aha1 to Hsp90 the C-terminal domain of Hsp90 is still free for interaction with TPR-containing co-chaperones. For example, interaction of Aha1 in the presence of the TPR-containing co-chaperone Cns1 was investigated in this work.

4.2. In vitro analysis of the Hsp90/Hsp70 interacting protein Cns1

4.2.1. Purification and structural characterization of Cns1

Hsp90, Cns1 and both its N-terminal and C-terminal domain were expressed in *E. coli*. Purification of Hsp90 was performed as described before (see Material and Methods). Cns1 and both the N-terminal and C-terminal domain of Cns1 were purified using the protocol which was previously described (HAINZL et al., 2004).

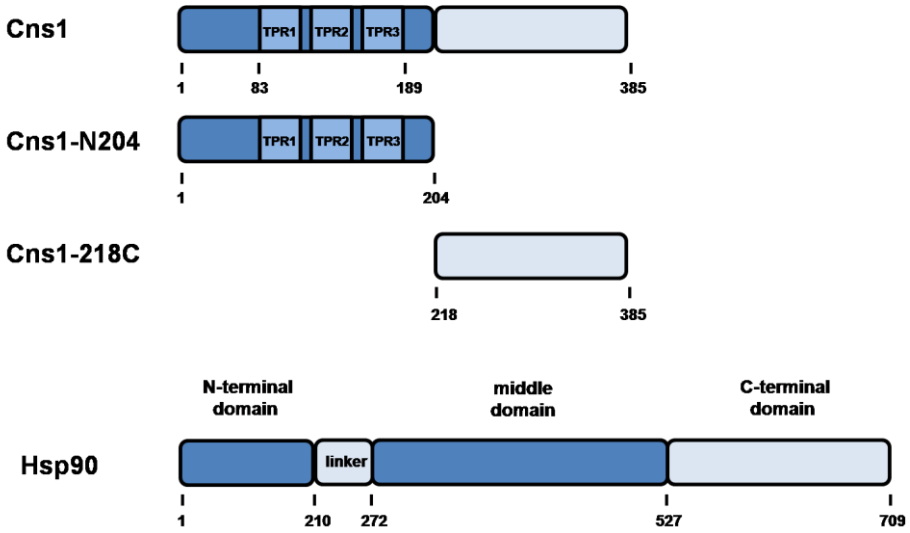

Figure 4-14: Schematic domain architecture of Hsp90 and Cns1.
The TPR-domain is located in the N-terminal domain of Cns1. Plasmids containing the subdivided constructs of Cns1 were purified as described before (HAINZL et al., 2004).

Confirmation of the purity of the protein preparations of Cns1 and both the N-terminal and C-terminal domain was done by SDS-PAGE. Additionally, Western-blots were performed. A polyclonal antibody against Cns1 was used as primary antibody in order to check if full length protein and both individual domains are detectable.

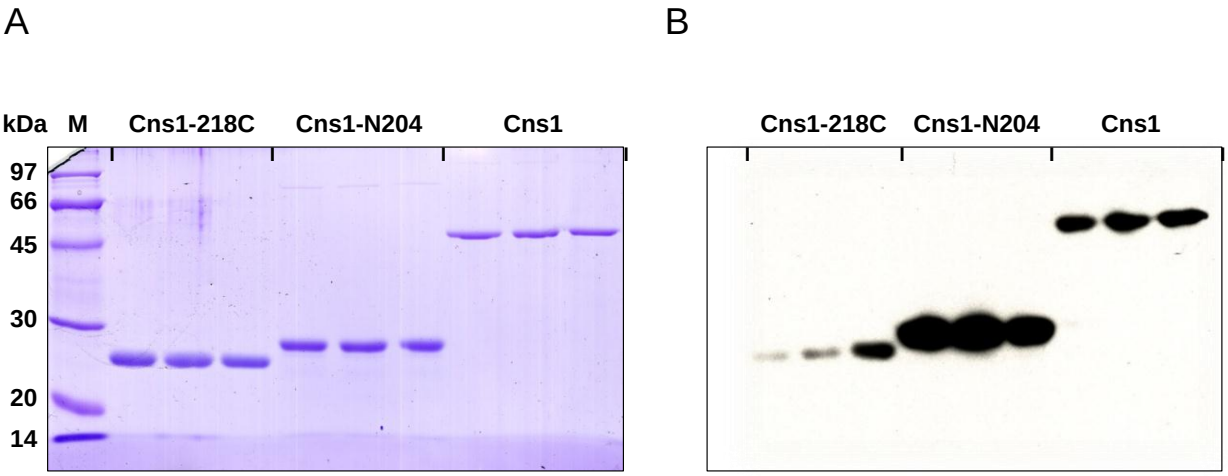

Figure 4-15: SDS-PAGE and Western Blot of Cns1, Cns1-218C and Cns1-N204.
(A) SDS-PAGE after protein purification using 12.5 % acrylamid-gel.
(B) Western Blot of the corresponding SDS-PAGE using the anti-Cns1-antibody.
Primary antibody (anti-Cns1-sera) was diluted 1:10000 in PBS. Anti-rabbit Peroxidase-conjugated IgG served as secondary antibody (1:8000). For detection the ECL detection kit was used (see Material and Methods).

As shown by SDS-PAGE (Figure 4-15, A), protein purification of Cns1 and both the N- and C-terminal domain revealed pure protein samples. Western Blot and incubation with the polyclonal anti-Cns1-antibody revealed that Cns1 and both the individual C- and N-terminal domain are detectable by use of this antibody. Additionally, no degradation of the proteins occurred during the preparation (Figure 4-15, B).

In order to test the correct folding of the individual N-terminal and C-terminal domains, CD-spectroscopy was performed.

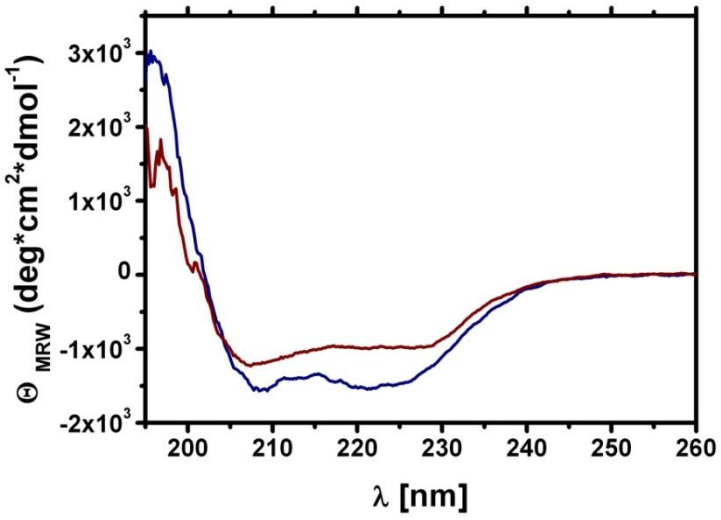

Figure 4-16: CD-spectra of Cns1-218C and Cns1-N204.
Cns1-218C (blue) and Cns1-N204 (red) were diluted in 40 mM KH_2PO_4/K_2HPO_4 (pH 7.5), 50 mM KCl to final concentrations of around 0.1 mg/ml. Spectra were recorded from 200 nm to 190 nm with 10 accumulations at 20°C.

Crystal formation of full length Cns1 was not observable. In order to get more structural information, an additional construct, Cns1-NΔ60, was generated. Here, the first 60 residues from the coding sequence of Cns1 were deleted. The N-terminal part in front of the TPR-domain is maybe rather flexible, which makes full length Cns1 not suitable for crystal formation. The coding sequence for Cns1-NΔ60 was cloned into pQE30 using BamH1 and SalI restriction sites. An additional thrombin cleavage site was introduced direct in front of the coding sequence of this construct in order to cleave the His_6-tag and the additional RGS-epitope derived from the vector. Cleavage of the His_6-tag was performed by using immobilized thrombin (SIGMA-ALDRICH). SDS-PAGE and Western blot was performed in order to check purity of the protein preparation and the thrombin cleavage reaction using the anti-His_6 Peroxidase-conjugated antibody.

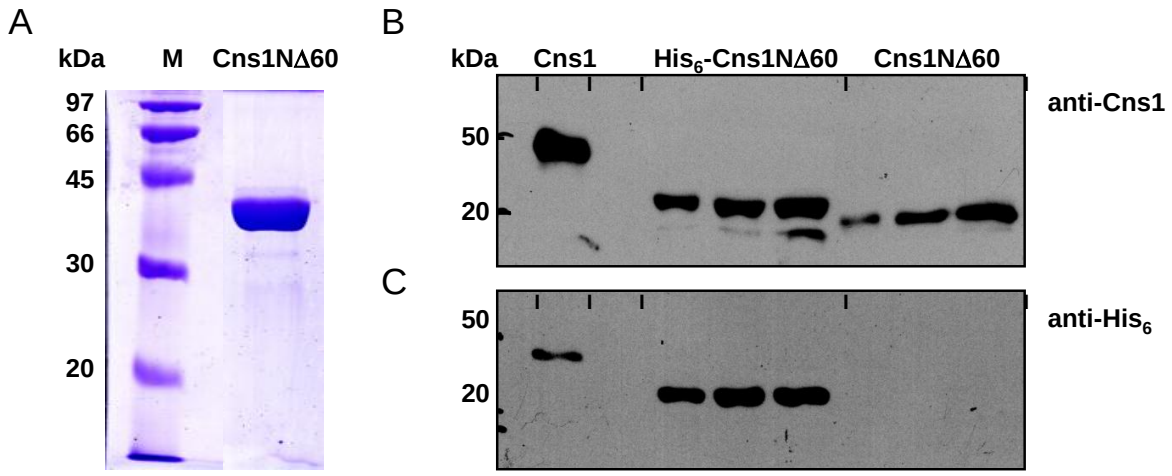

Figure 4-17: Characteristics of Cns1-NΔ60
(A) SDS-PAGE after protein purification using 12.5 % acrylamid-gel.
(B) Western Blot using the anti-Cns1-antibody as primary antibody. Primary antibody (anti-Cns1-antibody) was diluted 1:10000 in PBS, Anti-rabbit Peroxidase-conjugated IgG was used as secondary antibody (1:8000).
(C) Western Blot using the anti-His_6 Peroxidase-conjugated antibody. The antibody was diluted 1:12000. For detection the ECL detection kit was used (see Material and Methods). His_6-Cns1NΔ60 represents the protein before cleavage, Cns1NΔ60 the protein after cleavage with thrombin. His-tagged Cns1 (Cns1) was used as control.

Expression and purification of Cns1NΔ60 is working under the conditions used for Cns1-constructs (see Material and Methods). However, during preparation degradation occurred as shown by Western Blot. The anti-Cns1-antibody recognized an additional species whereas the anti-His-antibody did not. So, the protein was partially degraded from the N-terminus. Cleavage reaction with thrombin was proofed by Western Blot (Figure 4-17, B-C). As shown, digestion with thrombin leads to complete removal of the His-tag (Figure 4-17, C). CD-spectroscopy revealed correct folding of Cns1NΔ60 (Figure4-18).

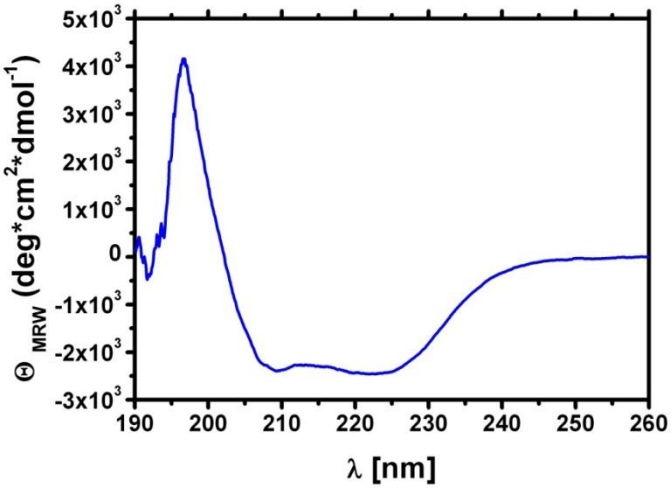

Figure 4-18: CD-spectrum of Cns1-NΔ60.
Cns1-NΔ60 was diluted in 40 mM KH_2PO_4/K_2HPO_4 (pH 7.5), 50 mM KCl to a final concentration of 0.1 mg/ml. Spectrum was recorded from 200 nm to 190 nm with 10 accumulations at 20°C.

This construct was generated for crystallization in order to get structural information of the TPR-domain. Different concentrations of this protein were used for crystallization experiments together with Eva Huber from the group of Prof. Michael Groll (Chair of Biochemistry, TU München). But it was not possible to obtain crystal formation even by using very high protein concentration (up to 40 mg/ml). Also addition of the TPR-binding peptide derived from Hsp90 (TEMEEVD) or Hsp70 (PTVEEVD) to the protein sample did not lead to crystal formation.

As purification of the TPR domain construct (residue 83-189, Figure 4-13) was not successful under conditions used before, different constructs containing the TPR domain of Cns1 were generated. Two constructs containing the TPR domain were cloned in the pET-SUMO vector for expression as SUMO-fusion proteins. Residues 60-204 and 70-204 of the coding sequence of Cns1 were used. Expression and purification of the SUMO-fusion proteins were performed as described before (see Material and Methods).

A B

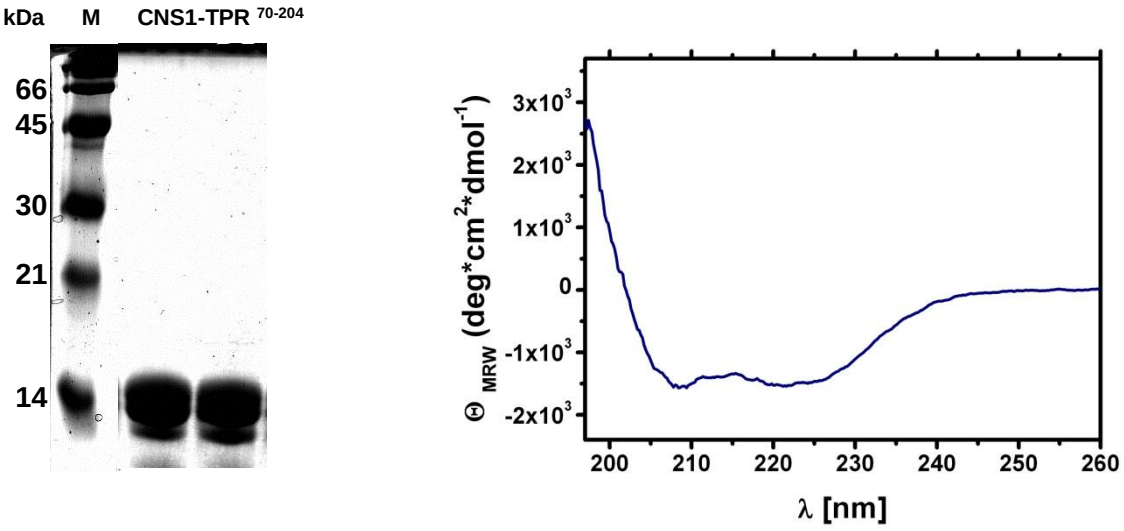

Figure 4-19: Characterization of Cns1-TPR$^{70-204}$.
(A) SDS-PAGE after protein purification using 15 % acrylamid-gel. M represents the LMW-Marker.
(B) CD-spectra of Cns1-TPR$^{70-204}$ was diluted in 40 mM KH_2PO_4/K_2HPO_4 (pH 7.5), 50 mM KCl to a final concentration of 0.1 mg/ml. Spectrum was recorded from 260 nm to 196 nm with 10 accumulations at 20°C.

As shown above purification of the TPR-domain, Cns1-TPR$^{70-204}$ was successful. However, the protein was partially degraded as shown by SDS-PAGE (Figure 4-19; A). Folding of Cns1-TPR$^{70-204}$ was proofed by CD-spectroscopy (Figure 4-19; B).

Expression and purification Cns1-TPR$^{60-204}$ lead to pure protein fractions (data not shown). However, mass analysis and an enzyme-coupled ATPase assay (data not shown) revealed that there is a contamination by DnaK, the Hsp70 of *E. coli*, in these protein preparations. The protein was concentrated up to around 50 mg/ml and the protein was used for crystallization experiments. Crystal formation of the TPR-domain of Sti1/Hop was successful in the presence of the Hsp90 (TEMEEVD) or Hsp70 peptide (PTVEEVD) (SCHEUFLER et al., 2000; SCHMID et al., 2012). The Hsp70 peptide PTVEEVD was added in a 2-fold molecular excess to the TPR-domains of Cns1 (Cns1-TPR$^{60-204}$, Cns1-TPR$^{70--204}$). However, no crystal formation was observed for the Cns1-TPR. Maybe the protein concentrations used for crystallization was still too low as crystallization of the TPR2B and TPR2A-TPR2B of Sti1 was done using protein concentrations of 70-120 mg/ml (SCHMID et al., 2012).

4.2.2. Protein-protein interaction by chemical crosslink

The structure of the C-terminal domain of Cns1 is already solved (unpublished, HAINZL PhD thesis, 2008). Pull down experiments with the C-terminal domain of Cns1 and yeast lysate showed no specific interaction with other proteins (data not shown). To identify specific binding of proteins to the C-terminal domain of Cns1 chemical crosslink was used. Therefore cysteine residues were introduced in the C-terminal domain of Cns1 by site directed mutagenesis (Figure 4-20, B). Based on the crystal structure different locations were used to introduce the cysteine residue. The residues that were changed are located at different sites of the molecule in order check different possible binding sites (Figure 4-20).

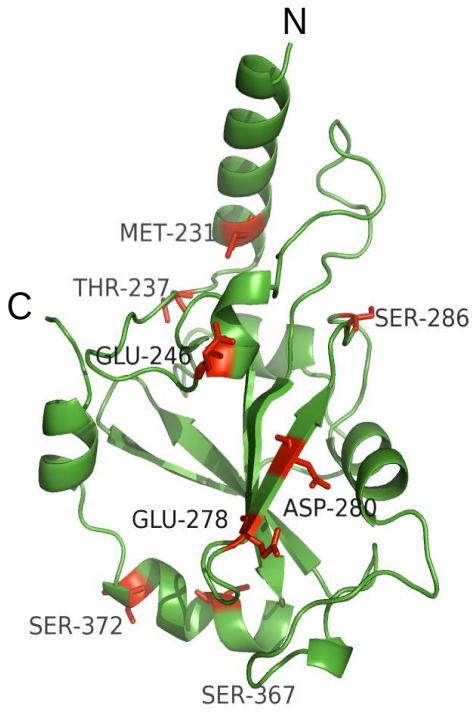

Figure 4-20: Crystal structure of C-terminal domain of Cns1 (unpublished; HAINZL, PhD thesis, 2008).
Overall structure of the C-terminal domain of Cns1, Cns1-213C, is shown in cartoon representation. The locations of the introduced cysteines in the overall structure are represented as sticks and are colored in red.

The Cns1-218C cysteine mutants were expressed and purified as described before (see Material and Methods). Folding of the single cysteine mutants was analyzed by CD-spectroscopy and revealed no changes in folding compared to Cns1-218C (data not shown). For cross linking, the single cysteine mutants of Cns1-218C were incubated with

50-fold molar excess of the hetero-bifunctional crosslinker 4-(N-malimido)-benzophenone. This crosslinking agent reacts with the sulfhydryl group of the cysteine residue via thioether formation. Site-specific reaction of the protein with the crosslinker was monitored by mass analysis (data not shown). During UV irradiation at 250 nm binding to a potential interacting protein occurs via a diradical excited state. Cns1-218C-Cys was incubated with 1 ml yeast lysate ($c_{protein}$ ~ 1 mg/ml) for 20 min at room temperature and were UV-irradiated. Various times of irradiation were tested. Cross linking was visualized by SDS-PAGE and Western blot. Additionally, cross linked complexes within the sample were purified using NiNTA Spin Columns as described before (see Material and Methods).

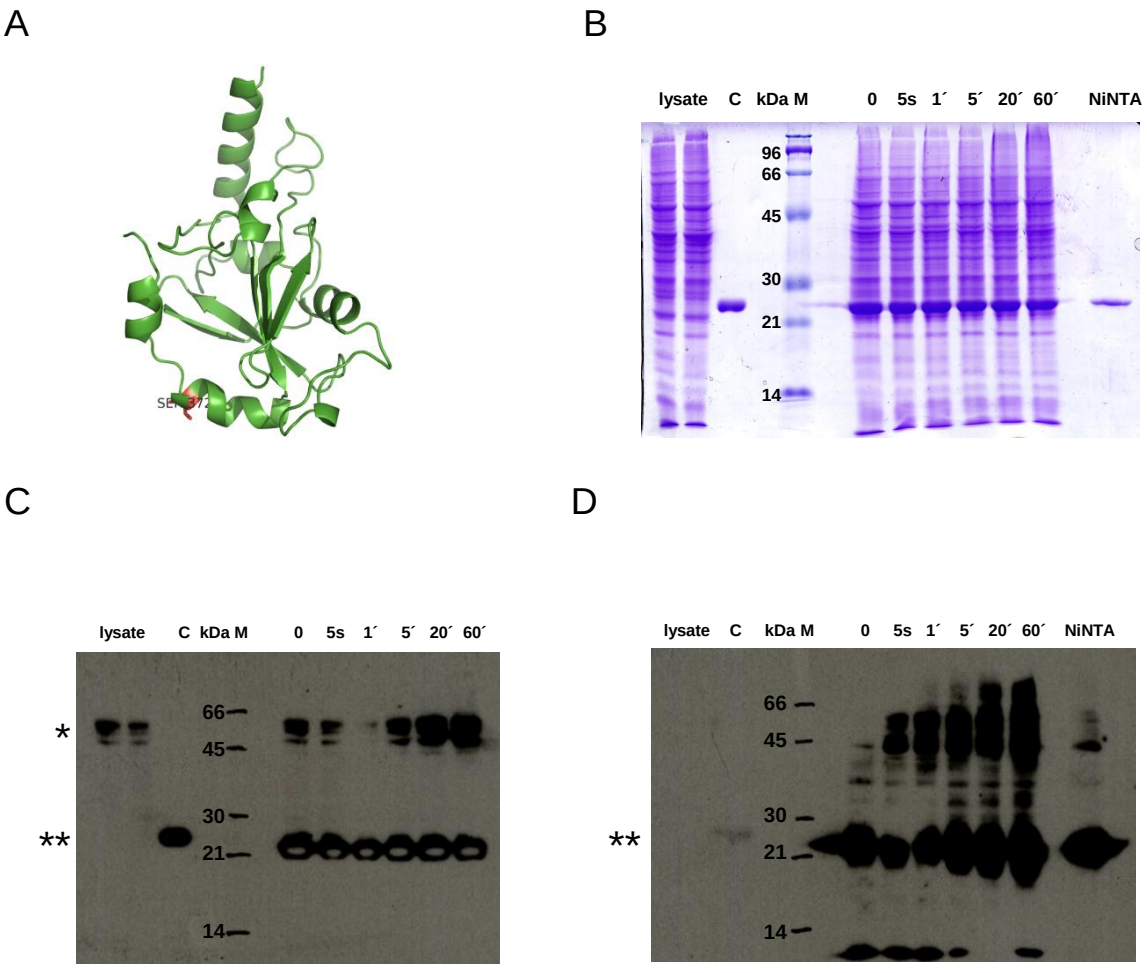

Figure 4-21: Chemical cross-linking of Cns1-218C-S372C with yeast lysate.
(A) Location of Ser 372 within the crystal structure of Cns1-218C.
(B) SDS-PAGE of the cross link reaction
(C) Western Blot of the corresponding SDS-PAGE. Anti-Cns1-antibody was used as primary antibody and was diluted 1:10000. Anti-rabbit Peroxidase-conjugated IgG served as secondary antibody (1:8000).
(D) Western Blot using the anti-His_6 Peroxidase-conjugated antibody. The antibody was diluted 1:12000. For detection the ECL detection kit was used (see Material and Methods).
C represents control sample (Cns1-218C), NiNTA the purified sample after the cross link reaction. Native Cns1 (*) and the C-terminal domain of Cns1 (**) are marked on the left side. Different irradiation times were used as indicated above the SDS-PAGE and the Western Blots.

As shown for the Cns1-218C-S372C mutant, no interacting protein could be cross-linked within the yeast lysate. After purification of the cross-linked complexes over NiNTA spin columns, no additional species was detected (Figure 4-21, B, D) indicating that either crosslinking was not successful or that no specific protein protein interaction occurred. By Western Blot using the anti-His_6-Peroxidase conjugated IgG a second dominant species could be detected (Figure 4-21, D). Mass analysis showed that only the Cns1 protein itself could be cross-linked implying a functional cross-link reaction under the used conditions. As protein interactions are site-specific other mutants were tested with this assay. But no protein interaction with the C-terminal domain of Cns1 could be detected within yeast lysate. Other cross-link reactions (EDC-NHS, see Material and Methods) which were also tested, did not lead to identification of a partner protein of the isolated C-terminal domain of Cns1 (data not shown).

4.2.3. Integration of Cns1 within the Hsp90 chaperone cycle

4.2.3.1. Interaction of Cns1 with Hsp90

Cns1 is known to interact with Hsp90 via its TPR domain, which is able to bind with the very C-terminal MEEVD peptide of Hsp90 (TESIC et al., 2003; HAINZL et al, 2004). Additionally, it could be shown that the interaction of Cns1 with Hsp90 is essential when the large PPIase Cpr7 is deleted. So, the C-terminal peptide of Hsp90 which mediates the binding to the TPR-containing co-chaperones is essential when Cpr7 is deleted and Cns1 function is impaired (TESIC et al., 2003).

To study specific interactions of Hsp90 and Cns1 in context of the chaperone cycle, purified proteins were used for ATPase assays and analytical ultracentrifugation. First, the influence of Cns1 on Hsp90 ATPase activity was tested.

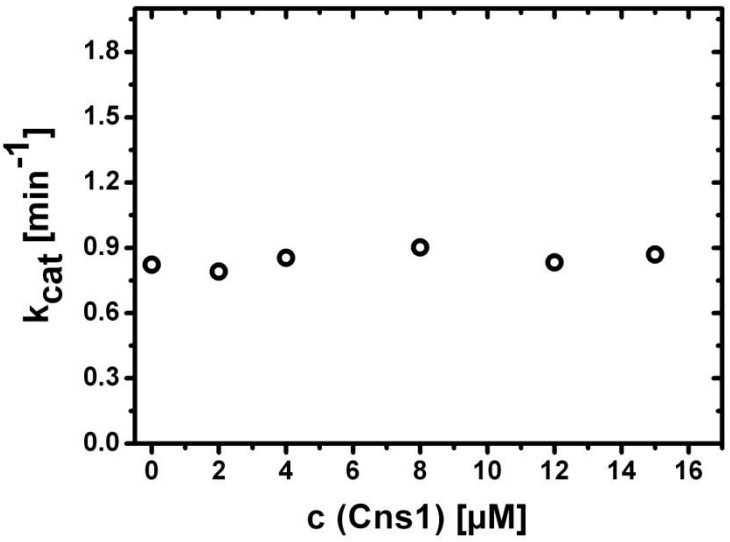

Figure 4-22: Influence of Cns1 on ATPase activity of Hsp90wt.
Hsp90wt was diluted in 40 mM HEPES/KOH (pH 7.5) 20 mM KCl, 5 mM $MgCl_2$, 2 mM PEP, 0.15 mM NADH, 0.1 %PK, and 0.4 % LDH to final concentration of 1.0 µM and was incubated with various amounts of Cns1. Assays were performed at 30°C and were started with addition of ATP to a final concentration of 500 µM.

As seen above, Cns1 has no influence on the ATPase activity of Hsp90. Also Cns1 itself showed no ATPase activity (data not shown) which is in agreement with previous work (HAINZL et al., 2004).

Analytical ultracentrifugation is a common method to study the association of proteins. Here, Cns1 was labeled with AlexaFluor488-dye which reacts with exposed lysine residues especially the primary amine. For labeling, Cns1 (5-7 mg/ml) was incubated with the AlexaFluor488. Afterwards the resulting labeling efficiency of 1.4 (c [protein]/c [Label]) was calculated according to manufacturer's protocol (see Material and Methods).

For analytical ultracentrifugation AlexaFluor488-Cns1 was diluted in buffer (40 mM HEPES/KOH (pH 7.5), 50 mM KCl, 5 mM $MgCl_2$) to a final concentration of 500 nM. In order to test complex formation with Hsp90, 500 nM AlexaFluor488-Cns1 were incubated with 1 µM Hsp90. Analytical ultracentrifugation was performed at 20°C and a constant rotational speed of 42000 rpm.

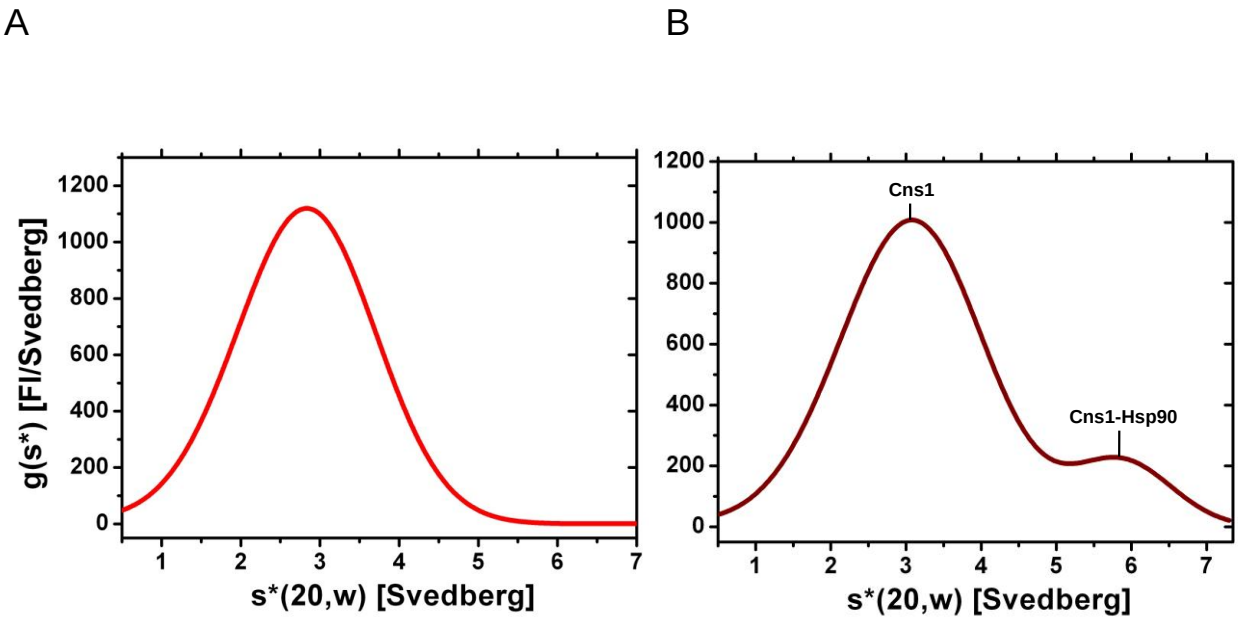

Figure 4-23: Sedimentation profile for Alexa488-Cns1 and association with Hsp90.
Analytical ultracentrifugation was performed with Alexa488-labeled Cns1. Sedimentation of Alexa488-Cns1 was detected by the fluorescence optical system. Analysis of aUC data was performed with DCDT+. A plot of g(s*) is shown, whereas s*(20,w) represents the sedimentation coefficient normalized for water and 20°C. Raw data of aUC were fitted according Gauss equation.
(A) Sedimentation profile of 500 nM Cns1.
(B) Sedimentation profile of 500 nM Cns1 in the presence of 1 µM Hsp90.
Resulting species are marked above, where Cns1 represents unbound Cns1 and Cns1-Hsp90 the associated complex.

AlexaFluor488-Cns1 showed a sedimentation coefficient of around 3 s (Figure 4-23; A). From data analysis and the corresponding fit, a molecular mass of around 41 kDa was calculated. Thus, in solution Cns1 is a monomer. This is in agreement with previous work (TESIC et al., 2003; HAINZL et al., 2004) indicating that the Alexa488-labeled Cns1 used for analytical ultracentrifugation showed no altered oligomerisation.

Addition of Hsp90 leads to complex formation with the labeled Cns1, which is detectable at higher sedimentation values of around 6 s (Figure 4-23; B). Thus, the binding affinity of Cns1 to Hsp90 seems to be quite low as the major fraction of Cns1 is not bound to Hsp90 under the used conditions. The binding affinity of Cns1 to Hsp90 was determined by SPR to around 5 µM (HAINZL et al., 2004). Labeling of Cns1 with AlexaFlour488 did not disturb binding to Hsp90.

To determine if the binding of Cns1 is dependent on Hsp90 conformation, analytical ultracentrifugation runs were performed. Here, Hsp90 was titrated to labeled Cns1. Addition of AMP-PNP, a non-hydrolysable ATP-analog, lead to the closed conformation of Hsp90 whereas in the presence ADP the open conformation is adopted. Labeled Cns1 (500 nM) was incubated with various amounts of Hsp90 in the presence of either AMP-PNP or ADP and analytical ultracentrifugation was performed at 20°C and a constant rotational speed of 42000 rpm.

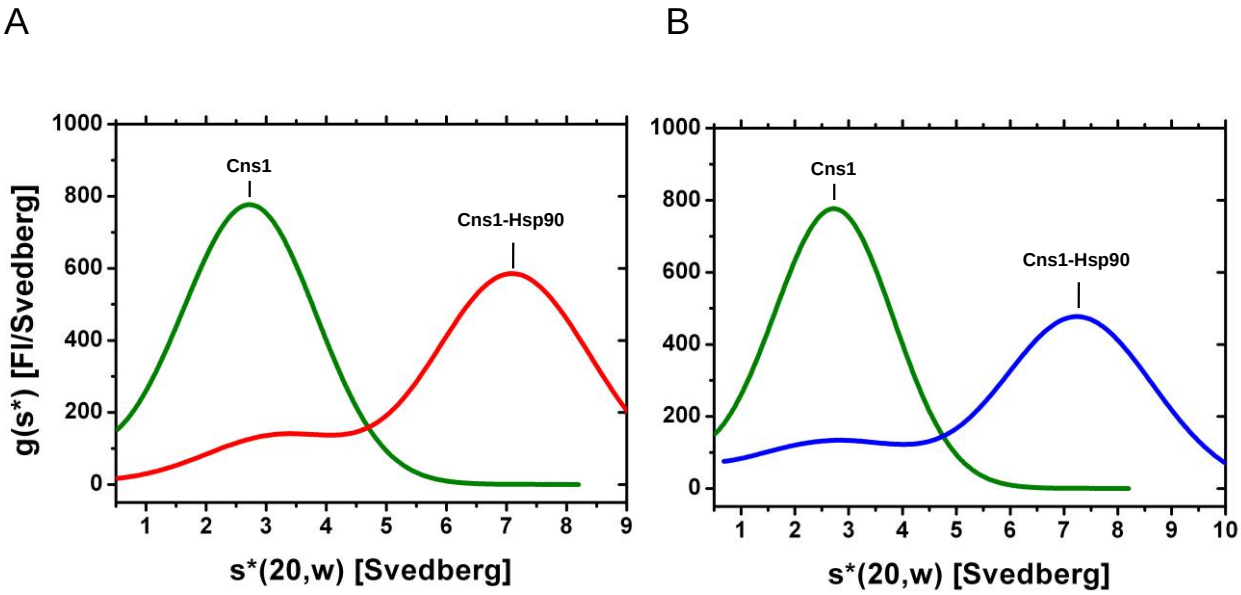

Figure 4-24: Sedimentation profile for Alexa488-Cns1 and association with Hsp90 in the presence of nucleotides.
Analytical ultracentrifugation was performed with Alexa488-labeled Cns1. Sedimentation of Alexa488-Cns1 was detected by the fluorescence optical system. Analysis of aUC data was performed with DCDT+. A plot of g(s*) is shown, whereas s*(20,w) represents the sedimentation coefficient normalized for water and 20°C. Raw data of aUC were fitted according Gauss equation.
(A) Sedimentation profile of 500 nM Cns1 (green curve) and complex formation with the ADP-bound, open conformation of Hsp90 (15 µM, red).
(B) Sedimentation profile of 500 nM Cns1 (green curve) and complex formation with the AMP-PNP-bound, closed conformation of Hsp90 (15 µM, blue curve).
Resulting species are marked above, where Cns1 represents unbound Cns1 and Cns1-Hsp90 the associated complex.

The complex formation of Cns1 with Hsp90 was also observable in the presence of defined conformational states of Hsp90 (Figure 4-24). Titration of various amounts of Hsp90 to Cns1 followed by analytical ultracentrifugation revealed that the binding affinities for both nucleotide-bound states of Hsp90 seem to be in a similar range (data not shown). Thus, Cns1 does not prefer a specific Hsp90 conformation in contrast to other co-chaperones like Sti1 and Sba1 (SULLIVAN et al., 2002; RICHTER et al.,2003 and 2004; MCLOUGHLIN et al., 2006; ONUOHA et al. 2008).

Subunit exchange reaction of Hsp90 can be detected using Förster resonance energy transfer (FRET) of labeled Hsp90 dimers (HESSLING et al., 2009). For Sti1, it could be shown that the subunit exchange reaction is nearly completely inhibited (LEE et al., 2012). Addition of Cns1 showed no effect on the subunit exchange reaction of Hsp90 (data not shown).

Cns1 contains a TPR domain which binds specifically to the C-terminus of Hsp90. In pull down experiments in yeast lysates with His_6-Hsp90ΔMEEVD as the sole source of Hsp90, Cns1 was also detected in Hsp90 complexes. In this yeast strain, the C-terminal peptide of

Hsp90 which mediates binding to the TPR-containing co-chaperones was deleted. Whether this interaction is direct or is mediated by another binding partner remained unclear (TESIC et al., 2003). Sgt1/Rar1, another TPR containing protein, is also able to associate with Hsp90 even when the carboxy terminus is truncated (PEARL et al., 2001; ZHANG et al., 2010). Furthermore, for client chaperoning it was proposed that TPR-containing co-chaperones may have additional binding sites in the N-terminal domain of Hsp90 which seems important to coordinate binding to multiple TPR-containing co-chaperones (CHADLI et al., 2008). To test if Cns1 is able to bind to purified Hsp90 lacking the C-terminal peptide (Hsp90ΔMEEVD), analytical ultracentrifugation was performed. However, no binding of Cns1 is observable to Hsp90ΔMEEVD even in the presence of a 40-fold molar excess of Hsp90ΔMEEVD (data not shown). Additionally, binding of Cns1 to either the N-terminal domain or the C-terminal domain of Hsp90 was tested using analytical ultracentrifugation.

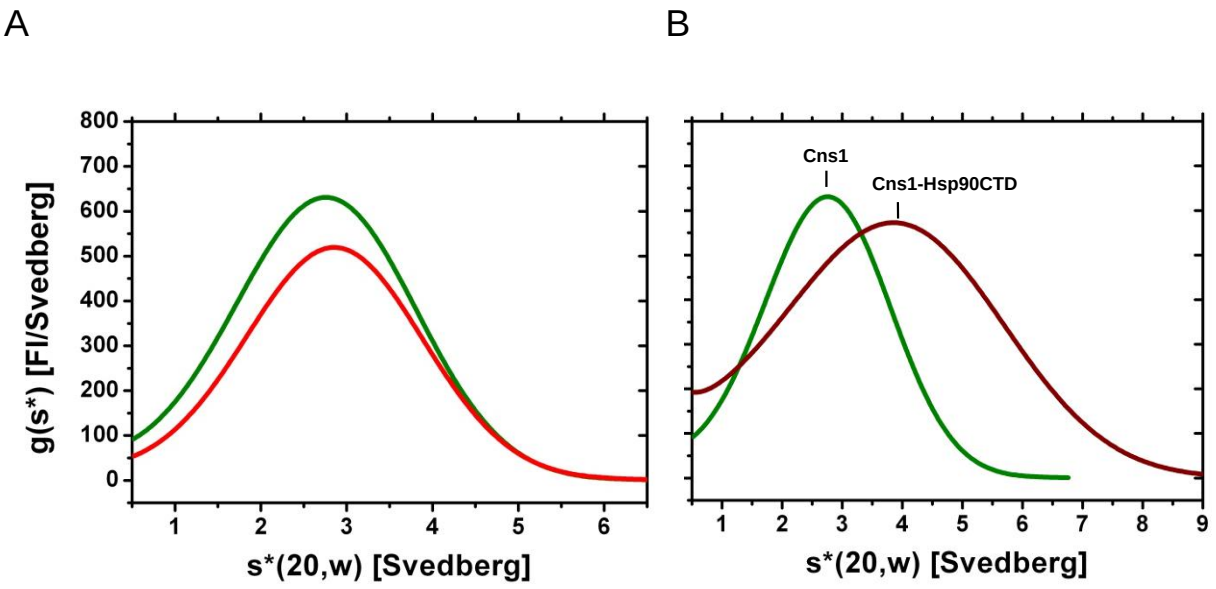

Figure 4-25: Sedimentation profile for Alexa488-Cns1 and association with individual Hsp90 domains.
Analytical ultracentrifugation was performed with Alexa488-labeled Cns1. Sedimentation of Alexa488-Cns1 was detected by the fluorescence optical system. Analysis of aUC data was performed with DCDT+. A plot of g(s*) is shown, where s*(20,w) represents the sedimentation coefficient normalized for water and 20°C. Raw data of aUC were fitted according to the Gauss equation.
(A) Sedimentation profile of 500 nM Cns1 (green curve) alone and in the presence of the N-terminal domain of Hsp90 (25 µM, red curve).
(B) Sedimentation profile of 500 nM Cns1 (green curve) and complex formation with the C-terminal domain of Hsp90 (Hsp90-CTD, 10 µM, dark red curve).
Resulting species are marked above, where Cns1 represents unbound Cns1 and Cns1-Hsp90-CTD the associated complex.

Cns1 formed no complexes with the individual N-terminal domain of Hsp90 even in the presence of a 50-fold molar excess of the Hsp90 N-terminal domain (Figure 4-25, A). Addition of the C-terminal domain of Hsp90 leads to complex formation with Cns1 (Figure 4-25, B). Titration of various amounts of the C-terminal domain to Cns1 followed by aUC revealed that in the presence of a 4-fold molar excess of Hsp90-CTD no unbound Cns1 is detectable (data not shown). So, Cns1 is bound specifically to the C-terminal domain of Hsp90. Additionally, Cns1-218C was labeled with AlexaFluor488 as described before. By analytical ultracentrifugation with labeled Cns1-218C it could be shown that the C-terminal domain of Cns1 is also monomeric in solution. Incubation with Hsp90 or individual Hsp90 domains did not lead to complex formation (data not shown). So, the binding site of Cns1 is located in the C-terminal domain of Hsp90. No additional binding site of Cns1 for binding to Hsp90 was found.

4.2.3.2. Influence of Co-chaperones on Cns1-Hsp90 complex formation

As shown for Sti1, Cpr6, Sba1 and Aha1 co-chaperones are able to form mixed complexes with Hsp90 (RICHTER et al., 2004; RETZLAFF et al., 2010, LI et al., 2011, LI, SOROKA AND BUCHNER, 2012). For progression of the chaperone cycle, it is essential to recruit co-chaperones at different stages within the chaperone cycle. Therefore it is important to determine where co-chaperones can form hetero-trimeric complexes with Hsp90.

4.2.3.2.1. Influence of Aha1 on Cns1-Hsp90-complex formation

As known from structural features and our work on the regulation of Hsp90 by its co-chaperone Aha1, the complete binding site of Aha1 to Hsp90 is determined (MEYER et al., 2004; RETZLAFF et al., 2010). In the case of binding of Aha1 to Hsp90, the C-terminal domain of Hsp90 is free for interaction with TPR containing co-chaperons to form ternary complexes. For Aha1 it was shown that it could form mixed Hsp90 complexes with Sba1 or Sti1 (RETZLAFF et al., 2010). Here, the influence of Aha1 on Cns1-Hsp90 complex formation was tested. Various amounts of Aha1 were incubated with the preformed Cns1-Hsp90 complex (Figure 4-23) in the presence of AMP-PNP and analytical ultracentrifugation runs were performed.

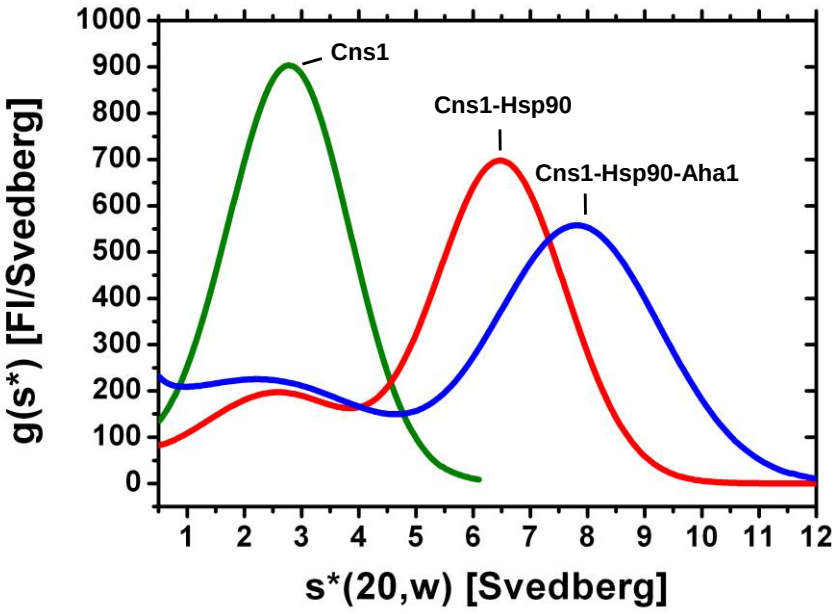

Figure 4-26: Influence of Aha1 on Cns1-Hsp90 complex formation.
Analytical ultracentrifugation was performed with Alexa488-labeled Cns1. Sedimentation of Alexa488-Cns1 was detected by the fluorescence optical system. Analysis of aUC data was performed with DCDT+. A plot of g(s*) is shown, where s*(20,w) represents the sedimentation coefficient normalized for water and 20°C. Raw data of aUC were fitted according to the Gauss equation.
Sedimentation profile of 500 nM Cns1 (green curve) alone and in the complex with the AMP-PNP-bound, closed state of Hsp90 (8 µM, red curve). Addition of Aha1 (15 µM) leads to a shift in sedimentation coefficient indicating the formation of a ternary complex (blue curve).
Resulting species are marked above, where Cns1 represents unbound Cns1, Cns1-Hsp90 the associated complex and Cns1-Hsp90-Aha1 the ternary complex.

Addition of Aha1 did not lead to the disruption of the Cns1-Hsp90 complex. As the complex peak was shifted towards higher Svedberg-values, a mixed complex remains possible (Figure 4-26). Additionally, Cns1 showed no binding to Aha1 under these conditions (data not shown). The binding sites of both co-chaperones are located in different parts of Hsp90, so there is no direct competition. As shown above, Cns1 did not prefer a specific conformation of Hsp90 (Figure 4-23). Cns1 itself did not influence the Hsp90 conformation. As shown by analytical ultracentrifugation, Aha1 did not disrupt the Cns1-Hsp90-complex. Maybe the stimulatory effect of Aha1 on the Hsp90 ATPase activity is influenced by simultaneous binding of Cns1 and Aha1 to Hsp90. Therefore, the ATPase activity of preformed Cns1-Hsp90-complexes in the presence of saturating amounts of Aha1 was measured.

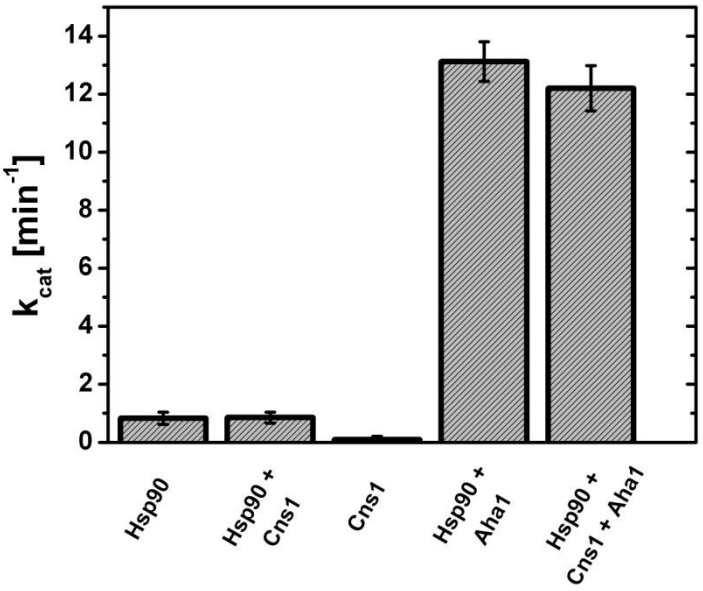

Figure 4-27: Influence of Cns1 on the ATPase activity of Hsp90 in the presence of Aha1.
Hsp90wt was diluted in 40 mM HEPES/KOH (pH 7.5) 20 mMKCl, 5 mM $MgCl_2$, 2 mM PEP, 0.15 mM NADH, 0.1 %PK, and 0.4 % LDH to a final concentration of 1.0 µM and was incubated with Aha1 (10 µM) or Aha1 (10 µM) and Cns1 (15 µM). Assays were performed at 30°C and were started with addition of ATP to a final concentration of 500 µM.

The ATPase activity of Hsp90 is stimulated by Aha1 whereas Cns1 has no effect (Figure 4-4; Figure 4-27). The presence of saturating amounts of Cns1did not influence the stimulatory effect on the ATP hydrolysis rate of Hsp90 by Aha1 (Figure 4-27).

Taken together, Hsp90 is able to form mixed complexes with Cns1 and Aha1. The specific stimulatory effect on the ATPase activity of Hsp90 by Aha1 is not influenced upon simultaneous binding of Cns1.

4.2.3.2.2. Influence of Sti1 on Cns1-Hsp90-complex

Sti1, the yeast homolog of Hop, connects the chaperone cycle of Hsp70 and Hsp90 (see introduction) and is therefore thought to be responsible for the substrate transfer between these chaperone cycles (WANDINGER et al., 2008; SMITH AND TOFT et al., 2008; SCHMID et al., 2012). It contains multiple TPR-domains which enabled Sti1 to bind Hsp90 and Hsp70 to

form the intermediate complex (SMITH, 1993). The TPR-domains within Sti1 and the human homolog Hop exhibit different affinities for Hsp90 and Hsp70, as shown previously (SCHEUFLER et al., 2003; SCHMID et al., 2012).

Sti1 and Cpr6, which are TPR-containing Co-chaperones, are able to bind simultaneously to Hsp90 resulting in the formation of ternary complexes (LI et al., 2011). In order to test if Sti1 is able to bind to the Cns1-Hsp90-complex, analytical ultracentrifugation was performed. Complex formation of labeled Cns1 and Hsp90 was achieved as described before (Figure 4-23). Various amounts of Sti1 were added to the preformed Cns1-Hsp90 complex.

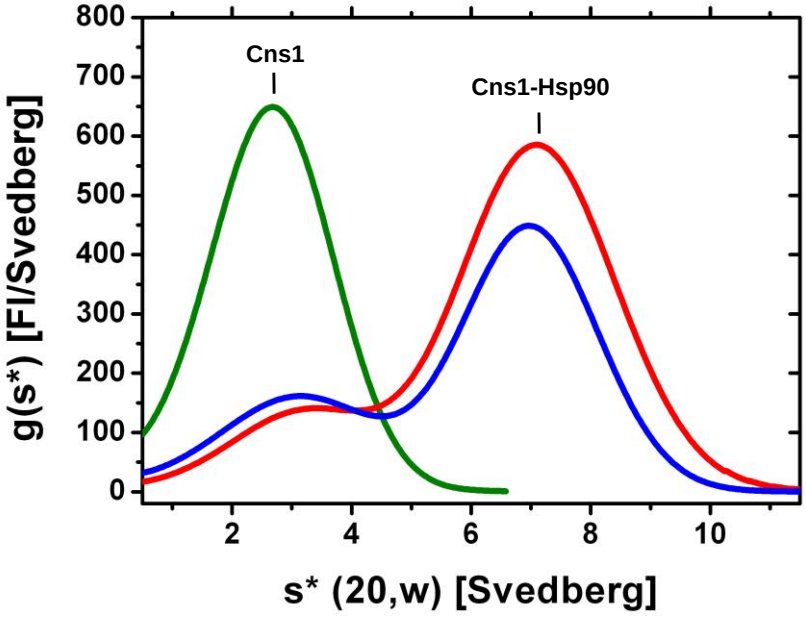

Figure 4-28: Influence of Sti1 on Cns1-Hsp90 complex formation
Analytical ultracentrifugation was performed with Alexa488-labeled Cns1. Sedimentation of Alexa488-Cns1 was detected by the fluorescence optical system. Analysis of aUC data was performed with DCDT+. A plot of g(s*) is shown, whereas s*(20,w) represents the sedimentation coefficient normalized for water and 20°C. Raw data of aUC were fitted according to the Gauss equation.
Sedimentation profile of 500 nM Cns1 (green curve) alone and in the complex with the ADP-bound, open state of Hsp90 (8 µM, red curve). Addition of Sti1 (20 µM) did not disrupt the associated complex of Cns1 and Hsp90 (blue curve).
Resulting species are marked above, where Cns1 represents unbound Cns1 and Cns1-Hsp90 the associated complex.

As shown by analytical ultracentrifugation, Sti1 did not disrupt the Cns1-Hsp90 complex nor was it integrated in the complex which would have resulted in a larger Svedberg-value (Figure 4-28). Interestingly, from ITC and SPR data it is known that Sti1 has a 5-fold higher

affinity to Hsp90 compared to Cns1 (HAINZL et al., 2003, SCHMID et al., 2012). Also, Hsp90 is in molecular excess to Cns1 indicating that only one Cns1 is bound to the Hsp90 dimer. So, in principle there is one binding site at the C-terminal domain of Hsp90 left for binding of other TPR containing co-chaperones. However, Sti1 is not forming a mixed complex with Hsp90 and Cns1. This was also proven by cross-linking of purified proteins and mass analysis. Only Cns1-Hsp90 or Sti1-Hsp90 complexes were detectable (data not shown). To check if Cns1 is able to disrupt a preformed Sti1-Hsp90 complex, FRET experiments were performed. To this end, FRET-complex of Sti1 and Hsp90 was used which was investigated previously (LI et al. 2011).

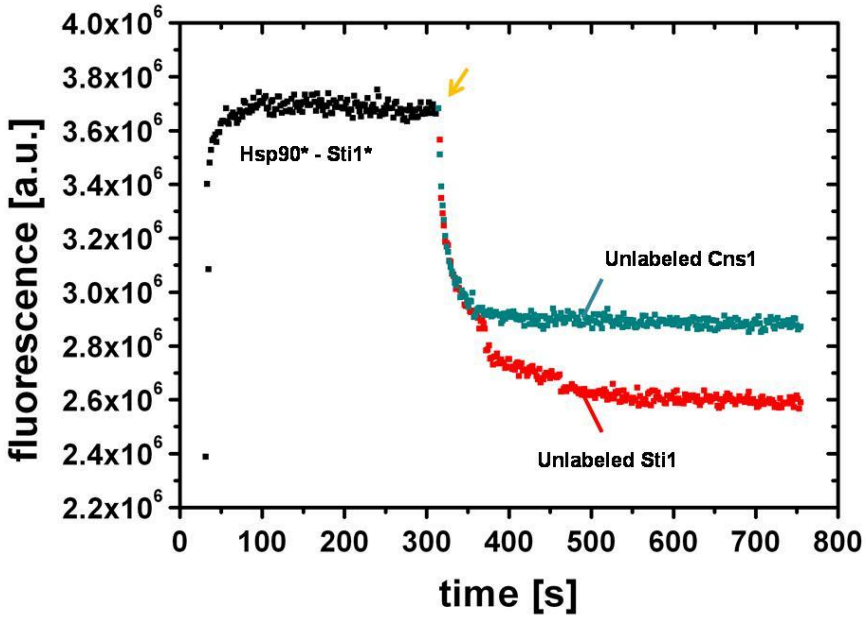

Figure 4-29: Release of Sti1 from the Hsp90 complex.
FRET assay of complex formation of Hsp90* (Atto550-labeled Hsp90) and Sti1* (Alexa488-labeled Sti1) is shown. 300 nM Hsp90* were added to 300 nM Sti1* and the binding kinetics of the complex formation were recorded (black plot). Addition of excess amounts of unlabeled Sti1 or Cns1 results in competition with donor fluorophore for the formation of Hsp90 complexes. The orange arrow indicates the addition of the unlabeled proteins. Measurement was performed by Jing Li.

The FRET assay revealed that Cns1 is able to release Sti1 from Hsp90 which was determined by disruption of the FRET complex (Figure 4-29). Data from analytical ultracentrifugation showed, that Sti1 is not able to bind to Hsp90 in the presence of Cns1. The FRET assay supports these findings, indicating that Cns1 disrupt the Sti1-Hsp90 complex.

To determine the binding constant (K_D) of Cns1 to Hsp90 in solution, ITC measurements were performed. Binding to full length Hsp90 was not detectable with ITC under the used conditions. So, binding studies with the TEMEEVD peptide were performed. ITC revealed a binding affinity of Cns1 of around 3 µM to the TPR-binding peptide of Hsp90 (data not shown). The binding affinity of Cns1 to full length Hsp90 was determined by SPR to ~ 6 µM (HAINZL et al., 2004). In solution binding of Cns1 to the TEMEEVD peptide showed a higher binding affinity to Hsp90. However, the binding affinity to full length Hsp90 seems to be lower compared to the TPR binding peptide. The dissociation constants of the individual TPR-domains of Sti1 to the TPR-binding peptide of Hsp90 were also determined by ITC and ranged from 1 µM (TPR2A) to 17 µM (TPR1) (SCHMID et al., 2012). So, the binding affinities of Cns1 and Sti1 to Hsp90 are in a same range. In the presence of both Sti1 and Cns1, the dominant species is the Cns1-Hsp90 complex.

Sti1 is known as non-competitive inhibitor of the Hsp90 ATPase activity as binding of Sti1 to Hsp90 arrests conformational states (RICHTER et al., 2003; HESSLING et al., 2009). Sti1 did not influence Cns1-Hsp90 complex formation and Cns1 was shown to displace Sti1 from Hsp90 (Figure 4-28). So, the ability of Sti1 to inhibit the ATPase activity of Hsp90 in presence of Cns1 was tested.

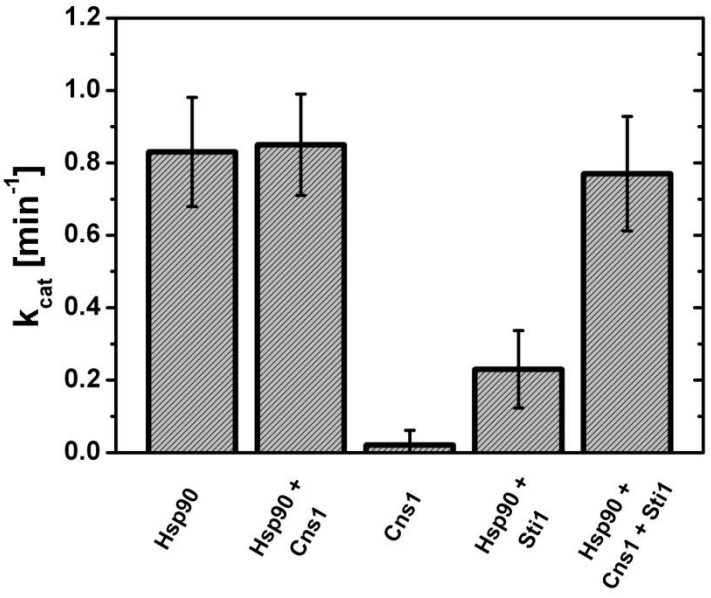

Figure 4-30: Influence of Cns1 on the ATPase activity of Hsp90 in the presence of Sti1.
Hsp90wt was diluted in 40 mM HEPES/KOH (pH 7.5) 20 mMKCl, 5 mM $MgCl_2$, 2 mM PEP, 0.15 mM NADH, 0.1 %PK, and 0.4 % LDH to a final concentration of 1.0 µM and was incubated with Sti1 (4 µM) or Sti1 (4 µM) and Cns1 (10 µM). Assays were performed at 30°C and were started with addition of ATP to a final concentration of 500 µM.

As shown above, Sti1 is able to inhibit the ATPase activity Hsp90. However, addition of Cns1 restores the Hsp90 ATPase activity indicating release of Sti1 from Hsp90 by Cns1. Taken together, Hsp90 is not able to form mixed complexes with Cns1 and Sti1 in contrast to ternary complex formation of Hsp90 and the TPR-containing co-chaperones Sti1 and Cpr6 (LI et al., 2011).

4.2.3.2.3. Influence of Cpr6, Cpr7 and Ppt1 on Cns1-Hsp90-complex

Another group of co-chaperones in yeast are the TPR-containing peptidyl-prolyl-isomerases (PPIases), Cpr6 and Cpr7. They were identified from studies with steroid hormone receptor complexes (DUINA et al., 1996). In addition to the TPR-domain which is responsible for binding to Hsp90, these proteins contain a PPIase domain, which catalyze the interconversion of cis-trans-isomers of proline peptide bonds (FANGHANEL et al., 2004). Furthermore, an independent chaperone function was shown for most of the large PPIases (BOSE et al., 1996; FREEMAN et al., 1996; PIRKL AND BUCHNER; 2001).

Cns1 was found as a suppressor of a Cpr7 deletion strain, which showed a slow growth phenotype (DOLINSKI et al., 1999). Additionally, overexpression of Cpr7 could rescue viability when Cns1 function is impaired. Additionally, an interaction of Cns1 with Cpr7 was observed but whether this interaction is direct or mediated by an additional interaction partner remained unclear (TESIC et al., 2003). Cpr7 and Cns1 are thought to share an essential function within the Hsp90 cycle. In order to test the influence of Cpr6 and Cpr7 on Cns1-complex formation, analytical ultracentrifugation was performed.

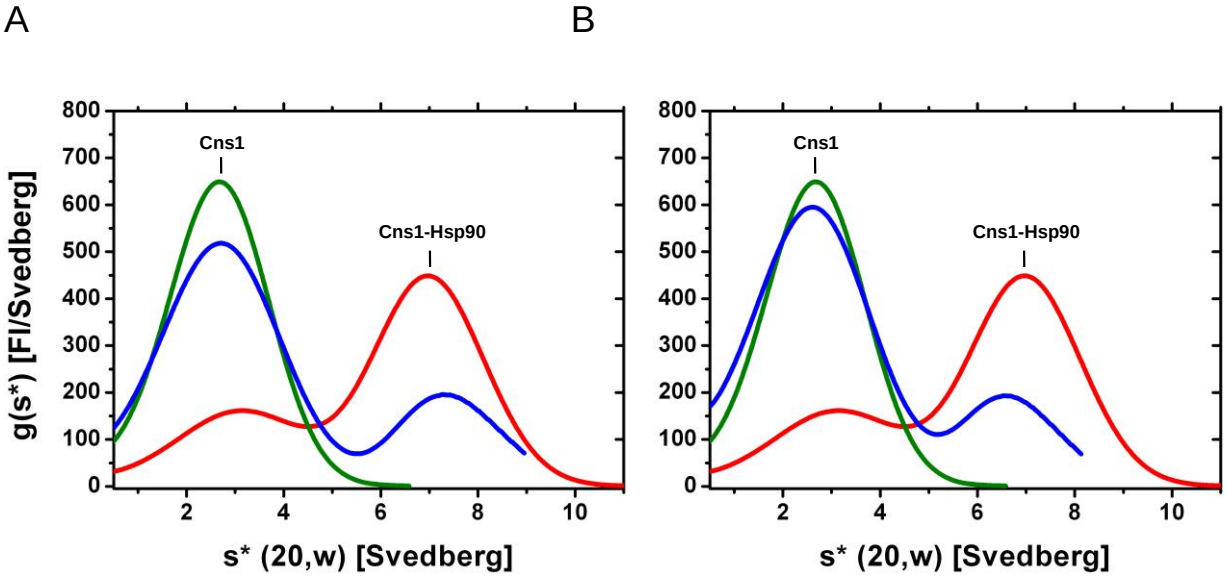

Figure 4-31: Influence of Cpr6 and Cpr7 on Cns1-Hsp90 complex formation
Analytical ultracentrifugation was performed with Alexa488-labeled Cns1. Sedimentation of Alexa488-Cns1 was detected by the fluorescence optical system. Analysis of aUC data was performed with DCDT+. A plot of g(s*) is shown, where s*(20,w) represents the sedimentation coefficient normalized for water and 20°C. Raw data of aUC were fitted according to the Gauss equation.
(A) Sedimentation profile of 500 nM Cns1 (green curve) alone and in the complex with Hsp90 (8 µM, red curve). Addition of Cpr6 (20 µM) leads to disruption of the Cns1-Hsp90-complex (blue curve).
(B) Sedimentation profile of 500 nM Cns1 (green curve) alone and in the complex with Hsp90 (8 µM, red curve). Addition of Cpr7 (20 µM) leads to disruption of the Cns1-Hsp90-complex (blue curve).
Resulting species are marked above, where Cns1 represents unbound Cns1 and Cns1-Hsp90 the associated complex.

As detected by analytical ultracentrifugation, Cpr6 and Cpr7 release Cns1 from Hsp90 (Figure 4-31). So, neither Cpr6 nor Cpr7 are able to bind simultaneously with Cns1 to Hsp90. Cpr6 is able to form mixed complexes with Hsp90 and the TPR-containing Co-chaperone Sti1 (LI et al., 2011). However, in the presence of Cns1, no mixed complexes were observable. As proven by analytical ultracentrifugation, Cns1 showed no direct binding to either Cpr6 or Cpr7 (data not shown).

Ppt1 is also a member of the TPR-containing co-chaperones. Additionally, the C-terminal domain of this protein is a phosphatase. Binding of Ppt1 to Hsp90 leads to abrogation of the autoinhibition of the phosphatase function of Ppt1 (KANG et al., 2001). Ppt1 is responsible for specific dephosphorylation of Hsp90 and Cdc37 (WANDINGER et al., 2006; VAUGHAN et al., 2008).

Here, complex formation of Cns1 and Hsp90 in the presence of Ppt1 was tested by use of analytical ultracentrifugation.

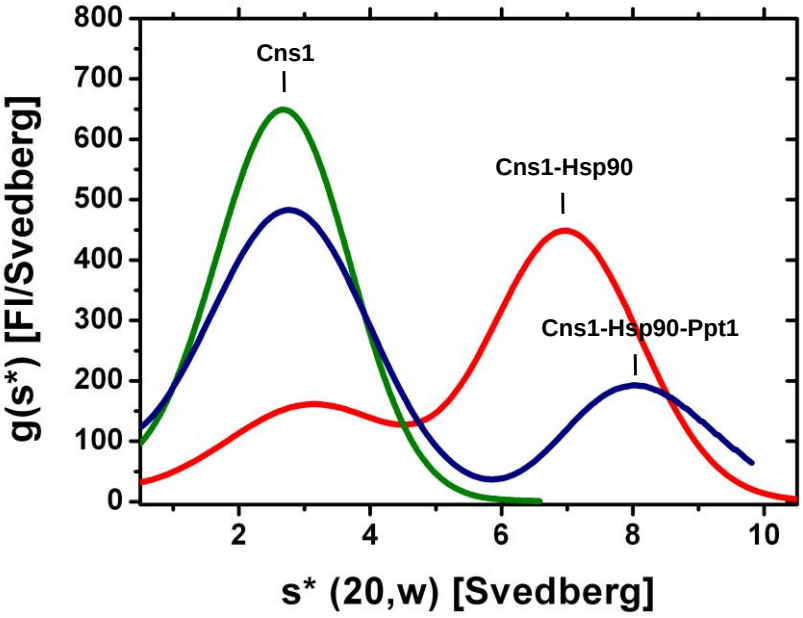

Figure 4-32: Influence of Ppt1 on Cns1-Hsp90 complex formation
Analytical ultracentrifugation was performed with Alexa488-labeled Cns1. Sedimentation of Alexa488-Cns1 was detected by the fluorescence optical system. Analysis of aUC data was performed with DCDT+. A plot of g(s*) is shown, where s*(20,w) represents the sedimentation coefficient normalized for water and 20°C. Raw data of aUC were fitted according to the Gauss equation.
Sedimentation profile of 500 nM Cns1 (green curve) alone and in the complex with Hsp90 (8 µM, red curve). Addition of Ppt1 (30 µM) leads to partial release of Cns1. Additionally, a shift in sedimentation coefficient occurs indicating the formation of a ternary complex (blue curve).
Resulting species are marked above, where Cns1 represents unbound Cns1, Cns1-Hsp90 the associated complex and Cns1-Hsp90-Ppt1 the potential ternary complex.

Addition of Ppt1 leads to partial release of Cns1 from Hsp90. As the sedimentation coefficient shifts to higher Svedberg-values a mixed complex seem to be likely. In addition, Ppt1 does not dephosphorylate Cns1 when Hsp90 is present (WANDINGER et al., 2006).

4.2.4. Integration of Cns1 within the Hsp70 chaperone cycle

4.2.4.1. Influence of Cns1 on the Ssa1 ATPase activity

The Ssa subfamily from *S. cerivisiae* consist of four proteins (Ssa1-Ssa4) and shows the strongest homology to the Hsp70 proteins from mammals (see introduction). Protein members from the Ssa subfamily are involved in regulation of the heat shock response and translocation of proteins (DESHAIES et al., 1988). Cns1 is known to interact with Ssa1 and Ssa2. Interaction of Cns1 with Ssa1 leads to the activation of the Ssa1 ATPase activity around 10-fold (HAINZL et al., 2004).

Ssa1 was expressed and purified from *Pichia pastoris* as described before (SCHMID et al. 2012). Like other Hsp70 proteins, Ssa1 is characterized by an intrinsically low ATPase activity and a low affinity for ATP (SADIS et al., 1992; WILBANKS et al., 1994, MAYER et al. 2005). Ssa1 purified during this work showed an ATPase activity with a k_{cat} of around 0.2 - 0.4 min^{-1} (data not shown). This is in agreement with the kinetic properties observed for Ssa1 using the described expression and purification protocol (SCHMID, PhD thesis 2009). The basal ATPase activity of Ssa1 purified from *Pichia pastoris* is around five-fold higher compared to previous work (ZIEGELHOFFER et al., 1995). This effect could derive from intramolecular activation of the ATPase activity of Ssa1 with its N-terminal peptide sequence which contains a His_6-tag. This N-terminal peptide contains stretches of hydrophobic amino acids and could bind to the substrate binding domain of Ssa1 which leads to stimulation of the ATPase activity. Stimulation of the Ssa1 ATPase activity by hydrophobic peptides was already shown (RICHARME et al., 1993; FOURIE et al., 1994; TAKENAKA et al., 1995; CROUY-CHANEL et al., 1996). The used concentration of Ssa1 in the enzyme-coupled ATPase assays (1.0-4.0 µM) could also lead to higher rate constants for the ATP turnover. The effect of autostimulation of Hsp70 at higher concentration caused by oligomerisation at the peptide binding domain was also previously observed (RICHARME et al., 1993; BENAROUDJ et al., 1997).

Hsp70 is interacting with various co-chaperones which regulate the activity of Hsp70 and influence steps of the ATPase cycle (BUKAU AND HORWICH, 1998; LU et al., 1998; TZANKOV et al., 2008). The Hsp40 Co-chaperone Ydj1 is known to interact with Ssa1 and activate the ATPase activity of Ssa1 (CHEETHAM AND CAPLAN, 1998, LANDRY, 2003, HAN et al., 2003). In order to proof the functionality of the purified Ssa1, its stimulation by Ydj1 was tested. Ssa1 was incubated with various amounts of Ydj1 and the ATPase activity was measured by an enzyme-coupled ATPase assay in the presence of saturating amounts of ATP.

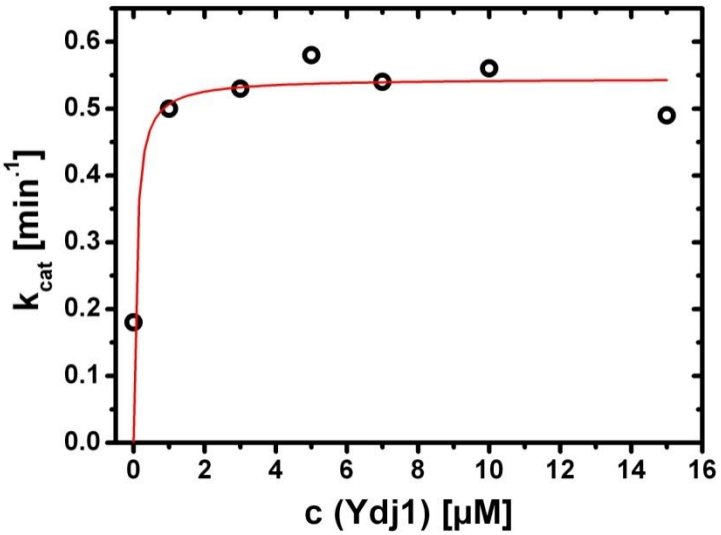

Figure 4-33: Influence of Ydj1 on the ATPase activity of Ssa1.
Ssa1 was diluted in buffer to a final concentration of 2.0 µM. After incubation with various amounts of Ydj1 the ATPase activity was measured at 30°C. Consumption of NADH was monitored at 340 nm and the rate of ATP hydrolysis was calculated using the slope of the linear decrease in absorption. Data points were fitted using following equation: $y=y_0+K_{MAX}+x/K_M+x$.

The ATPase activity of Ssa1 is enhanced upon addition of Ydj1 which was shown previously (CYR et al., 1992 and 1994; LU et al., 1998). As displayed by the apparent KM value of 0.1 µM, only catalytic amounts of Ydj1 are required to fully stimulate the Ssa1 ATPase activity. Binding of Ydj1 to Ssa1 could lead to conformational changes of Ssa1 which is described by a higher ATP hydrolysis rate. Full stimulation of the Ssa1 ATPase activity is achieved by addition of equimolar amounts of Ydj1. However, the specific mechanism of stimulation of the Ssa1 ATPase activity by Ydj1 is not yet understood. These results show that the purified Ssa1 is functional and possesses the same kinetic properties as described before (SCHMID et al., 2012).

Cns1 was described as activator of the Ssa1 ATPase activity (HAINZL et al., 2004). In order to proof the ability of Cns1 to activate the ATPase activity of Ssa1, ATPase assays were performed.

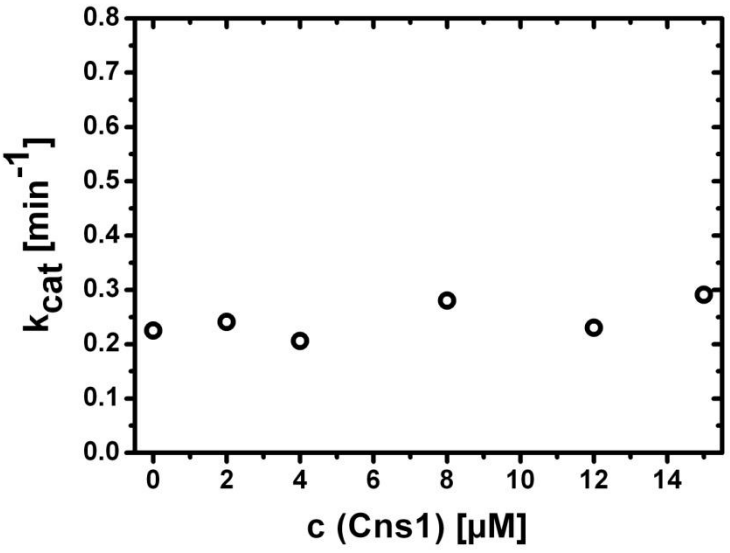

Figure 4-34: ATPase activity of Ssa1 in presence of Cns1.
Ssa1 was diluted in buffer to a final concentration of 2.0 µM. After incubation with various amounts of Cns1 the ATPase activity was measured at 30°C. Consumption of NADH was monitored at 340 nm and the rate of ATP hydrolysis was calculated using the slope of the linear decrease in absorption.

The ATPase activity of Ssa1 is not altered upon addition of Cns1. In previous work which used the same Ssa1 preparation, the stimulating effect of the Hsp90/Hsp70 co-chaperone Sti1 on Ssa1 ATPase activity could also not be detected (SCHMID, PhD thesis, 2009). Perhaps, impurity and/or co-purification of proteins due to the previous Ssa1 preparation protocol (WEGELE et al., 2003) are responsible as discussed in previous work (SCHMID, PhD thesis, 2009), for the previously observed stimulatory effect of Cns1 on the ATPase activity of Ssa1. With the purified Ssa1 used in this work Cns1 is not an activator of the Ssa1 ATPase activity.

4.2.4.2. Interaction of Cns1 with Ssa1

Cns1 is a TPR-containing co-chaperone which is known to interact with the substrate binding domain of Ssa1, especially the very C-terminal peptide EEVD of Ssa1 (HAINZL et al, 2004). In order to proof binding to Ssa1 analytical ultracentrifugation was performed. Cns1 was labeled with AlexaFlour488 as described before. For analytical ultracentrifugation 500 nM AlexaFluor488-Cns1 were used. Binding to Ssa1 was tested by addition of 10 µM Ssa1.

Analytical ultracentrifugation was performed at 25°C and a constant rotational speed of 42000 rpm.

Addition of Ssa1 to Cns1 leads to shift of the sedimentation velocity to higher Svedberg values. As the concentration of Ssa1 was set to 1 µM only a minor fraction of the associated complex was observable. However, it revealed that Cns1 is forming a complex with Ssa1 under the used conditions (data not shown). Compared to the interaction of Cns1 with Hsp90, again unbound Cns1 is detectable suggesting also a low affinity for the complex formation with Ssa1. Interestingly, Alexa488 labeled Cns1 with a labeling efficiency (c [label]/ c [protein] over 2 is not able to form complexes with Ssa1 (data not shown).

Ssa1 can adopt different conformational states upon nucleotide binding (SWAIN et al. 2006; VOGEL et al., 2006; JIANG et al. 2006; GOLUOUBINOFF et al, 2007; BERTELSEN et al., 2009). In order to test, if Cns1 prefers a defined conformational state of Ssa1 analytical ultracentrifugation was performed in presence of nucleotides. Here, labeled Cns1 was incubated with Ssa1 in the presence of either ADP or the non-hydrolysable ATP homologue AMP-PNP.

A

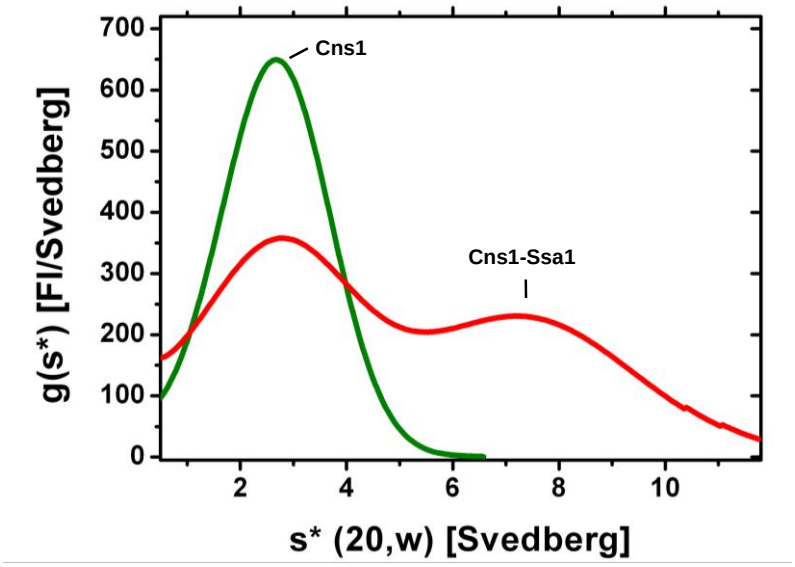

B

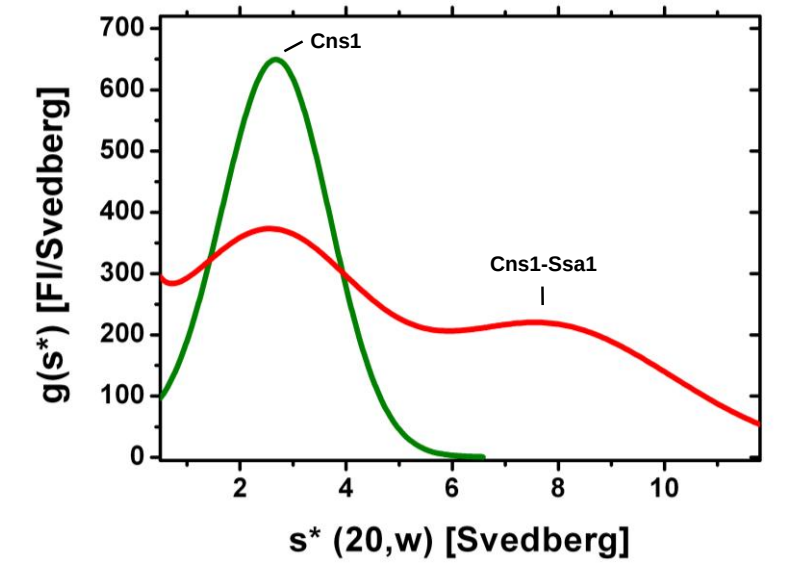

Figure 4-35: Sedimentation profile for Alexa488-Cns1 and association with Ssa1 in the presence of nucleotides.
Analytical ultracentrifugation was performed with Alexa488-labeled Cns1. Sedimentation of Alexa488-Cns1 was detected by the fluorescence optical system. Analysis of aUC data was performed with DCDT+. A plot of g(s*) is shown, where s*(20,w) represents the sedimentation coefficient normalized for water and 20°C. Raw data of aUC were fitted according to the Gauss equation.
(A) Sedimentation profile of 500 nM Cns1 (green curve) and complex formation with the ADP-bound state of Ssa1 (6 µM, red).
(B) Sedimentation profile of 500 nM Cns1 (green curve) and complex formation with the AMP-PNP-bound state of Ssa1 (6 µM, blue).
Resulting species are marked above, where Cns1 represents unbound Cns1 and Cns1-Ssa1 the associated complex.

Complex formation of Cns1 with Ssa1 was observable in the presence of both nucleotides (Figure 4-35). Titration of various amounts of Ssa1 to labeled Cns1 in the presence of nucleotides revealed that Cns1 binds to both nucleotide-sates of Ssa1 with nearly the same affinities (data not shown). As shown for the Hsp90 complex formation (Figure 4-24), Cns1 do not prefer a defined conformational state in the case of binding to Ssa1.

4.2.4.3. Interaction of Ydj1 with Ssa1

Ydj1 is a member of the Hsp40 family in *S. cerevisae*. It was shown that it regulates Hsp70 function in a vast set of cellular processes, like targeting degradation of misfolded proteins, protection of newly synthesized protein chains against degradation and membrane transport (CAPLAN et al., 1992; LEE et al., 1996; MANDAL et al., 2008).

In order to test how Cns1 can influence the Hsp70 cycle, especially its interaction with Ydj1, analytical ultracentrifugation was used. Only negligible effects were observed upon addition of Ydj1 on complex formation of Alexa488-Cns1 and Ssa1 (data not shown). So, formation of the Ydj1-Ssa1 complex detectable with analytical ultracentrifugation was established.

First, complex formation of the Hsp40 Co-chaperone Ydj with Ssa1 was tested. Therefore Ydj1 was labeled with AlexaFluor488. Labeling efficiency (c(label)/c(protein)) of 1.3 was calculated using equation of manufacturer´s protocol (see Material and Methods).

Labeled Ydj1 was diluted into buffer (40 mM HEPES/KOH (pH 7.5), 50 mM KCl, 5 mM $MgCl_2$) to a final concentration of 300 nM and analytical ultracentrifugation was performed.

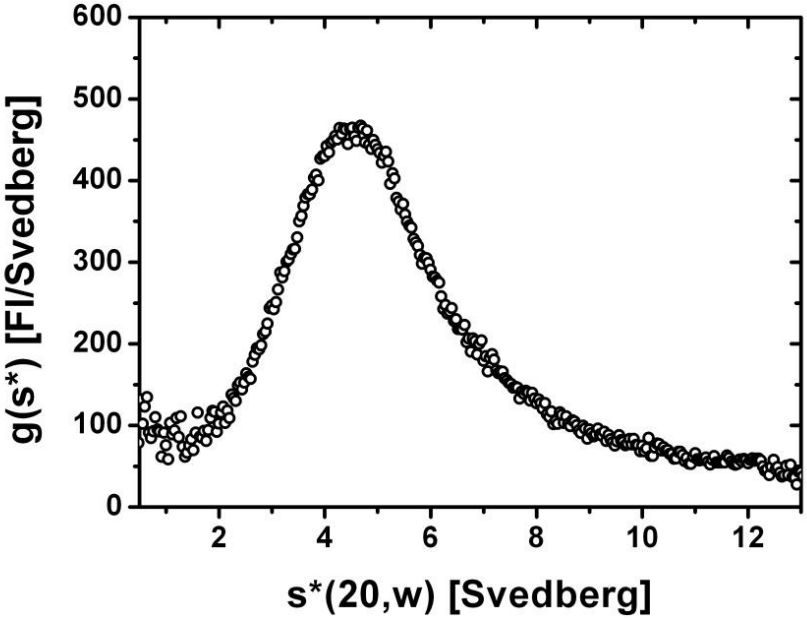

Figure 4-36: Sedimentation profile for Alexa488-Ydj1.
Analytical ultracentrifugation was performed with Alexa488-labeled Ydj1. Sedimentation of Alexa488-Ydj1 was detected by the fluorescence optical system. Analysis of aUC data was performed with DCDT+. A plot of g(s*) is shown, where s*(20,w) represents the sedimentation coefficient normalized for water and 20°C.

The labeled Ydj1 displayed a sedimentation coefficient of around 4.4 S. Compared to proteins of approximately equal molecular weight (for example: AlexaFluor488-Cns1) the predominant species of Ydj1 seem to be dimers which is in agreement with previous work (LANDRY, 2003).

Hsp40 interacts with Hsp70 as one of the first steps during the chaperone cycle (see Introduction). Hsp40s are able to bind unfolded polypeptides and a mechanism of substrate transfer to Hsp70 proteins was postulated (SCHRODER et al., 1993; HERNANDEZ et al., 2003).

Labeled Ydj1 (300 nM) was incubated with various amounts of Ssa1. To adopt defined conformational states of Ssa1, saturating amounts of either ADP or AMP-PNP were added.

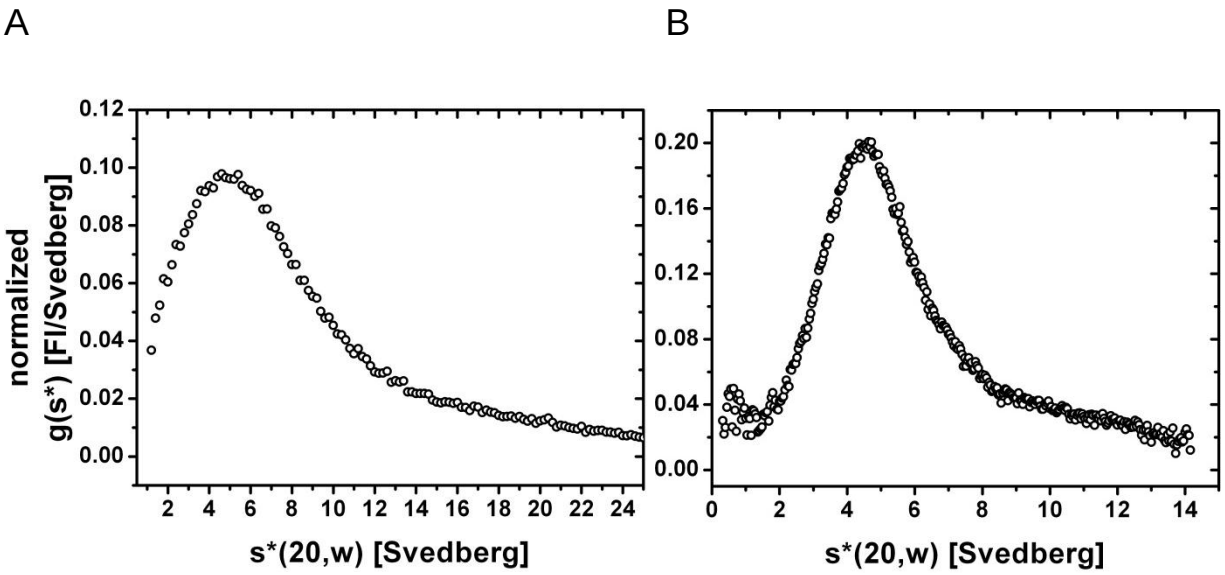

Figure 4-37: Sedimentation profile for Alexa488-Ydj1 in the presence of Ssa1.
Analytical ultracentrifugation was performed with Alexa488-labeled Ydj1. Sedimentation of Alexa488-Ydj1 was detected by the fluorescence optical system. Analysis of aUC data was performed with DCDT+. A plot of normalized g(s*) is shown, whereas s*(20,w) represents the sedimentation coefficient normalized for water at temperature of 20°C.
(A) Sedimentation profile of 300 nM Cns1 in the presence of 10 µM Ssa1 and ADP.
(B) Sedimentation profile of 300 nM Cns1 in the presence of 10 µM Ssa1 and AMP-PNP.

Complex formation of Ydj1 and Ssa1 could not be observed as only the unbound Ydj1 is detectable (Figure 4-37). In case of both nucleotide-bound states of Ssa1, Ydj1 is not able to form stable complexes. Additionally, the influence of ATP on complex formation of Ydj1 and Ssa1 was tested with analytical ultracentrifugation according to the experimental set up used before.

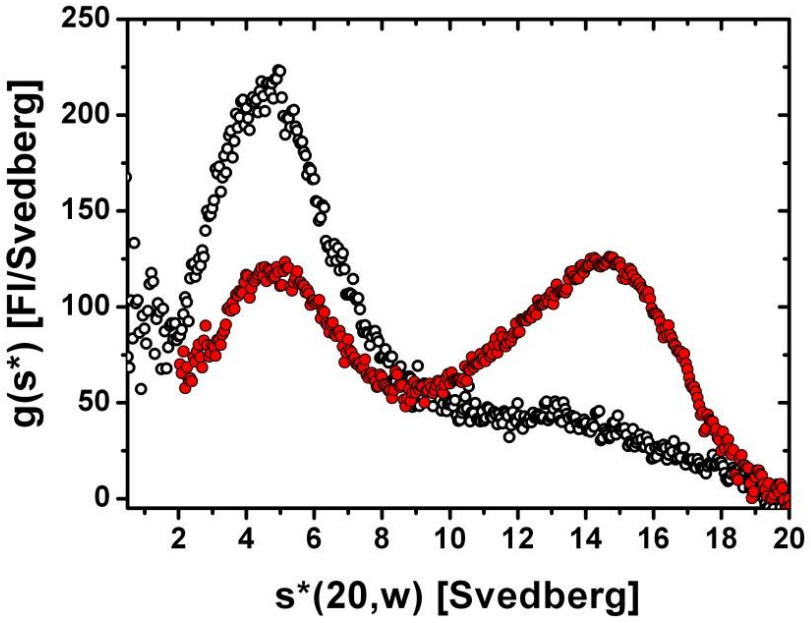

Figure 4-38: Sedimentation profile for Alexa488-Ydj1 in the presence of Ssa1 and ATP. Analytical ultracentrifugation was performed with 300 nM Alexa488-labeled Ydj1 in the presence of 8 µM Ssa1 and 1 mM ATP. Analysis of aUC data was performed with DCDT+. A plot of normalized g(s*) is shown, whereas s*(20,w) represents the sedimentation coefficient normalized for water at temperature of 20°C. Ydj1 is shown by black dots, whereas red dots represent association of Ydj1 and Ssa1 in the presence of ATP.

In presence of ATP, complex formation between Ydj1 and Ssa1 could be observed (Figure 4-38). The sedimentation coefficient for the Ydj1-Ssa1 complex is around 18 S. In this case, it is not possible that only one Ssa1 is bound to an Ydj1 dimer (see also aUC with Cns1-Ssa1 complex). So, the complex formed by Ydj1 and Ssa1 seems to consist of multiple copies of both proteins. These data are also in agreement with the complex formation of Hsp40, Hsp70 and a nucleotide exchange factor from *C. elegans* (SUN et al., 2012).

4.2.4.4. Influence of Sti1 on Ydj1-Ssa1-complex formation

During the multichaperone cycle, clients of Hsp90 have to be transferred from Hsp70 to Hsp90 (PRATT et al., 1999 and 2003; WEGELE et al., 2003 and 2006; FELTS et al., 2007). In order to form the complex of Hsp70 and Hsp90, the protein Sti1 serves as an adaptor protein (CHEN et al., 1998; HERNANDEZ et al., 2002; ODUNUGA et al., CARRIGAN et al., 2005). Sti1 is

known to bind to Hsp90 and Hsp70 via its TPR-domains which contain different affinities for Hsp70 and Hsp90 (SCHEUFLER et al., 2000; CARRIGAN et al., 2004; FLOM et al., 2007; SCHMID et al., 2012 etc.). Here, the influence of Sti1 on Ydj1-Ssa1 complex formation was tested by analytical ultracentrifugation. Ydj1-Ssa1 complexes were formed as shown above (Figure 4-38). Furthermore, association of Ydj1 and Ssa1 was tested in the presence of various amounts of Sti1.

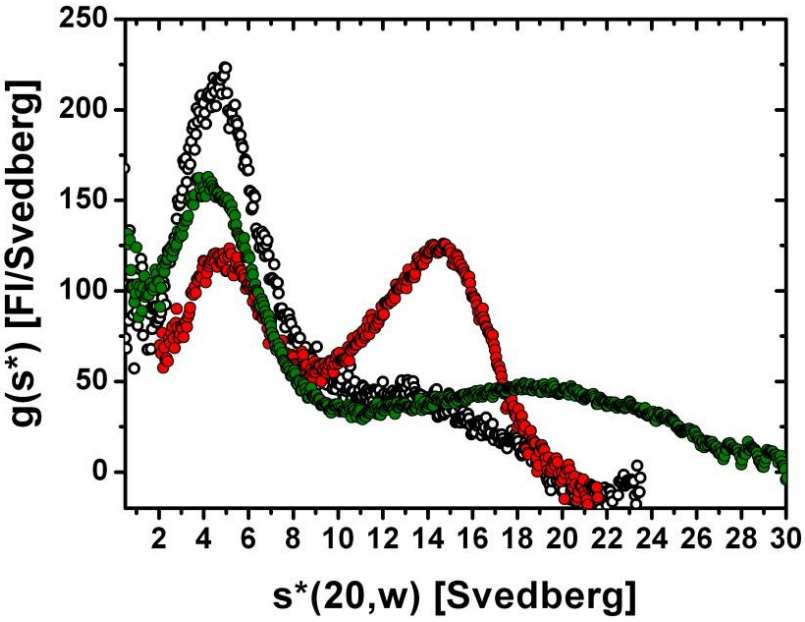

Figure 4-39: Sedimentation profile for Alexa488-Ydj1 in the presence of Ssa1 (ATP) and Sti1. Analytical ultracentrifugation was performed with 300 nM Alexa488-labeled Ydj1 in the presence of 8 µM Ssa1 and 1 mM ATP. Sedimentation of Alexa488-Ydj1 was detected by the fluorescence optical system. Analysis of aUC data was performed with DCDT+. A plot of normalized g(s*) is shown, whereas s*(20,w) represents the sedimentation coefficient normalized for water at temperature of 20°C. Ydj1 is shown by black dots, whereas red dots represent association of Ydj1 and Ssa1 in the presence of ATP. Influence of Sti1 is indicated by the green dots.

Addition of increasing amounts of Sti1 leads to partially disruption of the Ydj1-Ssa1-complex. As shown above, Sti1 seems to be able to release Ydj1 from Ssa1. Formation of a Ssa1-complex containing multiple co-chaperones is also possible. However, in the presence of Sti1, Ydj1 is partially released suggesting that mixed complexes with Sti1, Ydj1 and Ssa1 are not preferred.

Next, the influence of Sti1 on the stimulatory effect of Ydj1 on the Ssa1 ATPase activity was tested. To this end, Ssa1 were incubated with saturating amounts of Ydj1 and various

amounts of Sti1 were added. Afterwards the rates of ATP hydrolysis rate were determined by an enzyme-coupled ATPase assay.

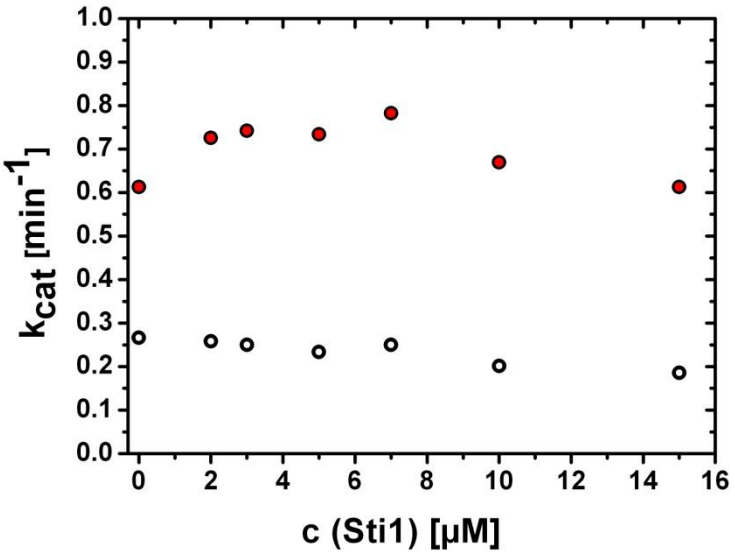

Figure 4-40: Influence of Ydj1 on the ATPase activity of Ssa1.
Ssa1 was diluted in buffer to a final concentration of 2.0 µM. After incubation with various amounts of Sti1, the ATPase activity of Ssa1 was measured at 30°C (white dots). Additionally, Ssa1 was incubated with saturating amounts of Ydj1 (3 µM) and various amounts of Sti1 (red dots). Consumption of NADH was monitored at 340 nm and the rate of ATP hydrolysis was calculated using the slope of the linear decrease in absorption.

In the presence of saturating amounts of Ydj1, the Ssa1 ATPase is not influenced by increasing amounts of Sti1. Sti1 itself showed no activation of the Ssa1 ATPase activity which is in agreement with previous work using the same Ssa1 preparation method (SCHMID, PhD thesis, 2009). Additionally, the stimulatory effect of Ydj1 on the Ssa1 ATPase activity in the presence of increasing amounts of Sti1 is not altered. Sti1 showed that it partially release Ydj1 from Ssa1 (figure 4-39). Together with the data from analytical ultracentrifugation, Sti1 is able to influence binding of Ydj1 to Ssa1 without altering the stimulatory effect of Ydj1 on the ATPase activity of Ssa1.

4.2.4.5. Influence of Cns1 on Ydj1-Ssa1-complex formation

As formation of the Ydj1-Ssa1 complex was established (Figure 4-38), the influence of Cns1 on association of Ydj1 and Ssa1 was tested. As shown above, the TPR-containing co-chaperone Sti1 is not able to release Ydj1 from Ssa1. Additionally, the effect of Ydj1 on Ssa1 ATPase activity is not altered in the presence of Sti1. Here, the influence of Cns1 was tested. As shown, Cns1 does not prefer a specific conformation of Ssa1 (Figure 4-35).

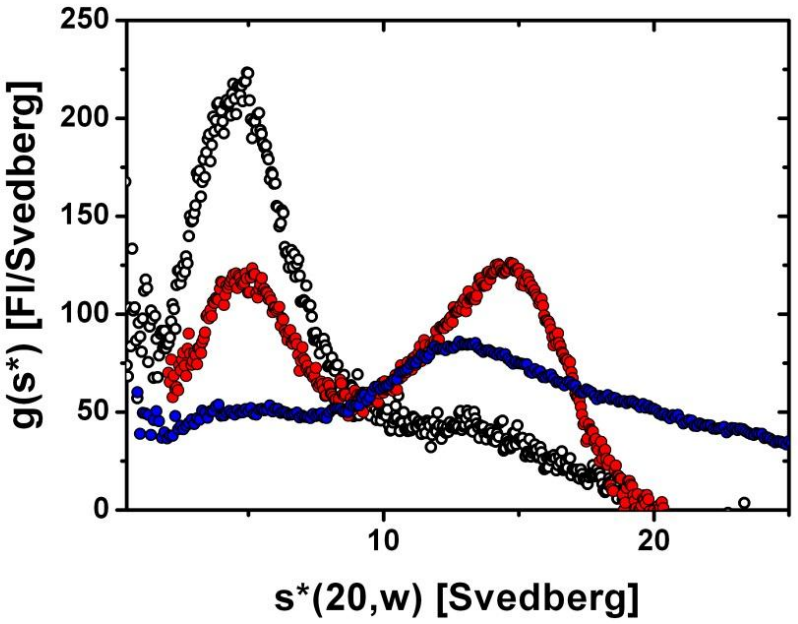

Figure 4-41: Sedimentation profile for Alexa488-Ydj1 in the presence of Ssa1 (ATP) and Cns1. Analytical ultracentrifugation was performed with 300 nM Alexa488-labeled Ydj1 in the presence of 8 µM Ssa1 and 1 mM ATP (red dots). Sedimentation of Alexa488-Ydj1 was detected by the fluorescence optical system. Analysis of aUC data was performed with DCDT+. A plot of normalized g(s*) is shown, where s*(20,w) represents the sedimentation coefficient normalized for water at temperature of 20°C. Ydj1 is shown by black dots, whereas red dots represent association of Ydj1 and Ssa1 in the presence of ATP. Influence of Cns1 is indicated by the blue dots.

Cns1 did not alter the sedimentation profile of labeled Ydj1 in the presence of ATP-bound Ssa1. Different populations of formed complexes are due to the used concentrations. Thus, the TPR-containing co-chaperone Cns1 is not able to disrupt the Ydj1-Ssa1 complex. In addition, the ability of Ydj1 to stimulate the ATPase activity of Ssa1 was tested in the presence of Cns1.

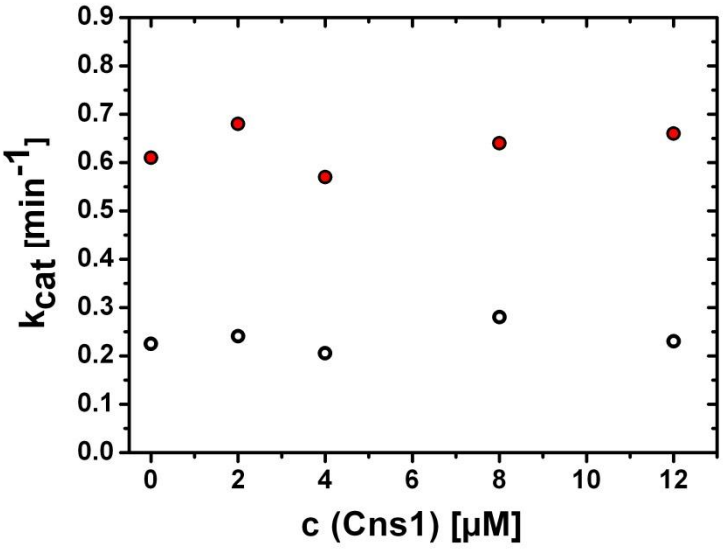

Figure 4-42: Stimulatory effect of Ydj1 on the ATPase activity of Ssa1 in the presence of Cns1. Ssa1 was diluted in buffer to a final concentration of 2.0 µM. After incubation with various amounts of Sti1, the ATPase activity of Ssa1 was measured at 30°C (white dots). Additionally, Ssa1 was incubated with saturating amounts of Ydj1 (3 µM) and various amounts of Cns1 (red dots). Consumption of NADH was monitored at 340 nm and the rate of ATP hydrolysis was calculated using the slope of the linear decrease in absorption.

As shown above, also Cns1 is not able to disrupt the Ydj1-complex (Figure 4-41). In addition, the stimulatory effect of Ydj1 on the ATPase activity of Ssa1 is not altered in the presence of Cns1. Taken together, Cns1 and Sti1 showed different influences on the complex formation of Ydj1 and Ssa1. Sti1 is able to release Ydj1 from Ssa1. Formation of the Ssa1-Sti1-Hsp90 complex was already shown (SCHMID et al., 2012). However, how formation of this complex is influenced by Ydj1 had not been tested.

4.2.5. TTC4, the human homolog of Cns1

The human TPR-containing protein, TTC4, was shown to be a putative co-chaperone as its binding to Hsp70 and Hsp90 could be detected (CREVEL et al., 2008). Additional studies showed, that the gene encoding for TTC4 is mutated in various cancer cells (POETSCH et al., 2000; SU et al., 2000). Furthermore, binding to Cdc6, a protein essential in the initiation of DNA replication, was observed (CREVEL et al., 2008).

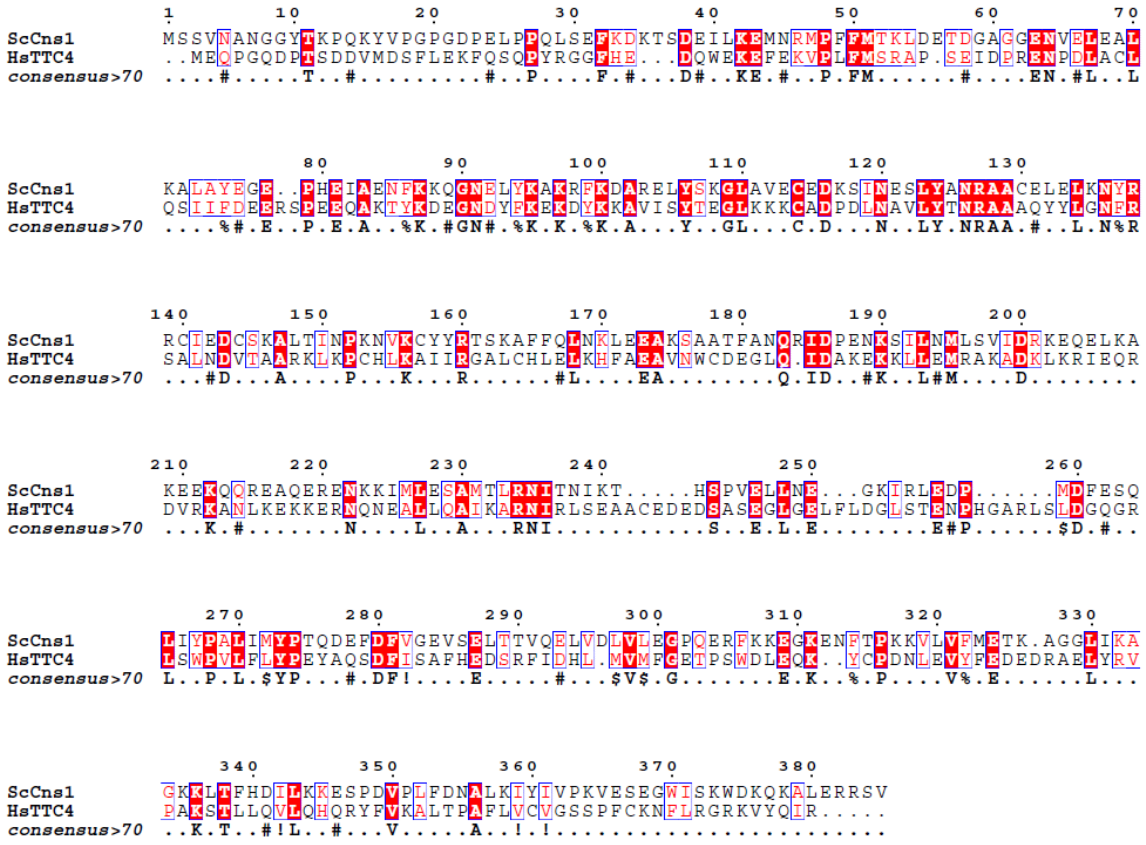

Figure 4-43: Sequence alignment of Cns1 and TTC4.
Sequence alignment was performed with yeast Cns1 (ScCns1) and human TTC4 (HsTTC4) using MULTALIN and ESPRIPT.

Sequence alignment of Cns1 and TTC4 revealed structural homologies and equal domain organization of Cns1 and TTC4. Structural alignments of the C-terminal domain of Cns1 did not identify structural homologues in the protein data bank. However, TTC4 shows sequence similarities to Cns1 also in the C-terminal domain and not only to the TPR-domain. Thus, TTC4 may have similar functions within the chaperone cycle compared to Cns1.

Expression in *E. coli* and purification of TTC4 is not yet established. In order to be able to compare effects of TTC4 in interacting with Hsp90 and Hsp70 with Cns1, expression and purification of TTC4 in *E. coli* was tested.

A plasmid containing the open reading frame from TTC4 was derived from IMAGENES. The coding sequence of TTC4 was amplified by PCR and was cloned into pET28a using NheI and XhoI restriction sites. Afterwards the plasmid was transformed into *E.coli* BL21CodonPlus. Gene expression was performed at 37°C and was induced by addition of 1 mM IPTG.

Purification of TTC4 was done according to the protocol used for Cns1. First, NiNTA was performed followed by anion exchange chromatography and Size Exclusion Chromatography.

A

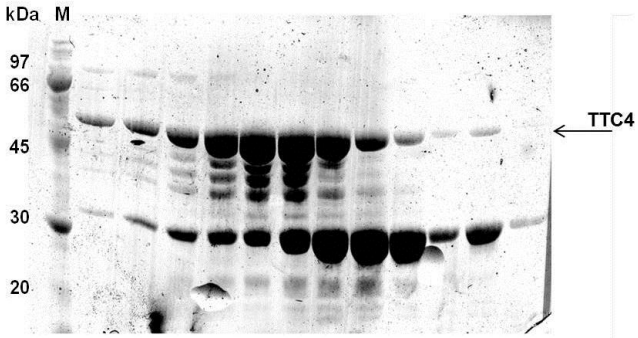

B

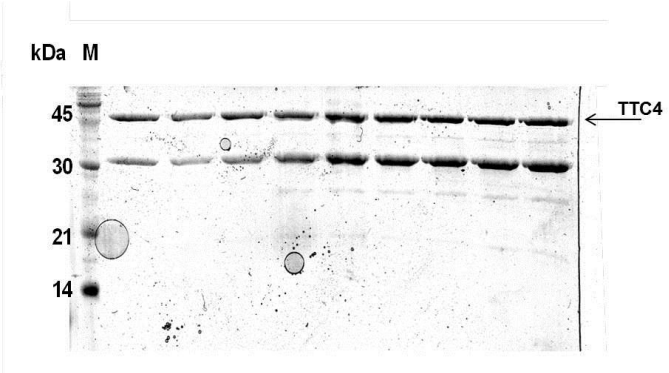

C

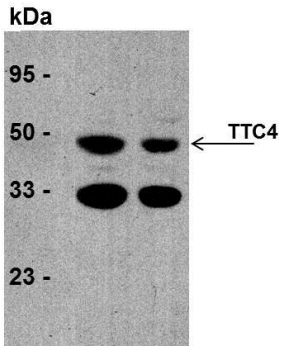

Figure 4-44: SDS-PAGE and Western Blot of TTC4.
(A) SDS-PAGE after protein purification using NiNTA column.
(B) SDS-PAGE after protein purification using Superdex 75 column.
(C) Western Blot using the anti-His_6 Peroxidase-conjugated antibody. For detection the ECL detection kit was used (see Material and Methods).

As shown by SDS-PAGE the protein showed two dominant species after the NiNTA column, indicating possible protein degradation (Figure 4-44; A). Fractions were pooled and loaded on a size exclusion chromatography (Superdex 75). SDS-PAGE of elution revealed that besides the full length TTC4, a second species co-eluated (Figure 4-44, B). In order to separate both proteins high salt conditions (500 mM KCl) were used for the SEC running buffer. But this did not lead to separation of the two species. In order to test whether the second band derived from degradation, Western blots were performed. This analysis, using an antibody against the N-terminal His-tag, revealed that the protein is partially degraded from the C-terminus as two bands are detectable (Figure 4-44, C). The bands could not be separated by ion exchange chromatography or a hydroxy apatite column (data not shown).

In order to reduce protein degradation gene expression was performed at 25°C. But also under these conditions, it was not possible to obtain pure protein fractions (data not shown).

In summary, it could be shown that the human homolog of Cns1, TTC4, could be expressed in *E.coli*. Purification revealed that this protein is partially degraded from the C-terminal end, the impurities could not be separated. As C-terminal degradation was detectable, expression with C-terminal fusion could be useful.

4.2.6. Discussion

Cloning, expression and purification of different fragments of Cns1 were established. To get further details of the structure of Cns1, these constructs were used for crystallization. But no crystal formation under the used conditions could be observed. For crystallization of the individual TPR-domains of Cns1, the protein concentrations should be increased which will require large scale production of the protein. In order to increase the protein yields during purification, expression should be performed high cell density cultivation in a fermenter. In order to obtain more information on the full length structure of Cns1, small angle x-ray scattering (SAXS) could perhaps lead to a solution structure of Cns1.

With different single cysteine mutants and chemical cross-linking in yeast lysate, specific protein-protein interaction of the individual C-terminal domain of Cns1 should be analyzed. However, this method did not lead to the identification of specific proteins which interact with the C-terminal domain of Cns1. As the C-terminal domain of Cns1 is not necessary for viability of yeast, a specific function of the C-terminal domain of Cns1 could not be determined. In order to obtain interacting proteins for specific domains of Cns1, a yeast two hybrid screen is a possible method. The individual domains of Cns1 should be used as pray which may lead to more information about potential interacting proteins. This could also point towards specific cellular pathways which may explain the essential function of the TPR-domain of Cns1.

The function of Cns1 within the Hsp90 chaperone cycle and the organization and recruitment of co-chaperones was tested *in vitro*. Analytical ultracentrifugation with fluorescence-labeled Cns1 was used to detect the Cns1-Hsp90 complex. As the ATPase activity of Hsp90 is not influenced in the presence of Cns1, binding to defined conformational states of Hsp90 was tested. A preferential binding of Cns1 to a specific conformation of Hsp90 was not detected. Cns1 binds with nearly the same affinities to the ADP-bound, open state and to the AMP-PNP bound, closed state of Hsp90. This also indicates that Cns1 is not regulating the ATP turnover of Hsp90 which was proven by the ATPase assays.

Binding of Cns1 to Hsp90 in the presence of different co-chaperones of Hsp90 was tested. Here, the activator of Hsp90 ATPase activity, Aha1, was used as an example for a co-chaperone which is known to bind to other parts of Hsp90 compared to Cns1 (PANARETOU et al., 2002; MEYER et al., 2004; RETZLAFF et al., 2010). In this case, addition of Aha1 did not lead to release of Cns1 from Hsp90. Additionally, in the presence of both co-chaperones the sedimentation coefficient of the complex changed to higher Svedberg-values indicating simultaneous binding of Cns1 and Aha1 to Hsp90. This effect was pconfirmed in the

enzyme-coupled ATPase assays. The presence of Cns1 did not alter the ability of Aha1 to activate the ATPase activity of Hsp90.

Additionally, the influence of various TPR-containing co-chaperones on Cns1-Hsp90 complex formation was tested. In this case, simultaneous or competitive binding of Cns1 and other TPR-containing chaperones was observable. Co-chaperones act at different stages of the Hsp90 chaperone cycle (Figure 1-11). Therefore, it is important to know how co-chaperones are recruited and organized within the Hsp90 chaperone cycle.

For Sti1, a known inhibitor of the Hsp90 ATPase activity, formation of mixed complexes with Hsp90 and Cpr6 was found. These hetero-trimeric complexes are important for progression of the chaperone cycle (RICHTER et al., 2003; LI et al., 2011). In this case, two TPR-containing co-chaperones are able to bind simultaneously to the Hsp90 dimer (LI et al., 2011). In contrast, Sti1 is not able to form ternary complexes with Hsp90 and Cns1. When Cns1 is present, Sti1 is not able to bind to Hsp90. Under the conditions used for analytical ultracentrifugation, Hsp90 was added in a 10-20fold molar excess to Cns1. In this case, only one Cns1 is bound to the Hsp90 dimer, so that the other binding site for TPR-containing co-chaperones of the Hsp90 dimer is free for interaction. However, in case of Sti1 no simultaneous binding was observable. This effect was also tested using the established FRET system to detect complex formation of Sti1 and Hsp90 (LI et al., 2011). In this assay, addition of Cns1 leads to displacement of Sti1 from the Hsp90 dimer. Furthermore, the ability of Sti1 to inhibit the Hsp90 ATPase activity was tested. Sti1 showed the inhibitory effect on the ATP turnover of Hsp90. However, presence of Cns1 restored the ATPase activity of Hsp90. Taken together, Sti1 is not able to bind to Hsp90 in the presence of Cns1. A competitive binding of Cns1 and Sti1 to the Hsp90 dimer was observed. Thus, Cns1 forms the predominant complex with Hsp90 in the presence of Sti1.

Another group of TPR-containing co-chaperones are the large PPIases, Cpr6 and Cpr7. Cns1 was found to suppress the slow growth phenotype of yeast cells resulting from deletion of Cpr7 (MARSH et al., 1998). For Cpr7, it could be shown that it restores viability of yeast cell when Cns1 function is impaired (TESIC et al., 2003). Growth or viability of *S. cerevisiae* cells is not affected when the C-terminal EEVD motif is deleted (LOUVION et al., 1996). However, a requirement for the Hsp90 EEVD sequence was shown and revealed that co-chaperones are necessary for proper function of Hsp90 (TESIC et al., 2003). The influence of Cpr6 and Cpr7 on Cns1-Hsp90 complex formation was tested. Addition of either Cpr6 or Cpr7 leads to disruption of the complex formed by Hsp90 and Cns1. In both cases no simultaneous binding of the co-chaperones to Hsp90 was observable. So, in the presence of the PPIases Cpr6 and Cpr7, Cns1 is not able to bind to Hsp90.

Ppt1 is a phosphatase which is known to interact with Hsp90 to fulfill its function (WANDINGER et al., 2006; VAUGHN et al., 2008). As it contains a TPR-domain for interaction with Hsp90, the influence of Ppt1 on Cns1-Hsp90 complex formation was also tested. Cns1 was partially released from Hsp90 in the presence of Ppt1. However, the complex shifted to higher Svedberg-values indicating that formation of a mixed complex of Ppt1, Cns1 and Hsp90 is possible. Cns1 is not dephosphorylated by Ppt1 as shown previously (WANDINGER et al., 2006).

Taken together, Aha1 showed no influence on the Cns1-Hsp90 complex. Both co-chaperones can bind simultaneously to Hsp90. The specific stimulatory effect of Aha1 on the ATPase activity is not influenced by Cns1. That indicates the formation of mixed complexes of Aha1, Cns1 and Hsp90. The influence of TPR-containing co-chaperones on Cns1-Hsp90-complex was tested. Sti1 is not able to release Cns1 from Hsp90. However, the cyclophilins displace Cns1 from Hsp90. In case of Sti1 and the cyclophilins, formation of mixed complexes with Cns1 and Hsp90 were not detected. The presence of Ppt1 resulted in partially release of Cns1 from Hsp90. However, the complex shifted towards higher Svebderg-values. Thus, a mixed complex of Cns1, Ppt1 and Hsp90 remains possible.

Furthermore, the interaction of Cns1 within the Hsp70 cycle was tested. Purified Ssa1 was functional as shown by its intrinsic ATPase activity and the activation by Ydj1. However, Cns1 showed no ability to activate the ATPase activity of Ssa1 which is in contrast to previous works (HAINZL el al., 2004). Complex formation of Cns1 and Ssa1 were detectable using analytical ultracentrifugation. Additionally, the influence of nucleotides was analyzed. As shown by analytical ultracentrifugation, Cns1 did not prefer a specific conformational, nucleotide-bound state of Ssa1 to form the complex. In order to test the influence of Ydj1 on the Cns1-Ssa1 complex, analytical ultracentrifugation was performed. Ydj1 was labeled and complex formation with Ssa1 was observed. Interestingly, complex formation of Ydj1 and Ssa1 was only detectable in the presence of ATP. The complex of Ydj1 and Ssa1 consists of multiple copies of both proteins as the complex showed a sedimentation coefficient of around 16 S. This is in agreement with previous work (SUN et al., 2012).

The effect of Sti1 and Cns1 on Ydj1-Ssa1 complex formation showed that Cns1 is not able to release Ydj1 from Ssa1. Also the stimulatory effect of Ydj1 on the ATPase activity of Ssa1 is not altered in the presence of Cns1. Sti1, however, partially releases Ydj1 from Ssa1. That is in agreement with the proposed model that Sti1 serves as adaptor to connect the Hsp70 and Hsp90 chaperone cycle. The ability of Ydj1 to activate the ATPase activity was not changed in the presence of Sti1. Thus, a mixed complex of Sti1, Ydj1 and Ssa1 is also possible.

4.3. In vivo analysis of the Hsp90/Hsp70 interacting protein Cns1

In *S. cerevisiae*, Cns1 was found to be essential for viability. Additionally, it was found that overexpression of Cns1 can suppress the slow growth phenotype and the decreased Hsp90 activity resulting from deletion of the gene encoding for Cpr7 (DOLINSKI et al., 1998; MARSH et al., 1998). Cns1 was also shown to serve as a multicopy suppressor of several temperature-sensitive Hsp90 mutants (NATHAN et al., 1999). Further studies revealed that only the TPR-domain of Cns1 is essential for viability of yeast cells (TESIC et al., 2003; HAINZL et al., 2004). Binding of Cns1 to C-terminal MEEVD peptide of Hsp90 is mediated by the TPR-domain of Cns1 (TESIC et al., 2003, HAINZL et al., 2004). However, deletion of the conserved EEVD motif of Hsp90 does not affect the growth of *S. cerevisiae* cells (LOUVION et al., 1996). Additionally, an interaction of Cns1 with Cpr7 was observed but whether this interaction is direct or mediated by an additional interaction partner remained unclear (TESIC et al., 2003).

4.3.1. Overexpression of Cns1 and Cns1 fragments

As known, Cns1 is one of the most weakly expressed genes in *S.cerevisae*. In order to test if overexpression of Cns1 has any effect on growth or viability of the yeast cells, a plasmid containing Cns1wt under the GPD promoter (p425-GPD) was transformed into yeast wild type cells (BY4741). Additionally, different constructs of Cns1 were used in this assay.

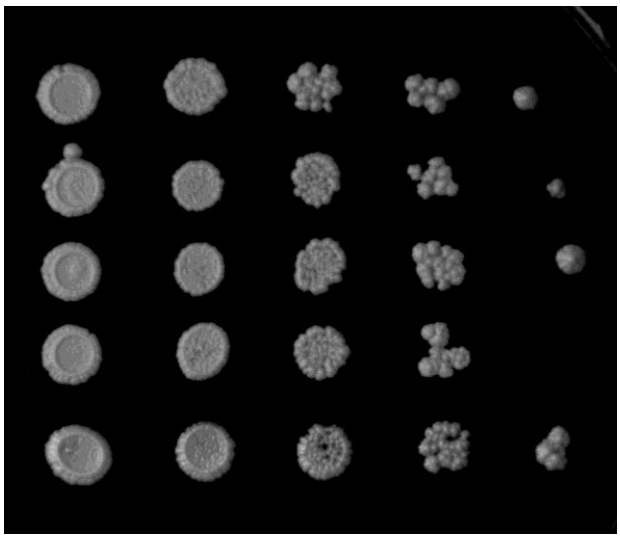

Figure 4-45: Overexpression of Cns1 in yeast wild type.
Yeast wild type cells were transformed with full length Cns1 or truncated Cns1 constructs (Cns1-TPR, Cns1-218C and Cns1-NΔ60) and were grown at 30°C until stationary phase were reached. 3 µl of 1:10 serial dilutions were spotted on LEU^- plates and were grown at 30°C for 2-3 days. Cell density decreases from left to right.

No phenotype of yeast cells could be observed when Cns1 or Cns1-constructs is overexpressed (Figure 4-45). The different fragments showed also no changes in viability or growth of the yeast cells compared to the wild type strain. No colonies were observed in the highest dilution for Cns1NΔ60. This is caused to the error in determination of the optical density of the yeast cultures. For this fragment an effect is not expected as growth of yeast strain containing the Cns1-TPR and Cns1-218C was not observed. Additionally, overexpression of Cns1 or Cns1 fragments showed no changes in growth of yeast cells at 37°C.

4.3.2. Maturation of the Hsp90 client v-Src

A known client of Hsp90 is v-Src kinase (BLAGOSKLONNY et al., 2002; STRAVOPODIS et al., 2007). For analysis of Cns1 in the context of client maturation by Hsp90, Cns1 and the TPR-domain of Cns1 were overexpressed in wild type yest cells. Expression of v-Src was induced on galactose media and the viability of cells was assessed (Figure 4-46).

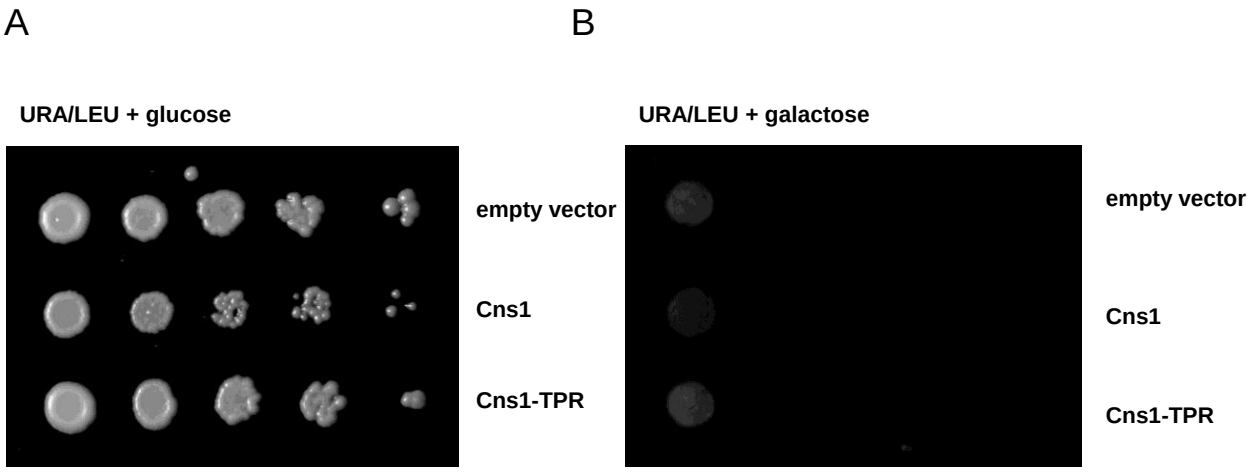

Figure 4-46: V-Src kinase activity assay with Cns1 and Cns1-TPR in yeast wild-type cells.
Yeast cells containing the galactose-inducible v-Src expression (URA) plasmid were transformed with plasmids expressing Cns1 or Cns1 fragments (LEU). Cells were grown at 30°C until stationary phase. Then 1:10 serial dilutions were made. 3 µl of each dilution were spotted (density decrease from left to right) on URA/LEU plates containing either glucose or galactose. Plates were incubated at 30°C for 3 days (plates containing galactose were incubated up to one week).

Overexpression of Cns1 and Cns1 fragments revealed no differences in Hsp90-mediated maturation of v-Src (Figure 4-46). So, Cns1 does not influence Hsp90 activity in the maturation of its kinase client.

4.3.3. Generation of haploid yeast Cns1-KO

For viability of *S. cerevisiae*, Cns1 was found to be essential (DOLINSKI et al., 1998). To test different construct of Cns1 for viability, a yeast strain where the locus for Cns1 is deleted was created. Therefore a diploid yeast strain containing an inserted YBR155w:kanMX4 was used for generation of the haploid yeast strain containing the Cns1 knockout and a URA3 plasmid encoding for Cns1 (see Material and Methods).

The diploid yeast strain (with YBR155w:kanMX4) was transformed with a plasmid containing a Cns1wt (p426GPD-Cns1wt; URA3). Afterwards, yeast cells were incubated on various media to obtain sporulation and formation of tetrads.

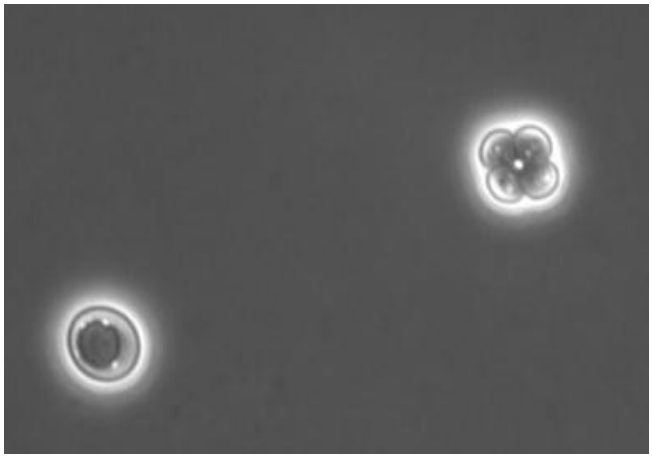

Figure 4-47: Microscopic image of yeast cells.
Diploid yeast cell (left) and yeast cell that formed 4 haploid spores (right).

As shown (Figure 4-47), sporulation of the diploid yeast cells was observable. Treatment with Lyticase was performed in order to digest the ascus of the yeast cells. Afterwards, tetrads were dissected using a micro-manipulator. Resulting haploid spores were then selected for the transformed p426GPD-Cns1 plasmid on –URA media. Selection for the kanMX4-cassette was achieved by spotting the haploid spores on media containing the aminoglycoside antibiotic G418 (Figure 4-48).

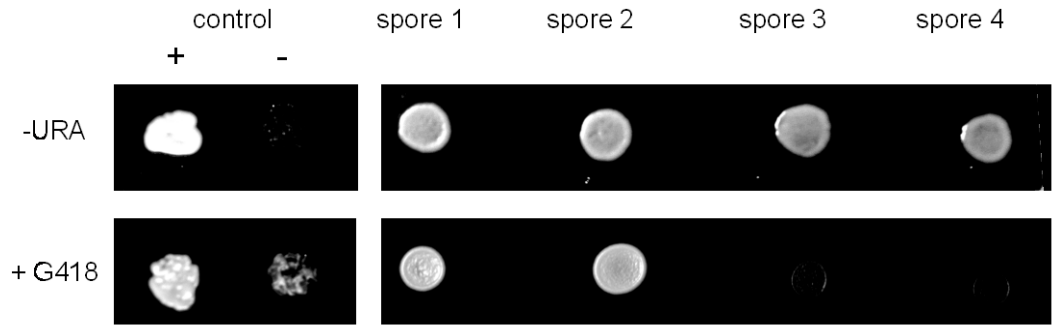

Figure 4-48: Haploid spores resulting from tetrad dissection.
Tetrad dissection followed by selection on URA$^-$-media and media containing G418. Diploid yeast strain (Cns1-KnockOut + p426GPD-Cns1) was used as positive control, yeast WT strain as negative control.

All of the four spores contain the p426-GPD-Cns1wt plasmid as they are growing on –URA media. The kanMX4-cassette carries a G418-resistance, so spores were incubated in the presence of G418. After sporulation, two of the spores contain the Cns1-ORF (YBR155w), the other two spores contain the deletion in the gene encoding for Cns1

(YBR155w:kanMX4). As shown above, only two spores are able to grow. This shows that these two spores are deleted for the Cns1 gene and harbor the plasmid encoding for Cns1.

In order to check the ploidy of the yeast strains resulting from sporulation and tetrad dissection, colony PCRs were performed. For PCR, primer were used which lead to the amplification of the locus for the mating type.

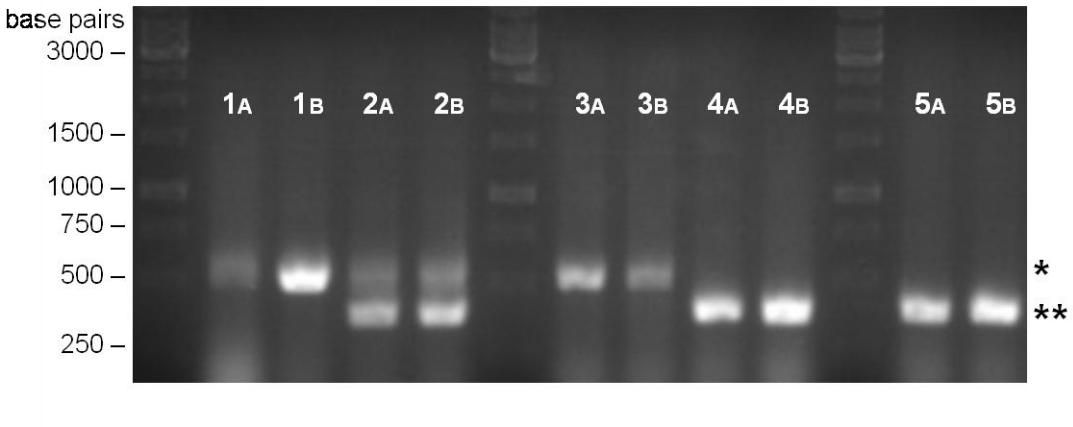

Figure 4-49: Colony PCRs of the yeast strains resulting from sporulation and tetrad dissection.
Colony PCRs of yeast cells and amplifying the mating type locus. Two colonies were analyzed for each yeast strain. Wild type yeast strain BY4741 (1) shown, is haploid with mating type alpha. The yeast strain (2n, YBR155w:kanMX4) was used as control for a diploid yeast strain containing both mating types (2). Yeast strains (spore 1-3) resulting from sporulation and tetrad dissection are haploid containing different mating types. (3-5)
Resulting PCR products of the mating type A (*) and mating type alpha (**) are marked on the right side.

Yeast strains resulting from sporulation followed by tetrad dissection are haploid as shown by colony PCR (Figure 4-49). The yeast strain containing the deletion for the Cns1 gene (YBR155w:kanMX4) have the mating type alpha and A (Figure, 4-49, 3 and 4). Additionally, colony-PCRs were performed to check the locus encoding for Cns1. Colony PCRs were performed with primer which leads to the amplification of either the open reading frame encoding for Cns1 or the inserted kanMX4 cassette.

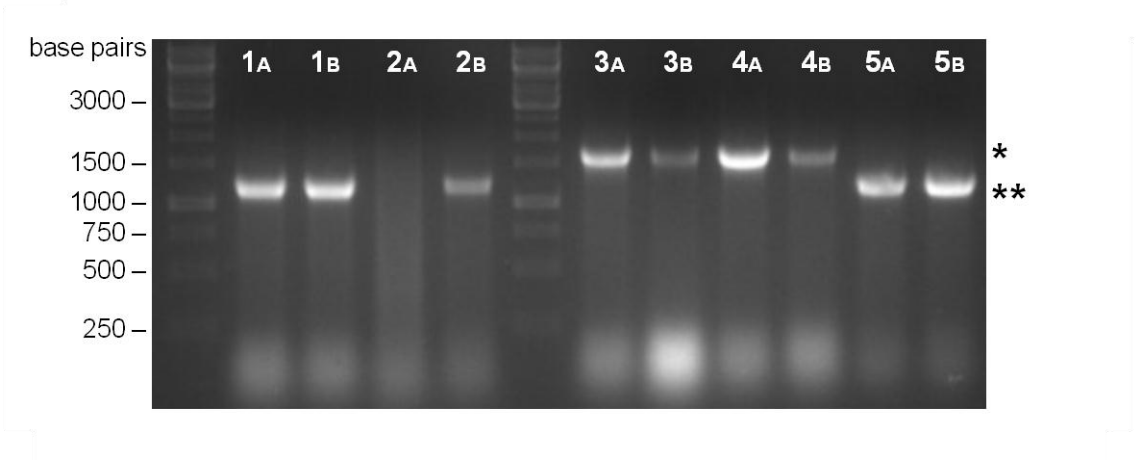

Figure 4-50: Colony PCRs of the yeast strains resulting from sporulation and tetrad dissection.
Colony PCRs of yeast cells amplifying the locus encoding for Cns1. Two colonies were analyzed for each yeast strain. Colony PCRs using wild type yeast strain BY4741 lead to amplification of the open reading frame of Cns1. The yeast strain (2n, YBR155w:kanMX4) was used as control for a diploid yeast strain containing the open reading frame and the deletion for CNs1 (2). Yeast strains (spore 1-2) contain the inserted deletion for Cns1 (YBR155w:kanMX4) (3,4). Spore 3 was used as control for the ORF of Cns1 (4).
Resulting PCR products of the inserted deletion for Cns1, YBR155w::kanMX4, (*) and the open reading frame of Cns1 (**) are marked on the right side.

As expected the two yeast strains resulting from sporulation and tetrad dissection, which showed the resistance against treatment with G418, contain the Cns1-kanMX cassette (Figure 4-50 and 4-48). As shown for the spore which was not able to grow on media containing G418, only the open reading encoding for Cns1 frame was amplified by colony-PCR.

By treatment with 5´-FOA, plasmids encoding for URA3 are digested. In a typical spot assay, the different spores were incubated on media containing 5´-FOA for 3 days at 30°C.

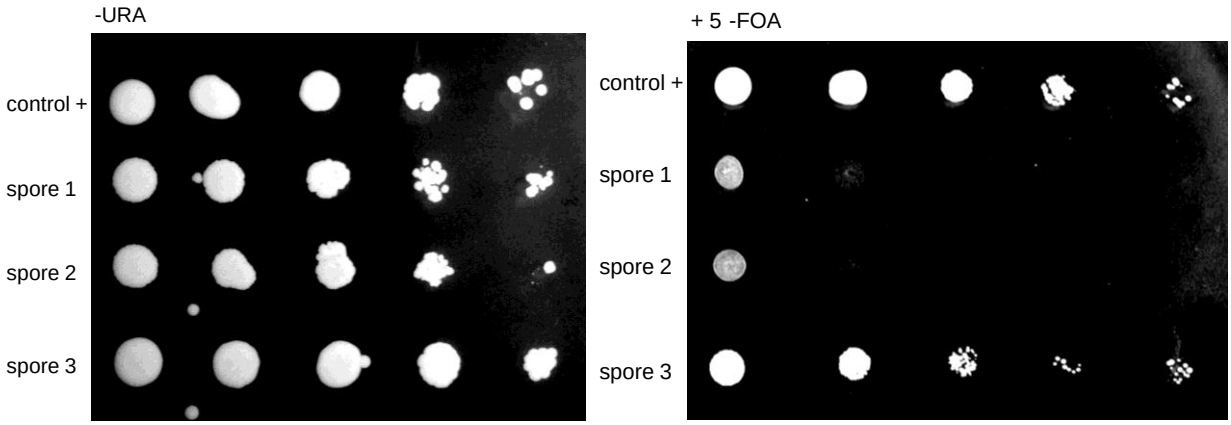

Figure 4-51: Growth of yeast strains resulting from sporulation and tetrad dissection.
Yeast strains (spores 1-3) containing the plasmid encoding for Cns1 (URA) and the diploid yeast strain (YBR155w::kanMX4; p426GPD-Cns1) used as positive control (control +). Cells were grown at 30°C until stationary phase. Then 1:10 serial dilutions were made. 3 µl of each dilution were spotted (density decrease from left to right) on URA$^-$-plates and plates containing 5´-FOA. Plates were incubated at 30°C for 3 days.

As shown above, both strains containing the deletion for Cns1 (YBR155w:kanMX4) are not able to grow on media containing 5´-FOA. This clearly shows that the plasmid encoding for Cns1 (URA3) was digested which resulted in lethality of the yeast cells resulting from deletion for the gene encoding for Cns1 (Figure 4-51). The yeast strain (spore 3) which contains the ORF encoding for Cns1 is still viable after treatment with 5´-FOA.

With the first viability assays and the PCR-based identification of the mating type and the ORF encoding for Cns1, the two resulting strain are haploid, contain the inserted YBR155w::kanMX4 and the plasmid encoding for Cns1 (p426GPD-Cns1).

4.3.4. Viability of different Cns1 fragments

After the yeast strain containing the deletion in Cns1-ORF and the Cns1wt copy on an URA3 plasmid, viability assays with different constructs of Cns1 were performed. Cns1 fragments were transformed into this strain. Treatment with 5´-FOA leads to digestion of the URA3-plasmid containing the Cns1wt copy (Figure 4-51). Only yeast cells containing plasmid with the essential part of Cns1 are viable. The essential function of the N-terminal domain of Cns1 containing the TPR-motifs could be shown. Deletion of the C-terminal domain of Cns1 did not affect growth of *S. cerevisiae* cells. Additionally, only the TPR-motifs are not able to rescue

viability of yeast strain where Cns1 is deleted. That implies importance of residues adjacent to the TPR domain (TESIC et al., HAINZL et al., 2004). However, the minimal fragment of Cns1, which is able to rescue viability of yeast cells, could not be targeted.

With the plasmid shuffling method, yeast cells expressing fragments containing the TPR-domain of Cns1 as sole source of Cns1 were tested for viability (Figure 4-52). Therefore the generated yeast strain (see 4.3.3.) was transformed with the different constructs of Cns1. After digestion of the plasmid encoding for Cns1 (p426GPD-Cns1, URA3) by treatment with 5´-FOA, viability of the yeast cells was checked.

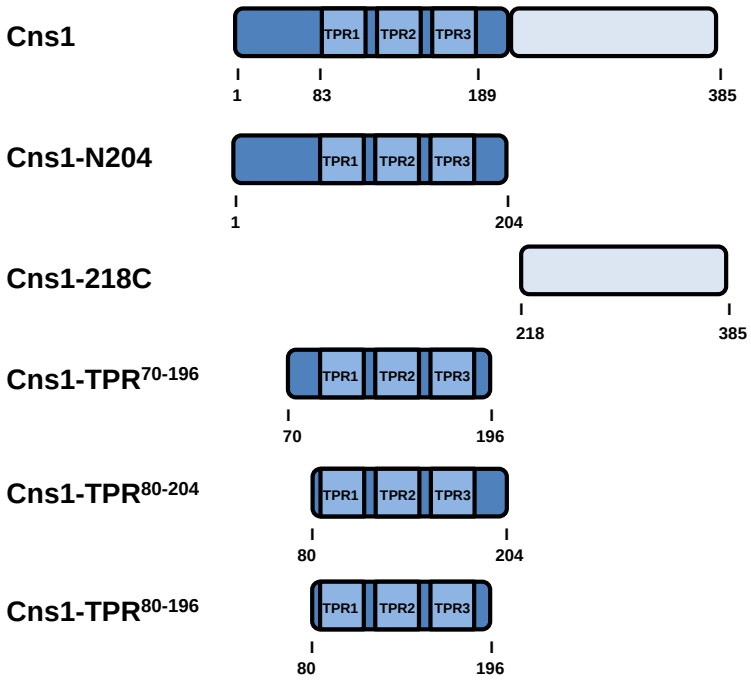

Figure 4-52: Schematic domain architecture of Cns1.
The TPR-domain is located in the N-terminal domain of Cns1. Plasmids containing the subdivided constructs of Cns1 were cloned into p425-GPD. Afterwards viability of yeast cells, expressing these constructs as sole source of Cns1, was tested.

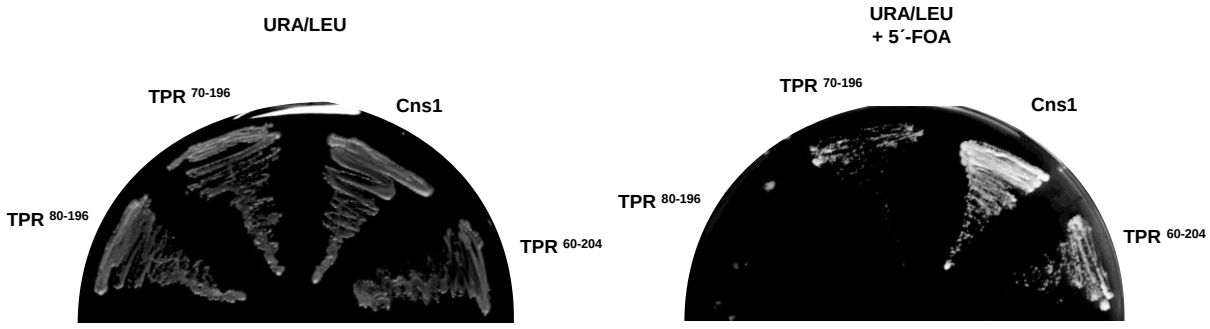

Figure 4-53: Growth of yeast strains resulting from sporulation and tetrad dissection.
Yeast strains (spores 1-3) containing the plasmid encoding for Cns1 (URA) were transformed with different construct of Cns1. Cells were grown at 30°C until stationary phase. Colonies were streaked on URA⁻/LEU⁻-plates and plates containing 5´-FOA. Plates were incubated at 30°C for 3 days.

Yeast cells expressing the C-terminal domain of Cns1 are not viable (Cns1-218C), whereas the N-terminal domain of Cns1 is able to restore viability (data not shown). That is in agreement with previous works (TESIC et al., 2003; HAINZL et al., 2004). Different construct of Cns1 showed that the amino acids adjacent to the TPR are essential for viability of the yeast cells. The TPR-domain (residues 83-189) is not able to restore viability (HAINZL et al., 2004). If the first 60 residues of Cns1 are truncated, yeast cells are still viable (data not shown). Yeast cell are not viable when the first 80 amino acids of Cns1 are deleted (Figure 4-52). Deletion of amino acids from the carboxy terminus lead to a decreased viability of the yeast cells (residues 70-196) (Figure 4-53).

4.3.5. Discussion

In order to test function of Cns1 in vivo, effects of Cns1 on growth and viability of yeast cells were analyzed. Cns1 was overexpressed and yeast cells were grown at different temperatures. That showed that overexpression of Cns1 did not influence growth or viability of yeast cells compared to wild type yeast cells. Also the function of Hsp90 in the maturation of its kinase client v-Src is not altered upon overexpression of Cns1.

In order to test different fragments of Cns1, a haploid yeast strain with a Cns1 knockout was created. With the plasmid shuffling method, fragments of Cns1 were tested for the ability to restore viability of the yeast cells. In this case, different fragments containing the

TPR-domain of Cns1 were used. As previously shown, amino acids adjacent to the TPR-domain of Cns1 are known to be essential for viability of yeast cells (TESIC et al., 2003; HAINZL et al., 2004). However, the minimal fragment of Cns1 that restores viability of the yeast cells was not determined so far. The TPR-motif (residues 83-189) is not able to fulfill the essential function of Cns1 (HAINZL et al., 2004). It was proposed, that the Cns1-Hsp90 interactions seems to be essential for viability of yeast cells (TESIC et al., 2003). If binding to Hsp90 is changed or disrupted in case of the TPR-domain (residues 83-189) remains unclear. When around 20 amino acids are present adjacent to the TPR-motif, viability of the yeast cells is restored (HAINZL et al., 2004). This Cns1 construct (residues 60-204) was further truncated at the N- and the C-terminus. N-terminal deletion leads to inviability of yeast cells.

When 80 N-terminal residues of Cns1 were deleted, yeast cells are not able to grow. Truncation of 70 residues from the N-terminal domain of Cns1 restores viability of yeast cells. With this assay, the minimal fragment of Cns1 which is able to grow, seem to be the TPR70-196. In order to test how binding to Hsp90 or Hsp70 is influenced with N- and C-terminal truncation, binding studies of the fragments should be done *in vitro*.

5. Summary

Hsp90 is a dedicated regulator of several substrate proteins. The ATPase activity of Hsp90 is regulated by several co-chaperones. The main activator of the ATPase activity of Hsp90 is Aha1. However, the specific mechanism of interaction of Aha1 and Hsp90 remains unclear. During this work, the mechanism of activation of the ATPase activity of Hsp90 by its co-chaperone Aha1 was solved with different biochemical and biophysical techniques. Both domains of Aha1 are involved to fully activate the ATPase activity of Hsp90. A second binding binding site for Aha1 to Hsp90 was identified. This pointed towards a binding mechanism of Aha1 to Hsp90, which includes both the middle and the N-terminal domain of Hsp90. Kinetic analysis with Hsp90 and several Hsp90 mutants implied a specific mechanism of activation by Aha1. With the heterodimer assays, it could be shown that Aha1 bridges the Hsp90 dimer. However, in contrast to this mechanism in *trans*, a mechanism in *cis* was also shown. Aha1 showed binding to both N-terminal domains of Hsp90. That favored the N-terminal closed conformation of the Hsp90 dimer. Kinetic analysis of different conformational states of Hsp90 showed that Aha1 is able to achieve a specific conformational state of the Hsp90 dimer. This effect leads to acceleration of the Hsp90 ATPase activity. Additionally, it was shown that only one Aha1 is sufficient to fully activate the Hsp90 ATPase activity.

For viability of yeast cells, the co-chaperone Cns1 exerts an essential function. However, it remained unclear how this protein is involved in the chaperone cycle. Cns1 is known to interact with Hsp90 and Hsp70. During this work, its specific recruitment and organization of Hsp90 co-chaperones complexes was investigated. For progression of the chaperone cycle of Hsp90, different co-chaperones act at different stages. It could be shown, that Cns1 did not prefer a specific conformational state of Hsp90. Binding assays with Hsp90 in the presence of various co-chaperones showed, that Cns1 is able to influence binding to other TPR-containing co-chaperones. Sti1, which serves as an adaptor for the Hsp70 and Hsp90 cycle, was not able to form complexes with Hsp90 in the presence of Cns1. Sti1 formed no mixed complexes with Cns1 and Hsp90. However, the cyclophilins Cpr6 and Cpr7 are able to disrupt the Cns1-Hsp90-complex. So, in contrast to Cpr6 and Sti1, no mixed complexes of Hsp90 were found in the presence of Cns1. However, for Ppt1, another TPR-containing co-chaperone, mixed complexes of Hsp90 and Cns1 seems possible. In the presence of Cns1, Aha1 and Hsp90, specific heterotrimeric complexes were detected. Aha1 did not

disrupt Cns1-Hsp90-complexes. Additionally, Cns1 did not influence stimulation of the ATPase activity by Aha1.

Cns1 is known to interact with Ssa1. In this work, it could be shown that Cns1 did not prefer specific conformational states of Ssa1. Additionally, the influence of Cns1 and Sti1 on complex formation of Ydj1 and Ssa1 was shown. The Ydj1-Ssa1 complex was only detectable in the presence of ATP. Sti1 is able to partially displace Ydj1 from Ssa1. However, Cns1 did not influence the Ydj1-Ssa1-complex formation.

For function of Cns1 in vivo, a yeast strain, which is deleted for genomically encoded Cns1, was generated. With the plasmid shuffling method, different constructs of Cns1 were tested for the ability to rescue viability of yeast cells. The experiments revealed that the TPR-domain of Cns1 and residues adjacent to the TPR-domain are essential for the *in vivo* function of Cns1.

6. Abbreviations

A	Ampere
A_{280}	absorption at 280 nm
AB	antibody
APS	Ammoniumpersulfate
ATPase	ATP hydrolase
BSA	bovine serum albumine
CD	circular dichroism
C. elegans	*Caenorhabditis elegans*
Da	Dalton
D. melanogaster	*Drosophila melanogaster*
DNA	Desoxyribunucleic acid
ε	Molar extinction cooefficient
E. coli	*Escherichia coli*
EDC	1-Ethyl-3-(dimethylaminopropyl)-carbodiimid-HCl
EDTA	Ethylenediamine-tetraacetic acid
FPLC	fast protein liquid chromatography
g	gram
GR	glucocorticoid receptore
h	hour
HCl	hydrochloric acid
HEPES	N-(2-Hydroxyethyle)-piperazine-N´-2-ethanesulfonic acid
Hsp(s)	Heat shock protein(s)

ITC	isothermic titration calorimetry
kDa	kilo Dalton
k_{cat}	unimolecular rate constant
K_D	dissociation constant
λ	Wavelength
l	liter
LBD	ligand binding domain
min	Minute
ml	milliliter
mM	Millimolar
µM	micromolar
MW	molecular weight
NHS	N-hydroxy-succineimide
nm	nanometer
nM	nanomolar
OD	optical density
PAGE	polyacrylamide gel electrophoresis
PEP	phosphoenole pyruvate
pH	potentia hydrogenii
pI	isoelectric point
PK	pyruvate kinase
P. pastoris	*Pichia pastoris*
PPIase	pepdidyl-prolyl-isomerase
RNA	ribuncleic acid
RNAse	ribunuclease
RT	room temperature
s	second

S. cerevisiae	*Saccharomyces cerevisiae*
SDS	Sodium dodecylsulfate
SHR	steroid hormone receptor
SPR	surface plasmon resonance
TEMED	N, N, N´,N´-Tetramethylethylenediamine
Tris/HCl	Trihydroxymethylaminomethan-hydrochloride
Rpm	rounds per minute
UV	ultraviolet
V	Volt
v/v	volume per volume
w/v	weight per volume

7. Literature

Akerfelt, M., D. Trouillet, et al. (2007). "Heat shock factors at a crossroad between stress and development." Ann N Y Acad Sci **1113**: 15-27.

Ali, M. M., S. M. Roe, et al. (2006). "Crystal structure of an Hsp90-nucleotide-p23/Sba1 closed chaperone complex." Nature **440**(7087): 1013-1017.

Andreasson, C., J. Fiaux, et al. (2008). "Insights into the structural dynamics of the Hsp110-Hsp70 interaction reveal the mechanism for nucleotide exchange activity." Proc Natl Acad Sci U S A **105**(43): 16519-16524.

Andreasson, C., J. Fiaux, et al. (2008). "Hsp110 is a nucleotide-activated exchange factor for Hsp70." J Biol Chem **283**(14): 8877-8884.

Anfinsen, C. B., E. Haber, et al. (1961). "The kinetics of formation of native ribonuclease during oxidation of the reduced polypeptide chain." Proc Natl Acad Sci U S A **47**: 1309-1314.

Banecki, B. and M. Zylicz (1996). "Real time kinetics of the DnaK/DnaJ/GrpE molecular chaperone machine action." J Biol Chem **271**(11): 6137-6143.

Bardwell, J. C. and E. A. Craig (1988). "Ancient heat shock gene is dispensable." J Bacteriol **170**(7): 2977-2983.

Beckmann, R. P., L. E. Mizzen, et al. (1990). "Interaction of Hsp 70 with newly synthesized proteins: implications for protein folding and assembly." Science **248**(4957): 850-854.

Beissinger, M., K. Rutkat, et al. (1999). "Catalysis, commitment and encapsulation during GroE-mediated folding." J Mol Biol **289**(4): 1075-1092.

Bergerat, A., B. de Massy, et al. (1997). "An atypical topoisomerase II from Archaea with implications for meiotic recombination." Nature **386**(6623): 414-417.

Bertelsen, E. B., L. Chang, et al. (2009). "Solution conformation of wild-type E. coli Hsp70 (DnaK) chaperone complexed with ADP and substrate." Proc Natl Acad Sci U S A **106**(21): 8471-8476.

Bhattacharya, A., A. V. Kurochkin, et al. (2009). "Allostery in Hsp70 chaperones is transduced by subdomain rotations." J Mol Biol **388**(3): 475-490.

Blond-Elguindi, S., S. E. Cwirla, et al. (1993). "Affinity panning of a library of peptides displayed on bacteriophages reveals the binding specificity of BiP." Cell **75**(4): 717-728.

Blond-Elguindi, S., A. M. Fourie, et al. (1993). "Peptide-dependent stimulation of the ATPase activity of the molecular chaperone BiP is the result of conversion of oligomers to active monomers." J Biol Chem **268**(17): 12730-12735.

Bocking, T., F. Aguet, et al. (2011). "Single-molecule analysis of a molecular disassemblase reveals the mechanism of Hsc70-driven clathrin uncoating." Nat Struct Mol Biol **18**(3): 295-301.

Borkovich, K. A., F. W. Farrelly, et al. (1989). "hsp82 is an essential protein that is required in higher concentrations for growth of cells at higher temperatures." Mol Cell Biol **9**(9): 3919-3930.

Bose, S., T. Weikl, et al. (1996). "Chaperone function of Hsp90-associated proteins." Science **274**(5293): 1715-1717.

Braig, K., Z. Otwinowski, et al. (1994). "The crystal structure of the bacterial chaperonin GroEL at 2.8 A." Nature **371**(6498): 578-586.

Breter, H. J., J. Ferguson, et al. (1983). "Isolation and transcriptional characterization of three genes which function at start, the controlling event of the Saccharomyces cerevisiae cell division cycle: CDC36, CDC37, and CDC39." Mol Cell Biol **3**(5): 881-891.

Brugge, J. S. (1986). "Interaction of the Rous sarcoma virus protein pp60src with the cellular proteins pp50 and pp90." Curr Top Microbiol Immunol **123**: 1-22.

Buchner, J. (1996). "Supervising the fold: functional principles of molecular chaperones." FASEB J **10**(1): 10-19.

Bukau, B. and A. L. Horwich (1998). "The Hsp70 and Hsp60 chaperone machines." Cell **92**(3): 351-366.

Bukau, B., J. Weissman, et al. (2006). "Molecular chaperones and protein quality control." Cell **125**(3): 443-451.

Carrello, A., E. Ingley, et al. (1999). "The common tetratricopeptide repeat acceptor site for steroid receptor-associated immunophilins and hop is located in the dimerization domain of Hsp90." J Biol Chem **274**(5): 2682-2689.

Carrigan, P. E., D. L. Riggs, et al. (2005). "Functional comparison of human and Drosophila Hop reveals novel role in steroid receptor maturation." J Biol Chem **280**(10): 8906-8911.

Cashikar, A. G., M. Duennwald, et al. (2005). "A chaperone pathway in protein disaggregation. Hsp26 alters the nature of protein aggregates to facilitate reactivation by Hsp104." J Biol Chem **280**(25): 23869-23875.

Chadli, A., E. S. Bruinsma, et al. (2008). "Analysis of Hsp90 cochaperone interactions reveals a novel mechanism for TPR protein recognition." Biochemistry **47**(9): 2850-2857.

Chakraborty, K., M. Chatila, et al. (2010). "Chaperonin-catalyzed rescue of kinetically trapped states in protein folding." Cell **142**(1): 112-122.

Cheetham, M. E. and A. J. Caplan (1998). "Structure, function and evolution of DnaJ: conservation and adaptation of chaperone function." Cell Stress Chaperones **3**(1): 28-36.

Chen, C. F., Y. Chen, et al. (1996). "A new member of the hsp90 family of molecular chaperones interacts with the retinoblastoma protein during mitosis and after heat shock." Mol Cell Biol **16**(9): 4691-4699.

Chen, J. and C. L. Brooks, 3rd (2008). "Implicit modeling of nonpolar solvation for simulating protein folding and conformational transitions." Phys Chem Chem Phys **10**(4): 471-481.

Chen, L. and P. B. Sigler (1999). "The crystal structure of a GroEL/peptide complex: plasticity as a basis for substrate diversity." Cell **99**(7): 757-768.

Chen, S. and D. F. Smith (1998). "Hop as an adaptor in the heat shock protein 70 (Hsp70) and hsp90 chaperone machinery." J Biol Chem **273**(52): 35194-35200.

Chen, S., W. P. Sullivan, et al. (1998). "Differential interactions of p23 and the TPR-containing proteins Hop, Cyp40, FKBP52 and FKBP51 with Hsp90 mutants." Cell Stress Chaperones **3**(2): 118-129.

Cheng, M. Y., F. U. Hartl, et al. (1989). "Mitochondrial heat-shock protein hsp60 is essential for assembly of proteins imported into yeast mitochondria." Nature **337**(6208): 620-625.

Chernoff, Y. O., S. L. Lindquist, et al. (1995). "Role of the chaperone protein Hsp104 in propagation of the yeast prion-like factor [psi+]." Science **268**(5212): 880-884.

Cintron, N. S. and D. Toft (2006). "Defining the requirements for Hsp40 and Hsp70 in the Hsp90 chaperone pathway." J Biol Chem **281**(36): 26235-26244.

Clare, D. K., D. Vasishtan, et al. (2012). "ATP-triggered conformational changes delineate substrate-binding and -folding mechanics of the GroEL chaperonin." Cell **149**(1): 113-123.

Costantino, E., F. Maddalena, et al. (2009). "TRAP1, a novel mitochondrial chaperone responsible for multi-drug resistance and protection from apoptotis in human colorectal carcinoma cells." Cancer Lett **279**(1): 39-46.

Craig, E. A., P. Huang, et al. (2006). "The diverse roles of J-proteins, the obligate Hsp70 co-chaperone." Rev Physiol Biochem Pharmacol **156**: 1-21.

Crevel, G., H. Bates, et al. (2001). "The Drosophila Dpit47 protein is a nuclear Hsp90 co-chaperone that interacts with DNA polymerase alpha." J Cell Sci **114**(Pt 11): 2015-2025.

Crevel, G., D. Bennett, et al. (2008). "The human TPR protein TTC4 is a putative Hsp90 co-chaperone which interacts with CDC6 and shows alterations in transformed cells." PLoS One **3**(3): e0001737.

Cyr, D. M. and M. G. Douglas (1994). "Differential regulation of Hsp70 subfamilies by the eukaryotic DnaJ homologue YDJ1." J Biol Chem **269**(13): 9798-9804.

Cyr, D. M., X. Lu, et al. (1992). "Regulation of Hsp70 function by a eukaryotic DnaJ homolog." J Biol Chem **267**(29): 20927-20931.

De Los Rios, P., A. Ben-Zvi, et al. (2006). "Hsp70 chaperones accelerate protein translocation and the unfolding of stable protein aggregates by entropic pulling." Proc Natl Acad Sci U S A **103**(16): 6166-6171.

Deshaies, R. J., B. D. Koch, et al. (1988). "The role of stress proteins in membrane biogenesis." Trends Biochem Sci **13**(10): 384-388.

Deshaies, R. J., B. D. Koch, et al. (1988). "A subfamily of stress proteins facilitates translocation of secretory and mitochondrial precursor polypeptides." Nature **332**(6167): 800-805.

Dey, B., J. J. Lightbody, et al. (1996). "CDC37 is required for p60v-src activity in yeast." Mol Biol Cell **7**(9): 1405-1417.

Diamant, S., A. P. Ben-Zvi, et al. (2000). "Size-dependent disaggregation of stable protein aggregates by the DnaK chaperone machinery." J Biol Chem **275**(28): 21107-21113.

Diamant, S. and P. Goloubinoff (1998). "Temperature-controlled activity of DnaK-DnaJ-GrpE chaperones: protein-folding arrest and recovery during and after heat shock depends on the substrate protein and the GrpE concentration." Biochemistry **37**(27): 9688-9694.

Dittmar, K. D., M. Banach, et al. (1998). "The role of DnaJ-like proteins in glucocorticoid receptor.hsp90 heterocomplex assembly by the reconstituted hsp90.p60.hsp70 foldosome complex." J Biol Chem **273**(13): 7358-7366.

Dobson, C. M. (2004). "Principles of protein folding, misfolding and aggregation." Semin Cell Dev Biol **15**(1): 3-16.

Dolinski, K. J., M. E. Cardenas, et al. (1998). "CNS1 encodes an essential p60/Sti1 homolog in Saccharomyces cerevisiae that suppresses cyclophilin 40 mutations and interacts with Hsp90." Mol Cell Biol **18**(12): 7344-7352.

Dragovic, Z., S. A. Broadley, et al. (2006). "Molecular chaperones of the Hsp110 family act as nucleotide exchange factors of Hsp70s." EMBO J **25**(11): 2519-2528.

Dragovic, Z., Y. Shomura, et al. (2006). "Fes1p acts as a nucleotide exchange factor for the ribosome-associated molecular chaperone Ssb1p." Biol Chem **387**(12): 1593-1600.
Duina, A. A., H. C. Chang, et al. (1996). "A cyclophilin function in Hsp90-dependent signal transduction." Science **274**(5293): 1713-1715.

Duina, A. A., J. A. Marsh, et al. (1996). "Identification of two CyP-40-like cyclophilins in Saccharomyces cerevisiae, one of which is required for normal growth." Yeast **12**(10): 943-952.

Eaglestone, S. S., L. W. Ruddock, et al. (2000). "Guanidine hydrochloride blocks a critical step in the propagation of the prion-like determinant [PSI(+)] of Saccharomyces cerevisiae." Proc Natl Acad Sci U S A **97**(1): 240-244.

Echtenkamp, F. J. and B. C. Freeman (2012). "Expanding the cellular molecular chaperone network through the ubiquitous cochaperones." Biochim Biophys Acta **1823**(3): 668-673.

Ehrnsperger, M., S. Graber, et al. (1997). "Binding of non-native protein to Hsp25 during heat shock creates a reservoir of folding intermediates for reactivation." EMBO J **16**(2): 221-229.

Fang, Y., A. E. Fliss, et al. (1998). "SBA1 encodes a yeast hsp90 cochaperone that is homologous to vertebrate p23 proteins." Mol Cell Biol **18**(7): 3727-3734.

Fanghanel, J. and G. Fischer (2004). "Insights into the catalytic mechanism of peptidyl prolyl cis/trans isomerases." Front Biosci **9**: 3453-3478.

Felts, S. J., B. A. Owen, et al. (2000). "The hsp90-related protein TRAP1 is a mitochondrial protein with distinct functional properties." J Biol Chem **275**(5): 3305-3312.

Fenton, W. A. and A. L. Horwich (2003). "Chaperonin-mediated protein folding: fate of substrate polypeptide." Q Rev Biophys **36**(2): 229-256.

Ferguson, J., J. Y. Ho, et al. (1986). "Nucleotide sequence of the yeast cell division cycle start genes CDC28, CDC36, CDC37, and CDC39, and a structural analysis of the predicted products." Nucleic Acids Res **14**(16): 6681-6697.

Ferreira, L. R., K. Norris, et al. (1994). "Association of Hsp47, Grp78, and Grp94 with procollagen supports the successive or coupled action of molecular chaperones." J Cell Biochem **56**(4): 518-526.

Fersht, A. R. and V. Daggett (2002). "Protein folding and unfolding at atomic resolution." Cell **108**(4): 573-582.

Flaherty, K. M., C. DeLuca-Flaherty, et al. (1990). "Three-dimensional structure of the ATPase fragment of a 70K heat-shock cognate protein." Nature **346**(6285): 623-628.

Flaherty, K. M., D. B. McKay, et al. (1991). "Similarity of the three-dimensional structures of actin and the ATPase fragment of a 70-kDa heat shock cognate protein." Proc Natl Acad Sci U S A **88**(11): 5041-5045.

Flom, G., J. Weekes, et al. (2006). "Effect of mutation of the tetratricopeptide repeat and asparatate-proline 2 domains of Sti1 on Hsp90 signaling and interaction in Saccharomyces cerevisiae." Genetics **172**(1): 41-51.

Flynn, G. C., J. Pohl, et al. (1991). "Peptide-binding specificity of the molecular chaperone BiP." Nature **353**(6346): 726-730.

Freeman, B. C., S. J. Felts, et al. (2000). "The p23 molecular chaperones act at a late step in intracellular receptor action to differentially affect ligand efficacies." Genes Dev **14**(4): 422-434.

Freeman, B. C. and R. I. Morimoto (1996). "The human cytosolic molecular chaperones hsp90, hsp70 (hsc70) and hdj-1 have distinct roles in recognition of a non-native protein and protein refolding." EMBO J **15**(12): 2969-2979.

Frydman, J., E. Nimmesgern, et al. (1994). "Folding of nascent polypeptide chains in a high molecular mass assembly with molecular chaperones." Nature **370**(6485): 111-117.

Gaiser, A. M., A. Kretzschmar, et al. (2010). "Cdc37-Hsp90 complexes are responsive to nucleotide-induced conformational changes and binding of further cofactors." J Biol Chem **285**(52): 40921-40932.

Gamer, J., H. Bujard, et al. (1992). "Physical interaction between heat shock proteins DnaK, DnaJ, and GrpE and the bacterial heat shock transcription factor sigma 32." Cell **69**(5): 833-842.

Gao, B., Y. Emoto, et al. (1993). "Nucleotide binding properties of bovine brain uncoating ATPase." J Biol Chem **268**(12): 8507-8513.

Gasch, A. P., P. T. Spellman, et al. (2000). "Genomic expression programs in the response of yeast cells to environmental changes." Mol Biol Cell **11**(12): 4241-4257.

Gassler, C. S., A. Buchberger, et al. (1998). "Mutations in the DnaK chaperone affecting interaction with the DnaJ cochaperone." Proc Natl Acad Sci U S A **95**(26): 15229-15234.

Gautschi, M., H. Lilie, et al. (2001). "RAC, a stable ribosome-associated complex in yeast formed by the DnaK-DnaJ homologs Ssz1p and zuotin." Proc Natl Acad Sci U S A **98**(7): 3762-3767.

Gautschi, M., A. Mun, et al. (2002). "A functional chaperone triad on the yeast ribosome." Proc Natl Acad Sci U S A **99**(7): 4209-4214.

Georgopoulos, C. and W. J. Welch (1993). "Role of the major heat shock proteins as molecular chaperones." Annu Rev Cell Biol **9**: 601-634.

Gething, M. J. and J. Sambrook (1992). "Protein folding in the cell." Nature **355**(6355): 33-45.

Glover, J. R. and S. Lindquist (1998). "Hsp104, Hsp70, and Hsp40: a novel chaperone system that rescues previously aggregated proteins." Cell **94**(1): 73-82.

Go, N. and H. Taketomi (1978). "Respective roles of short- and long-range interactions in protein folding." Proc Natl Acad Sci U S A **75**(2): 559-563.

Goeckeler, J. L., A. P. Petruso, et al. (2008). "The yeast Hsp110, Sse1p, exhibits high-affinity peptide binding." FEBS Lett **582**(16): 2393-2396.

Goloubinoff, P. and P. De Los Rios (2007). "The mechanism of Hsp70 chaperones: (entropic) pulling the models together." Trends Biochem Sci **32**(8): 372-380.

Goloubinoff, P., A. A. Gatenby, et al. (1989). "GroE heat-shock proteins promote assembly of foreign prokaryotic ribulose bisphosphate carboxylase oligomers in Escherichia coli." Nature **337**(6202): 44-47.

Goloubinoff, P., A. Mogk, et al. (1999). "Sequential mechanism of solubilization and refolding of stable protein aggregates by a bichaperone network." Proc Natl Acad Sci U S A **96**(24): 13732-13737.

Graf, C., M. Stankiewicz, et al. (2009). "Spatially and kinetically resolved changes in the conformational dynamics of the Hsp90 chaperone machine." EMBO J **28**(5): 602-613.

Greene, L. E., R. Zinner, et al. (1995). "Effect of nucleotide on the binding of peptides to 70-kDa heat shock protein." J Biol Chem **270**(7): 2967-2973.

Greene, M. K., K. Maskos, et al. (1998). "Role of the J-domain in the cooperation of Hsp40 with Hsp70." Proc Natl Acad Sci U S A **95**(11): 6108-6113.

Ha, J. H., U. Hellman, et al. (1997). "Destabilization of peptide binding and interdomain communication by an E543K mutation in the bovine 70-kDa heat shock cognate protein, a molecular chaperone." J Biol Chem **272**(44): 27796-27803.

Ha, J. H. and D. B. McKay (1994). "ATPase kinetics of recombinant bovine 70 kDa heat shock cognate protein and its amino-terminal ATPase domain." Biochemistry **33**(48): 14625-14635.

Ha, J. H. and D. B. McKay (1995). "Kinetics of nucleotide-induced changes in the tryptophan fluorescence of the molecular chaperone Hsc70 and its subfragments suggest the ATP-induced conformational change follows initial ATP binding." Biochemistry **34**(36): 11635-11644.

Hageman, J. and H. H. Kampinga (2009). "Computational analysis of the human HSPH/HSPA/DNAJ family and cloning of a human HSPH/HSPA/DNAJ expression library." Cell Stress Chaperones **14**(1): 1-21.

Hagn, F., S. Lagleder, et al. (2011). "Structural analysis of the interaction between Hsp90 and the tumor suppressor protein p53." Nat Struct Mol Biol **18**(10): 1086-1093.

Hainzl, O., M. C. Lapina, et al. (2009). "The charged linker region is an important regulator of Hsp90 function." J Biol Chem **284**(34): 22559-22567.

Hainzl, O., H. Wegele, et al. (2004). "Cns1 is an activator of the Ssa1 ATPase activity." J Biol Chem **279**(22): 23267-23273.

Halfmann, R., D. F. Jarosz, et al. (2012). "Prions are a common mechanism for phenotypic inheritance in wild yeasts." Nature **482**(7385): 363-368.

Han, W. and P. Christen (2003). "Mechanism of the targeting action of DnaJ in the DnaK molecular chaperone system." J Biol Chem **278**(21): 19038-19043.

Harris, S. F., A. K. Shiau, et al. (2004). "The crystal structure of the carboxy-terminal dimerization domain of htpG, the Escherichia coli Hsp90, reveals a potential substrate binding site." Structure **12**(6): 1087-1097.

Harrison, C. (2003). "GrpE, a nucleotide exchange factor for DnaK." Cell Stress Chaperones **8**(3): 218-224.

Hartl, F. U. and M. Hayer-Hartl (2002). "Molecular chaperones in the cytosol: from nascent chain to folded protein." Science **295**(5561): 1852-1858.

Hartl, F. U. and M. Hayer-Hartl (2009). "Converging concepts of protein folding in vitro and in vivo." Nat Struct Mol Biol **16**(6): 574-581.

Haslbeck, M., A. Miess, et al. (2005). "Disassembling protein aggregates in the yeast cytosol. The cooperation of Hsp26 with Ssa1 and Hsp104." J Biol Chem **280**(25): 23861-23868.

Haslbeck, M., S. Walke, et al. (1999). "Hsp26: a temperature-regulated chaperone." EMBO J **18**(23): 6744-6751.

Hawle, P., M. Siepmann, et al. (2006). "The middle domain of Hsp90 acts as a discriminator between different types of client proteins." Mol Cell Biol **26**(22): 8385-8395.

Helsen, C. W. and J. R. Glover (2012). "Insight into molecular basis of curing of [PSI+] prion by overexpression of 104-kDa heat shock protein (Hsp104)." J Biol Chem **287**(1): 542-556.

Hendrick, J. P. and F. U. Hartl (1993). "Molecular chaperone functions of heat-shock proteins." Annu Rev Biochem **62**: 349-384.

Hernandez, M. P., W. P. Sullivan, et al. (2002). "The assembly and intermolecular properties of the hsp70-Hop-hsp90 molecular chaperone complex." J Biol Chem **277**(41): 38294-38304.

Herrmann, J. M. and W. Neupert (2000). "Protein transport into mitochondria." Curr Opin Microbiol **3**(2): 210-214.

Hessling, M., K. Richter, et al. (2009). "Dissection of the ATP-induced conformational cycle of the molecular chaperone Hsp90." Nat Struct Mol Biol **16**(3): 287-293.

Hickey, E., S. E. Brandon, et al. (1989). "Sequence and regulation of a gene encoding a human 89-kilodalton heat shock protein." Mol Cell Biol **9**(6): 2615-2626.

Hoff, K. G., J. J. Silberg, et al. (2000). "Interaction of the iron-sulfur cluster assembly protein IscU with the Hsc66/Hsc20 molecular chaperone system of Escherichia coli." Proc Natl Acad Sci U S A **97**(14): 7790-7795.

Hofmann, H., F. Hillger, et al. (2010). "Single-molecule spectroscopy of protein folding in a chaperonin cage." Proc Natl Acad Sci U S A **107**(26): 11793-11798.

Horwich, A. L., W. Neupert, et al. (1990). "Protein-catalysed protein folding." Trends Biotechnol **8**(5): 126-131.

Horwitz, J. (1992). "Alpha-crystallin can function as a molecular chaperone." Proc Natl Acad Sci U S A **89**(21): 10449-10453.

Hua, G., Q. Zhang, et al. (2007). "Heat shock protein 75 (TRAP1) antagonizes reactive oxygen species generation and protects cells from granzyme M-mediated apoptosis." J Biol Chem **282**(28): 20553-20560.

Huang, P., M. Gautschi, et al. (2005). "The Hsp70 Ssz1 modulates the function of the ribosome-associated J-protein Zuo1." Nat Struct Mol Biol **12**(6): 497-504.

Hundley, H., H. Eisenman, et al. (2002). "The in vivo function of the ribosome-associated Hsp70, Ssz1, does not require its putative peptide-binding domain." Proc Natl Acad Sci U S A **99**(7): 4203-4208.

Hupp, T. R., D. W. Meek, et al. (1992). "Regulation of the specific DNA binding function of p53." Cell **71**(5): 875-886.

Itoh, T., H. Matsuda, et al. (1999). "Phylogenetic analysis of the third hsp70 homolog in Escherichia coli; a novel member of the Hsc66 subfamily and its possible co-chaperone." DNA Res **6**(5): 299-305.

Jaenicke, R. and R. Rudolph (1986). "Refolding and association of oligomeric proteins." Methods Enzymol **131**: 218-250.

Jakob, U. and J. Buchner (1994). "Assisting spontaneity: the role of Hsp90 and small Hsps as molecular chaperones." Trends Biochem Sci **19**(5): 205-211.

Jakob, U., T. Scheibel, et al. (1996). "Assessment of the ATP binding properties of Hsp90." J Biol Chem **271**(17): 10035-10041.

Jiang, J., E. G. Maes, et al. (2007). "Structural basis of J cochaperone binding and regulation of Hsp70." Mol Cell **28**(3): 422-433.

Johnson, B. D., R. J. Schumacher, et al. (1998). "Hop modulates Hsp70/Hsp90 interactions in protein folding." J Biol Chem **273**(6): 3679-3686.

Johnson, J. L. and D. O. Toft (1994). "A novel chaperone complex for steroid receptors involving heat shock proteins, immunophilins, and p23." J Biol Chem **269**(40): 24989-24993.

Johnson, J. L. and D. O. Toft (1995). "Binding of p23 and hsp90 during assembly with the progesterone receptor." Mol Endocrinol **9**(6): 670-678.

Kabani, M. (2009). "Structural and functional diversity among eukaryotic Hsp70 nucleotide exchange factors." Protein Pept Lett **16**(6): 623-660.

Kabsch, W., H. G. Mannherz, et al. (1990). "Atomic structure of the actin:DNase I complex." Nature **347**(6288): 37-44.

Kampinga, H. H. and E. A. Craig (2010). "The HSP70 chaperone machinery: J proteins as drivers of functional specificity." Nat Rev Mol Cell Biol **11**(8): 579-592.

Kang, H., S. L. Sayner, et al. (2001). "Identification of amino acids in the tetratricopeptide repeat and C-terminal domains of protein phosphatase 5 involved in autoinhibition and lipid activation." Biochemistry **40**(35): 10485-10490.

Kim, K. K., R. Kim, et al. (1998). "Crystal structure of a small heat-shock protein." Nature **394**(6693): 595-599.

Kloss, E., N. Courtemanche, et al. (2008). "Repeat-protein folding: new insights into origins of cooperativity, stability, and topology." Arch Biochem Biophys **469**(1): 83-99.

Klostermeier, D., R. Seidel, et al. (1998). "Functional properties of the molecular chaperone DnaK from Thermus thermophilus." J Mol Biol **279**(4): 841-853.

Knarr, G., S. Modrow, et al. (1999). "BiP-binding sequences in HIV gp160. Implications for the binding specificity of bip." J Biol Chem **274**(42): 29850-29857.

Kortemme, T., M. Ramirez-Alvarado, et al. (1998). "Design of a 20-amino acid, three-stranded beta-sheet protein." Science **281**(5374): 253-256.

Kosano, H., B. Stensgard, et al. (1998). "The assembly of progesterone receptor-hsp90 complexes using purified proteins." J Biol Chem **273**(49): 32973-32979.

Kramer, G., D. Boehringer, et al. (2009). "The ribosome as a platform for co-translational processing, folding and targeting of newly synthesized proteins." Nat Struct Mol Biol **16**(6): 589-597.

Krishna, P. and G. Gloor (2001). "The Hsp90 family of proteins in Arabidopsis thaliana." Cell Stress Chaperones **6**(3): 238-246.

Kumar, D. P., C. Vorvis, et al. (2011). "The four hydrophobic residues on the Hsp70 inter-domain linker have two distinct roles." J Mol Biol **411**(5): 1099-1113.

Landry, S. J. (2003). "Swivels and stators in the Hsp40-Hsp70 chaperone machine." Structure **11**(12): 1465-1466.

Large, A. T., M. D. Goldberg, et al. (2009). "Chaperones and protein folding in the archaea." Biochem Soc Trans **37**(Pt 1): 46-51.

Large, A. T. and P. A. Lund (2009). "Archaeal chaperonins." Front Biosci **14**: 1304-1324.

Li, J., X. Qian, et al. (2003). "The crystal structure of the yeast Hsp40 Ydj1 complexed with its peptide substrate." Structure **11**(12): 1475-1483.

Li, J., K. Richter, et al. (2011). "Mixed Hsp90-cochaperone complexes are important for the progression of the reaction cycle." Nat Struct Mol Biol **18**(1): 61-66.

Li, J., J. Soroka, et al. (2012). "The Hsp90 chaperone machinery: Conformational dynamics and regulation by co-chaperones." Biochim Biophys Acta **1823**(3): 624-635.

Liang, P. and T. H. MacRae (1997). "Molecular chaperones and the cytoskeleton." J Cell Sci **110 (Pt 13)**: 1431-1440.

Lindquist, S. and E. A. Craig (1988). "The heat-shock proteins." Annu Rev Genet **22**: 631-677.

Liu, B. and Z. Li (2008). "Endoplasmic reticulum HSP90b1 (gp96, grp94) optimizes B-cell function via chaperoning integrin and TLR but not immunoglobulin." Blood **112**(4): 1223-1230.

Liu, X. D., K. A. Morano, et al. (1999). "The yeast Hsp110 family member, Sse1, is an Hsp90 cochaperone." J Biol Chem **274**(38): 26654-26660.

Lopez-Buesa, P., C. Pfund, et al. (1998). "The biochemical properties of the ATPase activity of a 70-kDa heat shock protein (Hsp70) are governed by the C-terminal domains." Proc Natl Acad Sci U S A **95**(26): 15253-15258.

Lotz, G. P., H. Lin, et al. (2003). "Aha1 binds to the middle domain of Hsp90, contributes to client protein activation, and stimulates the ATPase activity of the molecular chaperone." J Biol Chem **278**(19): 17228-17235.

Louvion, J. F., R. Warth, et al. (1996). "Two eukaryote-specific regions of Hsp82 are dispensable for its viability and signal transduction functions in yeast." Proc Natl Acad Sci U S A **93**(24): 13937-13942.

Lu, Z. and D. M. Cyr (1998). "The conserved carboxyl terminus and zinc finger-like domain of the co-chaperone Ydj1 assist Hsp70 in protein folding." J Biol Chem **273**(10): 5970-5978.

Lu, Z. and D. M. Cyr (1998). "Protein folding activity of Hsp70 is modified differentially by the hsp40 co-chaperones Sis1 and Ydj1." J Biol Chem **273**(43): 27824-27830.

Lu, Z., Y. Tao, et al. (2006). "Mitochondrial reactive oxygen species and nitric oxide-mediated cancer cell apoptosis in 2-butylamino-2-demethoxyhypocrellin B photodynamic treatment." Free Radic Biol Med **41**(10): 1590-1605.

Lutz, T., B. Westermann, et al. (2001). "The mitochondrial proteins Ssq1 and Jac1 are required for the assembly of iron sulfur clusters in mitochondria." J Mol Biol **307**(3): 815-825.

MacLean, M. and D. Picard (2003). "Cdc37 goes beyond Hsp90 and kinases." Cell Stress Chaperones **8**(2): 114-119.

Mandal, A. K., P. A. Gibney, et al. (2010). "Hsp110 chaperones control client fate determination in the hsp70-Hsp90 chaperone system." Mol Biol Cell **21**(9): 1439-1448.

Mandal, A. K., P. Lee, et al. (2007). "Cdc37 has distinct roles in protein kinase quality control that protect nascent chains from degradation and promote posttranslational maturation." J Cell Biol **176**(3): 319-328.

Marcinowski, M., M. Holler, et al. (2011). "Substrate discrimination of the chaperone BiP by autonomous and cochaperone-regulated conformational transitions." Nat Struct Mol Biol **18**(2): 150-158.

Marsh, J. A., H. M. Kalton, et al. (1998). "Cns1 is an essential protein associated with the hsp90 chaperone complex in Saccharomyces cerevisiae that can restore cyclophilin 40-dependent functions in cpr7Delta cells." Mol Cell Biol **18**(12): 7353-7359.

Maruya, M., M. Sameshima, et al. (1999). "Monomer arrangement in HSP90 dimer as determined by decoration with N and C-terminal region specific antibodies." J Mol Biol **285**(3): 903-907.

Masuda, Y., G. Shima, et al. (2004). "Involvement of tumor necrosis factor receptor-associated protein 1 (TRAP1) in apoptosis induced by beta-hydroxyisovalerylshikonin." J Biol Chem **279**(41): 42503-42515.

Mayer, M. P. and B. Bukau (2005). "Hsp70 chaperones: cellular functions and molecular mechanism." Cell Mol Life Sci **62**(6): 670-684.

Mayer, M. P., S. Rudiger, et al. (2000). "Molecular basis for interactions of the DnaK chaperone with substrates." Biol Chem **381**(9-10): 877-885.

Mayr, C., K. Richter, et al. (2000). "Cpr6 and Cpr7, two closely related Hsp90-associated immunophilins from Saccharomyces cerevisiae, differ in their functional properties." J Biol Chem **275**(44): 34140-34146.

McCarty, J. S., A. Buchberger, et al. (1995). "The role of ATP in the functional cycle of the DnaK chaperone system." J Mol Biol **249**(1): 126-137.

McClellan, A. J., Y. Xia, et al. (2007). "Diverse cellular functions of the Hsp90 molecular chaperone uncovered using systems approaches." Cell **131**(1): 121-135.

McLaughlin, S. H., H. W. Smith, et al. (2002). "Stimulation of the weak ATPase activity of human hsp90 by a client protein." J Mol Biol **315**(4): 787-798.

Melnick, J., S. Aviel, et al. (1992). "The endoplasmic reticulum stress protein GRP94, in addition to BiP, associates with unassembled immunoglobulin chains." J Biol Chem **267**(30): 21303-21306.

Meyer, P., C. Prodromou, et al. (2003). "Structural and functional analysis of the middle segment of hsp90: implications for ATP hydrolysis and client protein and cochaperone interactions." Mol Cell **11**(3): 647-658.

Meyer, P., C. Prodromou, et al. (2004). "Structural basis for recruitment of the ATPase activator Aha1 to the Hsp90 chaperone machinery." EMBO J **23**(3): 511-519.

Millson, S. H., A. W. Truman, et al. (2005). "A two-hybrid screen of the yeast proteome for Hsp90 interactors uncovers a novel Hsp90 chaperone requirement in the activity of a stress-activated mitogen-activated protein kinase, Slt2p (Mpk1p)." Eukaryot Cell **4**(5): 849-860.

Minami, M., M. Nakamura, et al. (2001). "Both the N- and C-terminal chaperone sites of Hsp90 participate in protein refolding." Eur J Biochem **268**(8): 2520-2524.

Mogk, A., T. Tomoyasu, et al. (1999). "Identification of thermolabile Escherichia coli proteins: prevention and reversion of aggregation by DnaK and ClpB." EMBO J **18**(24): 6934-6949.

Moreno-del Alamo, M., A. Sanchez-Gorostiaga, et al. (2010). "Structural analysis of the interactions between hsp70 chaperones and the yeast DNA replication protein Orc4p." J Mol Biol **403**(1): 24-39.

Morishima, Y., K. C. Kanelakis, et al. (2003). "The hsp90 cochaperone p23 is the limiting component of the multiprotein hsp90/hsp70-based chaperone system in vivo where it acts to stabilize the client protein: hsp90 complex." J Biol Chem **278**(49): 48754-48763.

Muresan, Z. and P. Arvan (1997). "Thyroglobulin transport along the secretory pathway. Investigation of the role of molecular chaperone, GRP94, in protein export from the endoplasmic reticulum." J Biol Chem **272**(42): 26095-26102.

Nathan, D. F., M. H. Vos, et al. (1999). "Identification of SSF1, CNS1, and HCH1 as multicopy suppressors of a Saccharomyces cerevisiae Hsp90 loss-of-function mutation." Proc Natl Acad Sci U S A **96**(4): 1409-1414.

Nelson, R. J., T. Ziegelhoffer, et al. (1992). "The translation machinery and 70 kd heat shock protein cooperate in protein synthesis." Cell **71**(1): 97-105.

Nemoto, T., T. Matsusaka, et al. (1996). "Dimerization characteristics of the 94-kDa glucose-regulated protein." J Biochem **120**(2): 249-256.

Obermann, W. M., H. Sondermann, et al. (1998). "In vivo function of Hsp90 is dependent on ATP binding and ATP hydrolysis." J Cell Biol **143**(4): 901-910.

O'Brien, M. C. and D. B. McKay (1995). "How potassium affects the activity of the molecular chaperone Hsc70. I. Potassium is required for optimal ATPase activity." J Biol Chem **270**(5): 2247-2250.

Odunuga, O. O., V. M. Longshaw, et al. (2004). "Hop: more than an Hsp70/Hsp90 adaptor protein." Bioessays **26**(10): 1058-1068.

Onuoha, S. C., E. T. Coulstock, et al. (2008). "Structural studies on the co-chaperone Hop and its complexes with Hsp90." J Mol Biol **379**(4): 732-744.

Ostermann, J., A. L. Horwich, et al. (1989). "Protein folding in mitochondria requires complex formation with hsp60 and ATP hydrolysis." Nature **341**(6238): 125-130.

Packschies, L., H. Theyssen, et al. (1997). "GrpE accelerates nucleotide exchange of the molecular chaperone DnaK with an associative displacement mechanism." Biochemistry **36**(12): 3417-3422.

Palleros, D. R., K. L. Reid, et al. (1993). "ATP-induced protein-Hsp70 complex dissociation requires K+ but not ATP hydrolysis." Nature **365**(6447): 664-666.

Panaretou, B., C. Prodromou, et al. (1998). "ATP binding and hydrolysis are essential to the function of the Hsp90 molecular chaperone in vivo." EMBO J **17**(16): 4829-4836.

Panaretou, B., G. Siligardi, et al. (2002). "Activation of the ATPase activity of hsp90 by the stress-regulated cochaperone aha1." Mol Cell **10**(6): 1307-1318.

Park, S. J., M. Kostic, et al. (2011). "Dynamic Interaction of Hsp90 with Its Client Protein p53." J Mol Biol **411**(1): 158-173.

Pearl, L. H. (2005). "Hsp90 and Cdc37 -- a chaperone cancer conspiracy." Curr Opin Genet Dev **15**(1): 55-61.

Pearl, L. H. and C. Prodromou (2000). "Structure and in vivo function of Hsp90." Curr Opin Struct Biol **10**(1): 46-51.

Pearl, L. H. and C. Prodromou (2001). "Structure, function, and mechanism of the Hsp90 molecular chaperone." Adv Protein Chem **59**: 157-186.

Pearl, L. H. and C. Prodromou (2006). "Structure and mechanism of the Hsp90 molecular chaperone machinery." Annu Rev Biochem **75**: 271-294.

Perdew, G. H., N. Hord, et al. (1993). "Localization and characterization of the 86- and 84-kDa heat shock proteins in Hepa 1c1c7 cells." Exp Cell Res **209**(2): 350-356.

Pfund, C., N. Lopez-Hoyo, et al. (1998). "The molecular chaperone Ssb from Saccharomyces cerevisiae is a component of the ribosome-nascent chain complex." EMBO J **17**(14): 3981-3989.

Philo, J. S. (2011). “Limiting the sedimentation coefficient for sedimentation velocity data analysis: partial boundary modeling and g(s) approaches revisited.” Anal Biochem **412**(2): 189-202

Picard, D. (2002). "Heat-shock protein 90, a chaperone for folding and regulation." Cell Mol Life Sci **59**(10): 1640-1648.

Pierpaoli, E. V., E. Sandmeier, et al. (1997). "The power stroke of the DnaK/DnaJ/GrpE molecular chaperone system." J Mol Biol **269**(5): 757-768.

Pierpaoli, E. V., E. Sandmeier, et al. (1998). "Control of the DnaK chaperone cycle by substoichiometric concentrations of the co-chaperones DnaJ and GrpE." J Biol Chem **273**(12): 6643-6649.

Pirkl, F. and J. Buchner (2001). "Functional analysis of the Hsp90-associated human peptidyl prolyl cis/trans isomerases FKBP51, FKBP52 and Cyp40." J Mol Biol **308**(4): 795-806.

Poetsch, M., T. Dittberner, et al. (2000). "TTC4, a novel candidate tumor suppressor gene at 1p31 is often mutated in malignant melanoma of the skin." Oncogene **19**(50): 5817-5820.

Polier, S., Z. Dragovic, et al. (2008). "Structural basis for the cooperation of Hsp70 and Hsp110 chaperones in protein folding." Cell **133**(6): 1068-1079.

Polier, S., F. U. Hartl, et al. (2010). "Interaction of the Hsp110 molecular chaperones from S. cerevisiae with substrate protein." J Mol Biol **401**(5): 696-707.

Pratt, W. B., L. C. Scherrer, et al. (1992). "A model of glucocorticoid receptor unfolding and stabilization by a heat shock protein complex." J Steroid Biochem Mol Biol **41**(3-8): 223-229.

Pratt, W. B. and D. O. Toft (1997). "Steroid receptor interactions with heat shock protein and immunophilin chaperones." Endocr Rev **18**(3): 306-360.

Pratt, W. B. and D. O. Toft (1997). "Steroid receptor interactions with heat shock protein and immunophilin chaperones." Endocr Rev **18**(3): 306-360.

Pratt, W. B. and D. O. Toft (2003). "Regulation of signaling protein function and trafficking by the hsp90/hsp70-based chaperone machinery." Exp Biol Med (Maywood) **228**(2): 111-133.

Prodromou, C. (2012). "The 'active life' of Hsp90 complexes." Biochim Biophys Acta **1823**(3): 614-623.

Prodromou, C., B. Panaretou, et al. (2000). "The ATPase cycle of Hsp90 drives a molecular 'clamp' via transient dimerization of the N-terminal domains." EMBO J **19**(16): 4383-4392.

Prodromou, C., S. M. Roe, et al. (1997). "Identification and structural characterization of the ATP/ADP-binding site in the Hsp90 molecular chaperone." Cell **90**(1): 65-75.

Prodromou, C., G. Siligardi, et al. (1999). "Regulation of Hsp90 ATPase activity by tetratricopeptide repeat (TPR)-domain co-chaperones." EMBO J **18**(3): 754-762.

Ramsey, A. J., L. C. Russell, et al. (2000). "Overlapping sites of tetratricopeptide repeat protein binding and chaperone activity in heat shock protein 90." J Biol Chem **275**(23): 17857-17862.

Ratajczak, T., B. K. Ward, et al. (2009). "Cyclophilin 40: an Hsp90-cochaperone associated with apo-steroid receptors." Int J Biochem Cell Biol **41**(8-9): 1652-1655.

Ratzke, C., M. Mickler, et al. (2010). "Dynamics of heat shock protein 90 C-terminal dimerization is an important part of its conformational cycle." Proc Natl Acad Sci U S A **107**(37): 16101-16106.

Raviol, H., H. Sadlish, et al. (2006). "Chaperone network in the yeast cytosol: Hsp110 is revealed as an Hsp70 nucleotide exchange factor." EMBO J **25**(11): 2510-2518.

Reed, S. I. (1980). "The selection of S. cerevisiae mutants defective in the start event of cell division." Genetics **95**(3): 561-577.

Retzlaff, M., F. Hagn, et al. (2010). "Asymmetric activation of the hsp90 dimer by its cochaperone aha1." Mol Cell **37**(3): 344-354.

Richter, K. and J. Buchner (2001). "Hsp90: chaperoning signal transduction." J Cell Physiol **188**(3): 281-290.

Richter, K. and J. Buchner (2006). "hsp90: twist and fold." Cell **127**(2): 251-253.

Richter, K., M. Haslbeck, et al. (2010). "The heat shock response: life on the verge of death." Mol Cell **40**(2): 253-266.

Richter, K., S. Moser, et al. (2006). "Intrinsic inhibition of the Hsp90 ATPase activity." J Biol Chem **281**(16): 11301-11311.

Richter, K., P. Muschler, et al. (2001). "Coordinated ATP hydrolysis by the Hsp90 dimer." J Biol Chem **276**(36): 33689-33696.

Richter, K., P. Muschler, et al. (2003). "Sti1 is a non-competitive inhibitor of the Hsp90 ATPase. Binding prevents the N-terminal dimerization reaction during the atpase cycle." J Biol Chem **278**(12): 10328-10333.

Richter, K., J. Reinstein, et al. (2002). "N-terminal residues regulate the catalytic efficiency of

the Hsp90 ATPase cycle." J Biol Chem **277**(47): 44905-44910.

Richter, K., S. Walter, et al. (2004). "The Co-chaperone Sba1 connects the ATPase reaction of Hsp90 to the progression of the chaperone cycle." J Mol Biol **342**(5): 1403-1413.

Riordan, J. R. (2005). "Assembly of functional CFTR chloride channels." Annu Rev Physiol **67**: 701-718.

Riordan, J. R. (2008). "CFTR function and prospects for therapy." Annu Rev Biochem **77**: 701-726.

Roe, S. M., C. Prodromou, et al. (1999). "Structural basis for inhibition of the Hsp90 molecular chaperone by the antitumor antibiotics radicicol and geldanamycin." J Med Chem **42**(2): 260-266.

Rothnie, A., A. R. Clarke, et al. (2011). "A sequential mechanism for clathrin cage disassembly by 70-kDa heat-shock cognate protein (Hsc70) and auxilin." Proc Natl Acad Sci U S A **108**(17): 6927-6932.

Ruddock, L. W. and P. Klappa (1999). "Oxidative stress: Protein folding with a novel redox switch." Curr Biol **9**(11): R400-402.

Rudiger, S., L. Germeroth, et al. (1997). "Substrate specificity of the DnaK chaperone determined by screening cellulose-bound peptide libraries." EMBO J **16**(7): 1501-1507.

Rudiger, S., M. P. Mayer, et al. (2000). "Modulation of substrate specificity of the DnaK chaperone by alteration of a hydrophobic arch." J Mol Biol **304**(3): 245-251.

Rye, H. S., S. G. Burston, et al. (1997). "Distinct actions of cis and trans ATP within the double ring of the chaperonin GroEL." Nature **388**(6644): 792-798.

Sadis, S. and L. E. Hightower (1992). "Unfolded proteins stimulate molecular chaperone Hsc70 ATPase by accelerating ADP/ATP exchange." Biochemistry **31**(39): 9406-9412.

Schaiff, W. T., K. A. Hruska, Jr., et al. (1992). "HLA-DR associates with specific stress proteins and is retained in the endoplasmic reticulum in invariant chain negative cells." J Exp Med **176**(3): 657-666.

Schatz, G. and B. Dobberstein (1996). "Common principles of protein translocation across membranes." Science **271**(5255): 1519-1526.

Scheibel, T., S. Neuhofen, et al. (1997). "ATP-binding properties of human Hsp90." J Biol Chem **272**(30): 18608-18613.

Scheufler, C., A. Brinker, et al. (2000). "Structure of TPR domain-peptide complexes: critical elements in the assembly of the Hsp70-Hsp90 multichaperone machine." Cell **101**(2): 199-210.

Schlecht, R., A. H. Erbse, et al. (2011). "Mechanics of Hsp70 chaperones enables differential interaction with client proteins." Nat Struct Mol Biol **18**(3): 345-351.

Schmid, A. B; (2009). “The adaptor protein Sti1/Hop connects the Hsp70 and Hsp90 chaperone cycle” PhD thesis

Schmid, A. B., S. Lagleder, et al. (2012). "The architecture of functional modules in the Hsp90 co-chaperone Sti1/Hop." EMBO J **31**(6): 1506-1517.

Schmid, D., A. Baici, et al. (1994). "Kinetics of molecular chaperone action." Science **263**(5149): 971-973.

Schroder, H., T. Langer, et al. (1993). "DnaK, DnaJ and GrpE form a cellular chaperone machinery capable of repairing heat-induced protein damage." EMBO J **12**(11): 4137-4144.

Schuermann, J. P., J. Jiang, et al. (2008). "Structure of the Hsp110:Hsc70 nucleotide exchange machine." Mol Cell **31**(2): 232-243.

Schumacher, R. J., W. J. Hansen, et al. (1996). "Cooperative action of Hsp70, Hsp90, and DnaJ proteins in protein renaturation." Biochemistry **35**(47): 14889-14898.

Schweizer, R. S., R. A. Aponte, et al. (2011). "Fine tuning of a biological machine: DnaK gains improved chaperone activity by altered allosteric communication and substrate binding." Chembiochem **12**(10): 1559-1573.

Sfatos, C. D., A. M. Gutin, et al. (1996). "Simulations of chaperone-assisted folding." Biochemistry **35**(1): 334-339.

Sha, B., S. Lee, et al. (2000). "The crystal structure of the peptide-binding fragment from the yeast Hsp40 protein Sis1." Structure **8**(8): 799-807.

Shaner, L., P. A. Gibney, et al. (2008). "The Hsp110 protein chaperone Sse1 is required for yeast cell wall integrity and morphogenesis." Curr Genet **54**(1): 1-11.

Shaner, L. and K. A. Morano (2007). "All in the family: atypical Hsp70 chaperones are conserved modulators of Hsp70 activity." Cell Stress Chaperones **12**(1): 1-8.

Shaner, L., R. Sousa, et al. (2006). "Characterization of Hsp70 binding and nucleotide exchange by the yeast Hsp110 chaperone Sse1." Biochemistry **45**(50): 15075-15084.

Shaner, L., A. Trott, et al. (2004). "The function of the yeast molecular chaperone Sse1 is mechanistically distinct from the closely related hsp70 family." J Biol Chem **279**(21): 21992-22001.

Shaner, L., H. Wegele, et al. (2005). "The yeast Hsp110 Sse1 functionally interacts with the Hsp70 chaperones Ssa and Ssb." J Biol Chem **280**(50): 41262-41269.

Sharma, S. K., P. De los Rios, et al. (2010). "The kinetic parameters and energy cost of the Hsp70 chaperone as a polypeptide unfoldase." Nat Chem Biol **6**(12): 914-920.

Siligardi, G., B. Panaretou, et al. (2002). "Regulation of Hsp90 ATPase activity by the co-chaperone Cdc37p/p50cdc37." J Biol Chem **277**(23): 20151-20159.

Smith, D. F. (1993). "Dynamics of heat shock protein 90-progesterone receptor binding and the disactivation loop model for steroid receptor complexes." Mol Endocrinol **7**(11): 1418-1429.

Smith, D. F. and D. O. Toft (1993). "Steroid receptors and their associated proteins." Mol Endocrinol **7**(1): 4-11.

Smith, D. F. and D. O. Toft (2008). "Minireview: the intersection of steroid receptors with molecular chaperones: observations and questions." Mol Endocrinol **22**(10): 2229-2240.

Smith, D. F., L. Whitesell, et al. (1995). "Progesterone receptor structure and function altered by geldanamycin, an hsp90-binding agent." Mol Cell Biol **15**(12): 6804-6812.

Sondermann, H., C. Scheufler, et al. (2001). "Structure of a Bag/Hsc70 complex: convergent functional evolution of Hsp70 nucleotide exchange factors." Science **291**(5508): 1553-1557.

Song, H. Y., J. D. Dunbar, et al. (1995). "Identification of a protein with homology to hsp90 that binds the type 1 tumor necrosis factor receptor." J Biol Chem **270**(8): 3574-3581.

Song, J., M. Takeda, et al. (2001). "Bag1-Hsp70 mediates a physiological stress signalling pathway that regulates Raf-1/ERK and cell growth." Nat Cell Biol **3**(3): 276-282.

Spence, J., A. Cegielska, et al. (1990). "Role of Escherichia coli heat shock proteins DnaK and HtpG (C62.5) in response to nutritional deprivation." J Bacteriol **172**(12): 7157-7166.

Spence, J. and C. Georgopoulos (1989). "Purification and properties of the Escherichia coli heat shock protein, HtpG." J Biol Chem **264**(8): 4398-4403.

Stebbins, C. E., A. A. Russo, et al. (1997). "Crystal structure of an Hsp90-geldanamycin complex: targeting of a protein chaperone by an antitumor agent." Cell **89**(2): 239-250.

Street, T. O., L. A. Lavery, et al. (2011). "Substrate binding drives large-scale conformational changes in the Hsp90 molecular chaperone." Mol Cell **42**(1): 96-105.

Su, G., G. Casey, et al. (2000). "Genomic structure of the human tetratricopeptide repeat-containing gene, TTC4, from chromosome region 1p31 and mutation analysis in breast cancers." Int J Mol Med **5**(2): 197-200.

Suh, W. C., W. F. Burkholder, et al. (1998). "Interaction of the Hsp70 molecular chaperone, DnaK, with its cochaperone DnaJ." Proc Natl Acad Sci U S A **95**(26): 15223-15228.

Sullivan, W. P., B. A. Owen, et al. (2002). "The influence of ATP and p23 on the conformation of hsp90." J Biol Chem **277**(48): 45942-45948.

Sun, L., F. T. Edelmann, et al. (2012). "The lid domain of Caenorhabditis elegans Hsc70 influences ATP turnover, cofactor binding and protein folding activity." PLoS One **7**(3): e33980.

Swain, J. F., G. Dinler, et al. (2007). "Hsp70 chaperone ligands control domain association via an allosteric mechanism mediated by the interdomain linker." Mol Cell **26**(1): 27-39.

Tesic, M., J. A. Marsh, et al. (2003). "Functional interactions between Hsp90 and the co-chaperones Cns1 and Cpr7 in Saccharomyces cerevisiae." J Biol Chem **278**(35): 32692-32701.

Theyssen, H., H. P. Schuster, et al. (1996). "The second step of ATP binding to DnaK induces peptide release." J Mol Biol **263**(5): 657-670.

Thulasiraman, V., C. F. Yang, et al. (1999). "In vivo newly translated polypeptides are sequestered in a protected folding environment." EMBO J **18**(1): 85-95.

Tsutsumi, S., M. Mollapour, et al. (2012). "Charged linker sequence modulates eukaryotic heat shock protein 90 (Hsp90) chaperone activity." Proc Natl Acad Sci U S A **109**(8): 2937-2942.

Tzankov, S., M. J. Wong, et al. (2008). "Functional divergence between co-chaperones of Hsc70." J Biol Chem **283**(40): 27100-27109.

Ungermann, C., W. Neupert, et al. (1994). "The role of Hsp70 in conferring unidirectionality on protein translocation into mitochondria." Science **266**(5188): 1250-1253.

Vaughan, C. K., U. Gohlke, et al. (2006). "Structure of an Hsp90-Cdc37-Cdk4 complex." Mol Cell **23**(5): 697-707.

Vaughan, C. K., M. Mollapour, et al. (2008). "Hsp90-dependent activation of protein kinases is regulated by chaperone-targeted dephosphorylation of Cdc37." Mol Cell **31**(6): 886-895.

Vogel, M., B. Bukau, et al. (2006). "Allosteric regulation of Hsp70 chaperones by a proline switch." Mol Cell **21**(3): 359-367.

Vogel, M., M. P. Mayer, et al. (2006). "Allosteric regulation of Hsp70 chaperones involves a conserved interdomain linker." J Biol Chem **281**(50): 38705-38711.

Voisine, C., Y. C. Cheng, et al. (2001). "Jac1, a mitochondrial J-type chaperone, is involved in the biogenesis of Fe/S clusters in Saccharomyces cerevisiae." Proc Natl Acad Sci U S A **98**(4): 1483-1488.

Walter, S. and J. Buchner (2002). "Molecular chaperones--cellular machines for protein folding." Angew Chem Int Ed Engl **41**(7): 1098-1113.

Wandinger, S. K., M. H. Suhre, et al. (2006). "The phosphatase Ppt1 is a dedicated regulator of the molecular chaperone Hsp90." EMBO J **25**(2): 367-376.

Wang, X., A. V. Koulov, et al. (2008). "Chemical and biological folding contribute to temperature-sensitive DeltaF508 CFTR trafficking." Traffic **9**(11): 1878-1893.

Weaver, A. J., W. P. Sullivan, et al. (2000). "Crystal structure and activity of human p23, a heat shock protein 90 co-chaperone." J Biol Chem **275**(30): 23045-23052.

Wegele, H., L. Muller, et al. (2004). "Hsp70 and Hsp90--a relay team for protein folding." Rev Physiol Biochem Pharmacol **151**: 1-44.

Wegele, H., S. K. Wandinger, et al. (2006). "Substrate transfer from the chaperone Hsp70 to Hsp90." J Mol Biol **356**(3): 802-811.

Weikl, T., P. Muschler, et al. (2000). "C-terminal regions of Hsp90 are important for trapping the nucleotide during the ATPase cycle." J Mol Biol **303**(4): 583-592.

Wendler, P. and H. R. Saibil (2010). "Cryo electron microscopy structures of Hsp100 proteins: crowbars in or out?" Biochem Cell Biol **88**(1): 89-96.

Werner-Washburne, M. and E. A. Craig (1989). "Expression of members of the Saccharomyces cerevisiae hsp70 multigene family." Genome **31**(2): 684-689.

Wickner, S., J. Hoskins, et al. (1991). "Function of DnaJ and DnaK as chaperones in origin-specific DNA binding by RepA." Nature **350**(6314): 165-167.

Wickner, S., J. Hoskins, et al. (1991). "Monomerization of RepA dimers by heat shock proteins activates binding to DNA replication origin." Proc Natl Acad Sci U S A **88**(18): 7903-7907.

Wilbanks, S. M., C. DeLuca-Flaherty, et al. (1994). "Structural basis of the 70-kilodalton heat shock cognate protein ATP hydrolytic activity. I. Kinetic analyses of active site mutants." J Biol Chem **269**(17): 12893-12898.

Wilbanks, S. M. and D. B. McKay (1995). "How potassium affects the activity of the molecular chaperone Hsc70. II. Potassium binds specifically in the ATPase active site." J Biol Chem **270**(5): 2251-2257.

Wu, S., F. Hong, et al. (2012). "The molecular chaperone gp96/GRP94 interacts with Toll-like receptors and integrins via its C-terminal hydrophobic domain." J Biol Chem **287**(9): 6735-6742.

Wu, Y., J. Li, et al. (2005). "The crystal structure of the C-terminal fragment of yeast Hsp40 Ydj1 reveals novel dimerization motif for Hsp40." J Mol Biol **346**(4): 1005-1011.

Xu, Z., A. L. Horwich, et al. (1997). "The crystal structure of the asymmetric GroEL-GroES-(ADP)7 chaperonin complex." Nature **388**(6644): 741-750.

Yamada, S., T. Ono, et al. (2003). "A hydrophobic segment within the C-terminal domain is essential for both client-binding and dimer formation of the HSP90-family molecular chaperone." Eur J Biochem **270**(1): 146-154.

Yang, Y., B. Liu, et al. (2007). "Heat shock protein gp96 is a master chaperone for toll-like receptors and is important in the innate function of macrophages." Immunity **26**(2): 215-226.

Yi, F., I. Doudevski, et al. (2010). "HOP is a monomer: investigation of the oligomeric state of the co-chaperone HOP." Protein Sci **19**(1): 19-25.

Young, J. C. and F. U. Hartl (2000). "Polypeptide release by Hsp90 involves ATP hydrolysis and is enhanced by the co-chaperone p23." EMBO J **19**(21): 5930-5940.

Zhang, Y. (2009). "Protein structure prediction: when is it useful?" Curr Opin Struct Biol **19**(2): 145-155.

Zhang, M., Y. Kadota, et al. (2010). "Structural basis for assembly of Hsp90-Sgt1-CHORD protein complexes: implications for chaperoning of NLR innate immunity receptors." Mol Cell **39**(2): 269-281.

Zhao, R., M. Davey, et al. (2005). "Navigating the chaperone network: an integrative map of physical and genetic interactions mediated by the hsp90 chaperone." Cell **120**(5): 715-727.

Zhu, X., X. Zhao, et al. (1996). "Structural analysis of substrate binding by the molecular chaperone DnaK." Science **272**(5268): 1606-1614.

Zolkiewski, M., T. Zhang, et al. (2012). "Aggregate reactivation mediated by the Hsp100 chaperones." Arch Biochem Biophys **520**(1): 1-6.

Zuiderweg, E. R., E. B. Bertelsen, et al. (2012). "Allostery in the Hsp70 Chaperone Proteins." Top Curr Chem.

8. Publications

L. Mitschke, C. Parthier, K. Schröder-Tittmann; J. Coy, S. Lüdtke, K. Tittmann (2010) "The crystal structure of human transketolase and new insights into its mode of action." J Biol Chem **285**(41): 31559-31570.

M. Retzlaff, F. Hagn, L. Mitschke, M. Hessling, F. Gugel, H. Kessler, K. Richter, J. Buchner (2010). "Asymmetric activation of the hsp90 dimer by its cochaperone aha1." Mol Cell **37**(3): 344-354.

Acknowledgemnents

This thesis was prepared at the Technische Univerität München, chair of biotechnology under the supervision of Prof. Dr. Johannes Buchner.

First of all, I would like to thank Prof. Dr. Johannes Buchner for giving me the opportunity to prepare the PhD thesis in his group, which provides excellent scientific equipment and knowledge. Additionally, I would like to thank him for the productive working atmosphere and the helpful discussions on scientific topics. Additionally, it was a pleasure to attend on two Hsp90 conferences in 2008 and 2010.

I would like to thank Maike Krause, Klaus Richter, Alexander Bepperling and Jirka Peschek for technical support with analytical ultracentrifugation and the data analysis. Additionally, thanks to all our lab technicians for their support.

Moreover, I would like to thank Prof. Dr. Michael Groll and his group for crystallization experiments.

I would like to thank all of my practical and bachelor students for their provided technical assistance. In this regard, thanks to Rudi and Herwin for their work on Cns1. It was a funny time.

Furthermore, I thank all my colleagues in the group. In this regards, I want to thank Moritz, Marco, Natalia, Matthias, Mathias and Eva from the lab 6. It was really funny to work with you! Especially, I want to thank Christoph, Marco and Moritz for all the technical support and the fruitful scientific and non-scientific discussions.

I would like to thank the girls from office 4 (Alina, Maike, Danae and Vroni) for the nice atmosphere in our office. Thanks for the productive and funny time!

I would like to thank my parents for all their support.

Especially, I want to thank my girlfriend Annette and my daughter Matilda.

Acknowledgemnents

Declaration

Hereby I declare that this thesis was composed independently without use of other resources or references than the stated ones. This work has not been presented to any examination board yet.

Hiermit erkläre ich, dass die vorliegende Arbeit selbständig verfasst wurde. Dabei wurden keine anderen als die hier angegebenen Hilfsmittel oder Quellen verwendet. Die Arbeit wurde noch keiner Prüfungskommission vorgelegt.

München, Juni 2012